STRUCTURAL GEOLOGY OF THE VEIN SYSTEM IN THE SAN ANTONIO GOLD MINE BISSETT, MANITOBA, CANADA

A thesis submitted to the
UNIVERSITY OF MANITOBA
in partial fulfillment of the requirements
for the degree of

Master of Science
by
MENG HOO SEBASTIAN LAU

Department of Geological Sciences
University of Manitoba
Winnipeg, Manitoba
Canada 1988

ISBN 0-315-44102-X

STRUCTURAL GEOLOGY OF THE VEIN SYSTEM
IN THE SAN ANTONIO GOLD MINE
BISSETT, MANITOBA, CANADA

BY

MENG HOO SEBASTIAN LAU

A thesis submitted to the Faculty of Graduate Studies of the University of Manitoba in partial fulfillment of the requirements of the degree of

MASTER OF SCIENCE

The University of Manitoba requires the signatures of all persons using or photocopying this thesis. Please sign below, and give address and date.

ABSTRACT

The San Antonio mine occurs in a mafic sill-like unit within the Rice Lake Group known as the San Antonio Mine (SAM) unit. Within the SAM unit there are five major fracture sets, each with distinct characteristics, now filled by dike and vein materials. The cross-cutting relationships between the five sets of fractures are very consistent and reveal age relationships, from oldest to youngest (1) dikes, (2) stockworks, (3) 16-type vein-filled shear zones, (4) NE/SE vein-filled shear zones and (5) NW/SW vein-filled fractures.

The dikes and the fractures in which they occur are coeval and were developed as the result of hydraulic tension fracturing of the SAM unit.

The stockworks are composed mainly of three components: marginal ladder-veins, central breccia zones and central veins. The ladder-veins were developed by hydraulic tension fracturing, and the central breccia zones developed as a result of either hydraulic or shear brecciation at advanced stages of ladder-vein development. The central veins which occur within the central breccia zones are in later fractures developed by shear or tension. In either case the fracturing was brittle.

The 16-type veins occur within 16-type ductile shear zones. The veins were emplaced by hydraulic dilation of the shear zone schistosity.

The NE/SE veins occur within pre-vein NE/SE ductile shear zones and were emplaced by process similar to the 16-type veins.

The NW/SW veins occur in brittle fractures which may have originated by either shear or tension.

The orientations of these sets of fractures, along with kinematics and/or stress orientation interpretations indicate that they were developed independently of each other at different times. In contrast the veins in the fractures have similar compositions indicating that vein forming fluids changed very little over the time span of the development of the four vein-filled fractures sets.

The 16-type shear zones are the only structures within the SAN unit which have been related to observed deformation in the surrounding Rice Lake Group. They represent spaced ductile shear zones that have caused segmentation of the SAM unit into elongate prisms. Kinematic analyses of these features have revealed that displacement of the segments is subparallel to their elongation and similar in direction and sense to the interpretation of displacement represented by the schistosity and lineations in the surrounding Rice Lake Group.

ACKNOWLEDGEMENT

Special thanks are due to Dr. W. C. Brisbin who suggested the topic of the study, patiently supervised the project and guided me through the process of conducting research, proper data documentation and reporting the results. His incessant encouragements and invaluable dicussions throughout the course of the study were of great benefit to the author. The author also gratefully acknowledges Dr. Brisbin for allotting financial support throughout this study.

Thanks are also due to Dr. K. H. Poulsen of the Geological Survey of Canada who also provided many invaluble dicussions during the course of this study and made many suggestions that improved the final manuscript. Dr. N. M. Halden of the Department of the Geological Sciences, University of Manitoba is also thanked for giving suggestions to improve the manuscript.

D. E. Ames of the Geological Survey of Canada has assisted the author in many ways. B. Whiting provided the author with the first underground geological tour of the San Antonio Mine.

The author is grateful to Lathwell Resources Ltd., Brinco Ltd. and INCO Ltd. for providing access to the mine records and underground of the San Antonio Mine. Lathwell Resources Ltd. also provided accomodation at the mine site in the summer of the 1984. Thanks are also due to the staffs at the mine for their hospitality.

Many colleages at the Department of Geological Sciences, University of Manitoba have provided much assistance.

Funding for this project was provided by the Federal side of the Canada-Manitoba Mineral Development Agreement (1984). Scientific Authority at the Federal Level was Dr. K. H. Poulsen, Mineral Resources Division, Geological Survey of Canada.

CONTENTS

LIST OF FIGURES

LIST OF TABLE

CHAPTER ONE

INTRODUCTION

1.1 OBJECTIVE

This thesis presents the result of a structural geologic study of the orebodies of the San Antonio gold mine in southeast Manitoba. The orebodies occur as vein-filled fractures within a particular mafic stratigraphic unit, known as the San Antonio Mine (**SAM**) unit, which is part of Rice Lake Supracrustal Group. The objectives of the study are: (1) to document the characteristics of, the orientation of, the spatial distribution of, the age relationships between, the nature of the vein-filling within, and the effect of the wall rock alteration adjacent to different sets of fractures within the SAM unit; (2) to interpret the origin of fracture sets, and the sequence of veining; and (3) to discuss these interpretations in the context of regional structural development.

1.2 LOCATION OF THE SAN ANTONIO MINE

The San Antonio gold mine is located on the north shore of Rice Lake, near Bissett, Manitoba (Figure 1). The 250 km all weather road (Provicial Highway 319) along the southeastern side of Lake Winnipeg provides good access to the site from Winnipeg.

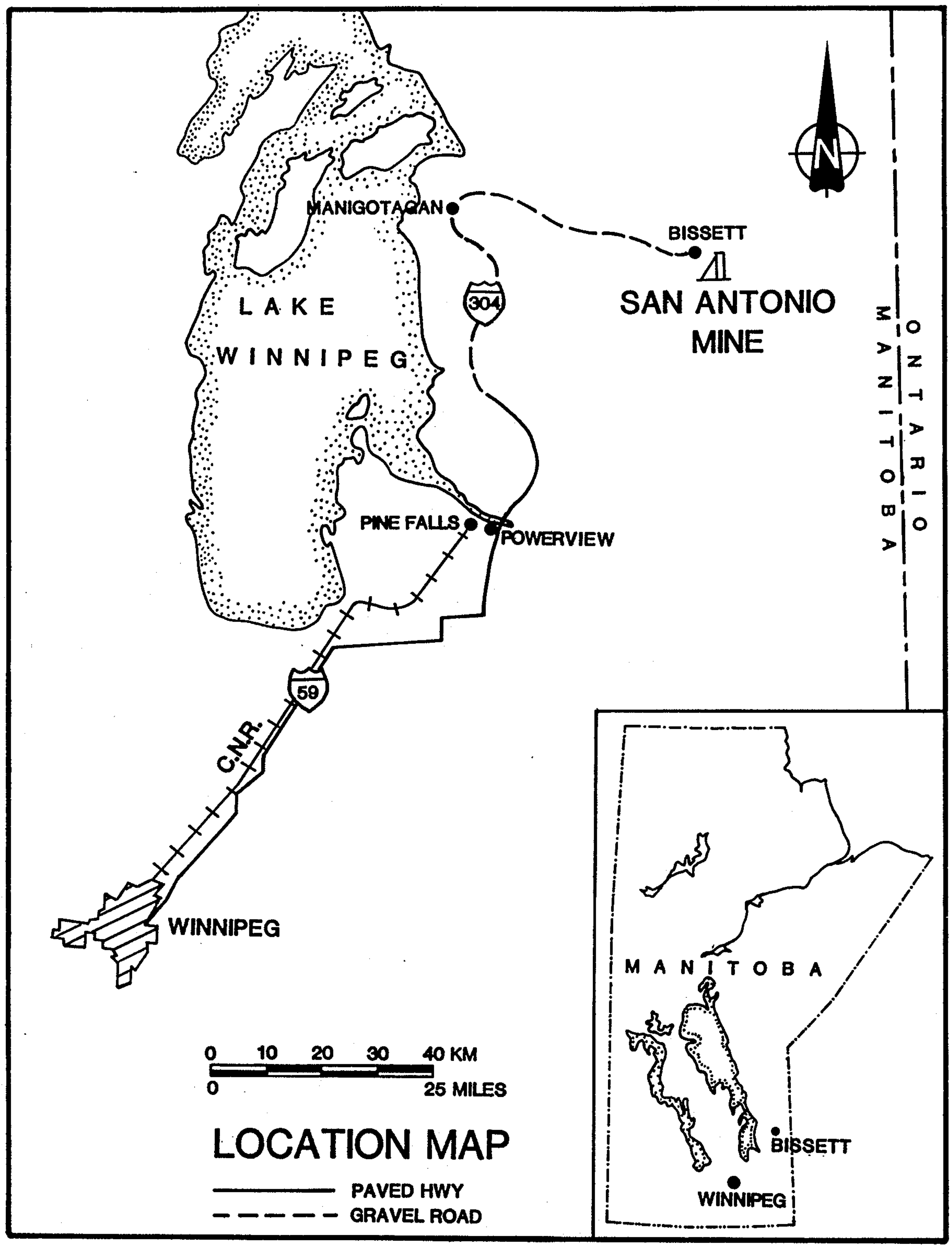

Figure 1: Location of the San Antonio Mine.

1.3 HISTORY OF THE SAN ANTONIO MINE PROPERTY

Gold was first discovered on the San Antonio property in 1911 but very little was done until 1928 (Henry, 1928). Two problems encountered in these early stages of exploration were the lack of exposure and the lack of finances. Although many poorly exposed but promising showings had attracted attention, the lack of funds for follow-up work inhibited full disclosure of the potential of these occurrences.

Serious exploration began in 1928 when the first shaft was sunk about 100 m east of the present main shaft. Following a sizable discovery underground, the mill was built and started operating in 1931. Since then 4,955,388 tonnes (4,875,748 tons) of ore with an average grade of 8.71 gram per tonnes (0.28 oz per ton) gold has been produced from the mine. The mine was closed in 1968. At that time a total of 42,918 kg (1.38 million oz) of gold and 6.065 kg (195,000 oz) of silver had been recovered from the mine. Further exploration in the mine resumed in the early 1980's. It was opened briefly for the purpose of underground exploration in 1984 and was closed again in 1986.

1.4 PREVIOUS STUDIES OF THE SAN ANTONIO MINE GEOLOGY

The vein system which has yielded good production at the San Antonio mine consists of complex sets of fractures that have been filled with vein material. The characteristics of the vein material and, to a lesser extent, of the fractures, have been dealt with by many authors (Reid 1933, Stockwell 1938, DeHuff 1940, Gibson and Stockwell 1948, Skerl 1955 and Stephenson 1971). These authors have recognised the fracture system as the primary control for the ore, but have limited their interpretation of the genesis of the fractures primarily to the orientation of, and angular relationships between fracture sets. The fact that the main orebodies were confined to two major fracture sets lead most of these authors to interpret that the fractures were generated as conjugate sets of shear fractures.

Various authors (Bragg 1943, Amukun and Turnock 1971, Stephenson 1971) also studied the relationships of the type and intensity of host rock alteration to the type of veins. These authors also dealt with possible sources of vein minerals. Stephenson (1971) concluded that both vein material and gold have come from the host rock, while Amukun and Turnock (1971) concluded that they were from external sources.

None of the previous work dealt with complete documentation of fracture characteristics, their spatial distribution, their age relationships, or the complex nature of vein filling. Similarly, none of the previous authors has dealt with the relationships of fracture development and veining to the development of regional structures. Consequently, the previous interpretations have tended to be somewhat simplistic. The present study attempts to address these matters.

1.5 METHODS OF THE PRESENT STUDY

The methods used for the present study involve: (1) examination of all previous records of mining operations including mine level plans, cross-sections, longitudinal sections and assay result; (2) detailed geologic documentation of members of individual fracture sets at various undergound locations; and (3) sampling, preparation, and examination of oriented polished sections and thin sections of veins, vein contacts, altered SAM unit, and sheared SAM unit.

1.6 CONCURRENT STUDIES

Three studies in the San Antonio mine area have been conducted concurrently by Poulsen et al (1984 onward), Geological Survey of Canada, with the present study: (1) a structural study of the Rice Lake greenstone belt in the vicinity of the San Antonio mine; (2) the study of the types and effects of alteration within and adjacent to the San Antonio mine unit; and (3) the determination of the composition and nature of the San Antonio mine unit.

CHAPTER TWO

GEOLOGIC SETTING OF THE SAN ANTONIO MINE

The Rice Lake gold district is confined geologically within the Rice Lake greenstone belt of the Archean Superior province (Figures 2 and 3). The greenstone belt stretches east from Lake Winnipeg to the other side of the Ontario border for a length of 130 km, and it has a maximum width of 16 km.

The rocks in the vicinity of the San Antonio mine strike east-west. They compose a sequence of volcanic and sedimentary rocks, known as the Rice Lake Group, which have been intruded by felsic and basic intrusions. Extending westward from Rice Lake and forming an angular unconformity against the Rice Lake Group is the younger San Antonio Formation, consisting of cross-bedded, arkosic quartzite.

There are four fault zones in the region, the influences of which may be reflected in the San Antonio mine area. These are shown on Figure 3. The Wanipigow fault is an east-west trending structure which forms the contact between the Wanipigow River plutonic complex to the north and the Rice Lake greenstone belt to the south. The fault is about 2.5 km north of Rice Lake. Movement on this fault has been interpreted as dextral transcurrent by McRitchie (1971) and Poulsen et al (1986). At the eastern end of Rice Lake the Rice Lake Group has been truncated and intensely deformed by the Normandy Creek shear zones. Poulsen et al (1986) have interpreted this zone as a ductile shear zone and movement on which has been sinistral and northwest side up. The third fault zone

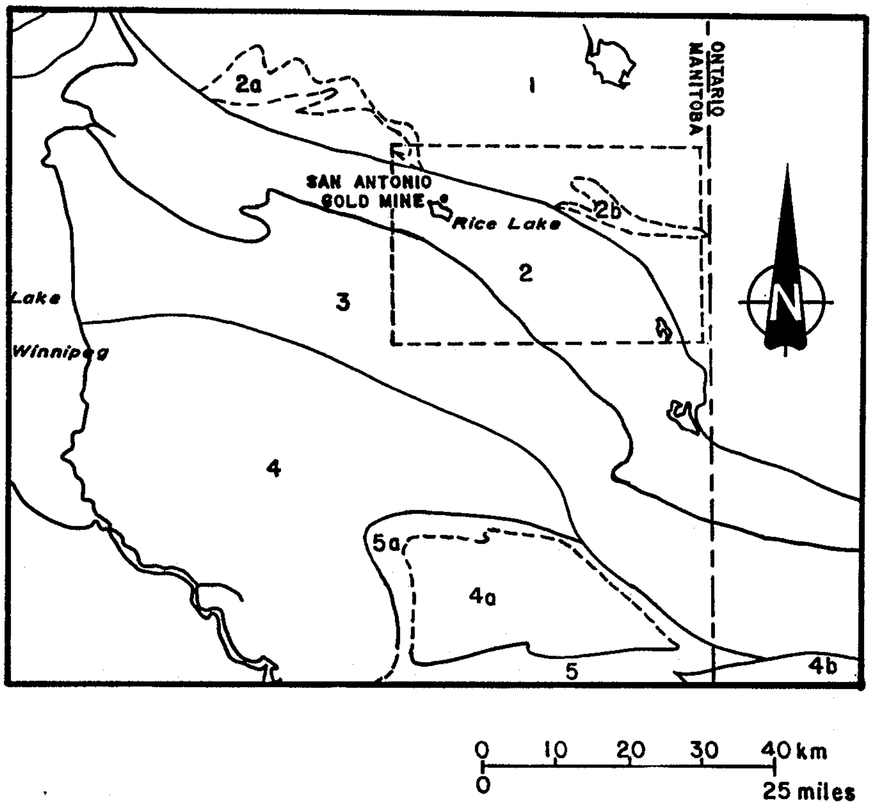

1 Wanipigow River plutonic complex

2 Rice Lake greenstone belt

a English Lake subsidiary greenstone belt

b Wallace Lake subsidiary greenstone belt

3 Manigotagan gneissic belt

4 Pine Falls plutonic complex

a Maskwa Lake pluton

b Marijane Lake pluton

5 Bird River greenstone belt

a Cat Lake subsidiary greenstone belt

Figure 2: The main geologic units in the Wanipigow Region, southeast Manitoba. Modified from McRitchie (1971). The boxed area is shown in Figure 3.

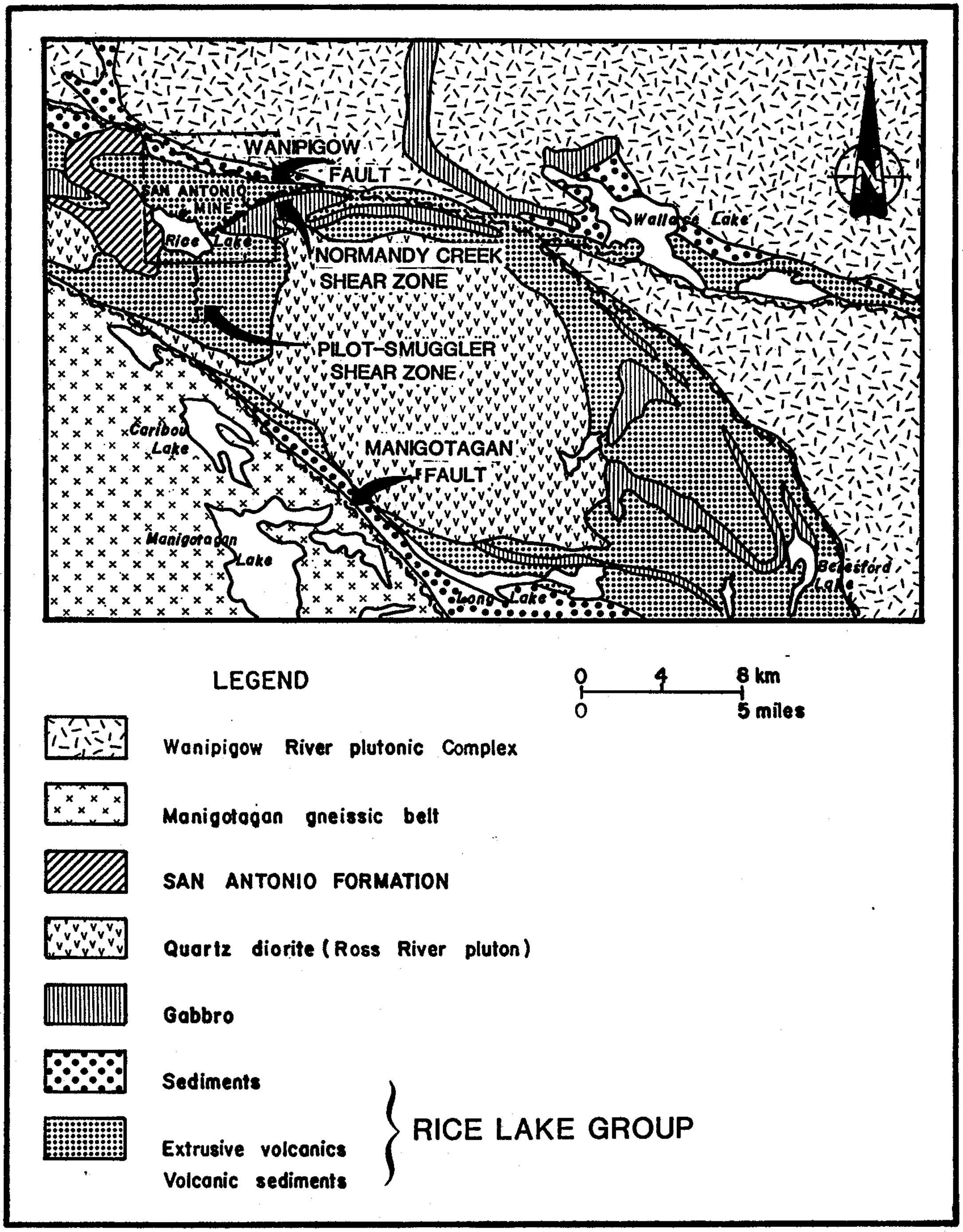

Figure 3: The regional geology of part of the Rice Lake greenstone belt. Modified from Amukun and Turnock (1971). The boxed area is shown in Figure 4.

is a northerly trending shear zone located in the southeast conrner of the Rice Lake. This zone is known as the Pilot-Smuggler shear zone; Bailes (1971) has interpreted apparent dextral strike-slip displacement on this zone. Finally, Manigotagan fault is a northwest-southeast trending structure which forms the contact between the Manigotagan gneissic belt to the south and the Rice Lake Group to the north. It is located 4 km southwest of the San Antonio mine. McRitchie (1971) has interpreted movement on this fault as dextral strike-slip.

The rocks in the Rice Lake Group in the neighbourhood of the mine have been subdivided into nine stratigraphic units (Poulsen et al, 1986) which all face and dip $40^0 - 50^0$ northward (Figure 4). The lowest stratigraphic unit of this Group is unsubdivided. Immediately overlying the lowest unit is a felsic-intermediate volcanic unit which includes a thin tabular mafic body in which the gold quartz veins occur. This body is called the San Antonio Mine (SAM) unit (Theyer, 1983). The felsic-intermediate volcanic unit is succeeded by a thin unit of basalt flow and breccia. The successive units stratigraphically above the basalt flow and breccia unit are intermediate feldspar-phyric volcanic flows, intermediate-felsic heterolithic breccias and tuff breccias, felsic tuff and tuff breccias, a quartz-feldspar porphyry unit, and finally an argillite unit.

The rocks in the Rice Lake area contain a secondary metamorphic foliation and metamorphic lineations. The foliation is penetrative and varies from continuous to spaced and is formed by the planar alignment of micaceous minerals (Poulsen et al 1986). The foliation is often discordant to bedding. Poulsen et al have interpreted the lineations as stretch lineations defined by elongation of volcanic clasts. The orientation of foliation and lineations is shown in Figure 5.

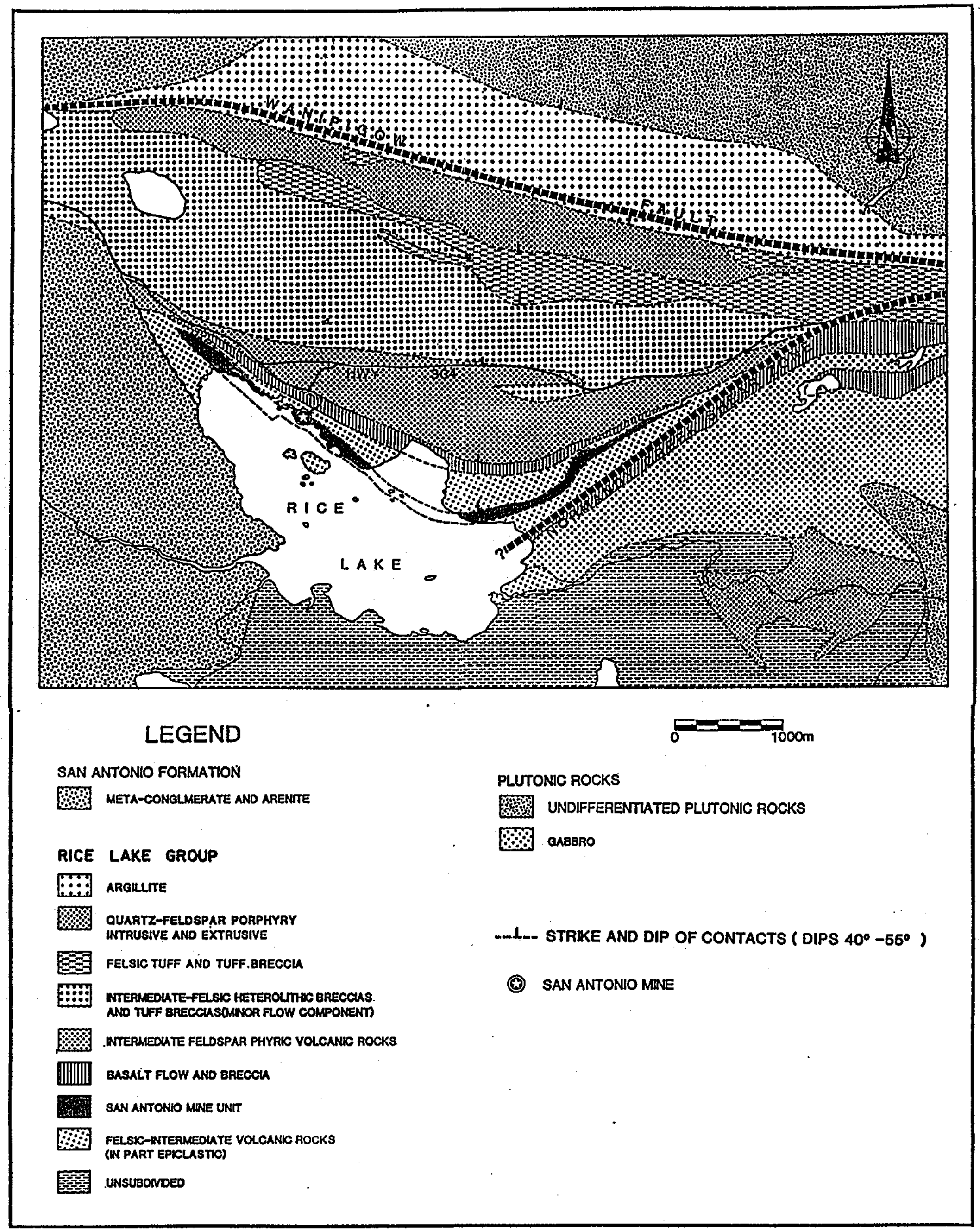

Figure 4: The general geology in the vicinity of the San Antonio Mine. Modified from Poulsen et al (1986).

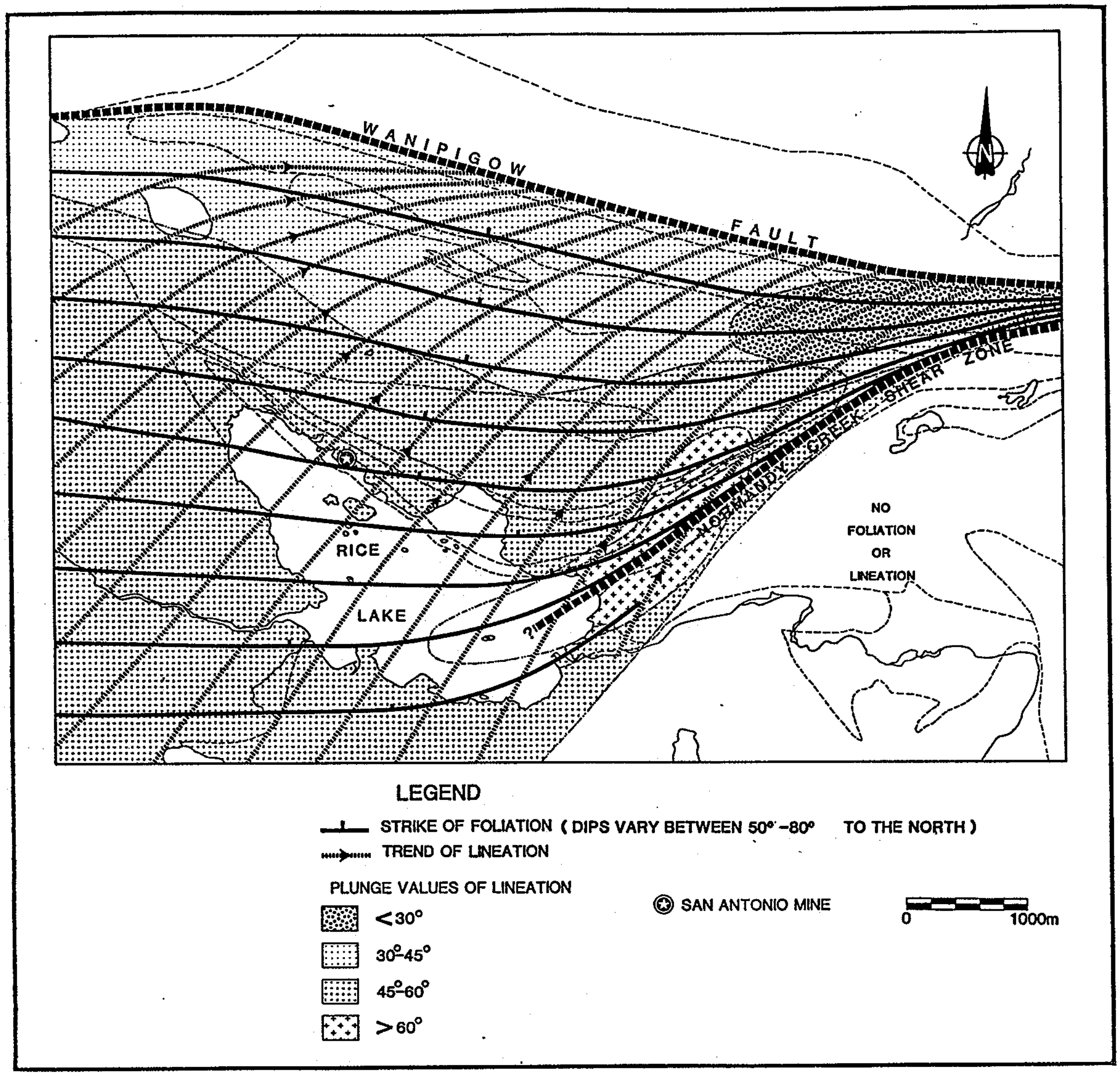

Figure 5: Structural map showing variation in foliation and stretch lineation orientations within Rice Lake Group. From Poulsen et al (1986).

CHAPTER THREE

GEOLOGY OF THE SAN ANTONIO MINE (SAM) UNIT AND HANGINGWALL AND FOOTWALL ROCK

3.1 SAN ANTONIO MINE (SAM) UNIT

The gold-quartz veins of the San Antonio mine are confined exclusively to a single tabular mafic body (SAM unit) which follows the east-west crescent-shaped outline of the enclosing Rice Lake Group (Figure 4). This unit generally has an apparent thickness of about 15 m to 90 m over a strike length of 6 km. But at the mine site the apparent thickness is from 60 m to 195 m. Figure 6 is an equal area plot of the poles to the hangingwall and footwall contacts of the SAM unit. This figure shows a strong concentration of poles reflecting the attitude of the SAM unit at the mine as $N49^0W/47^0NE$.

Traditionally, the sam unit has been viewed as a sill of metadiabase (Stockwell 1938, Gibson and Stockwell 1948), and recently interpreted as a unit of mafic volcanic flows and tuffs (Theyer 1983). Others (e.g. DeWit 1933) have simply called it a greenstone unit in contrast to the buff coloured sericite schist which occur stratigraphically above and below.

The latest work on the SAM unit has been conducted by Poulsen et al (1986). Their geochemical and textural data indicate that the unit has an igneous texture, a tholeiitic composition, and is geochemically related to the overlying basalt flows. They interpreted the SAM unit as a synvolcanic, layered metagabbro sill (Poulsen et al 1986). The results of this recent work are compelling and the interpretation presented by Poulsen et al (1986) is accepted for this thesis.

The SAM unit was subjected to metamorphic conditions which developed a regional foliation and stretch lineation in the rest of the Rice Lake Group.

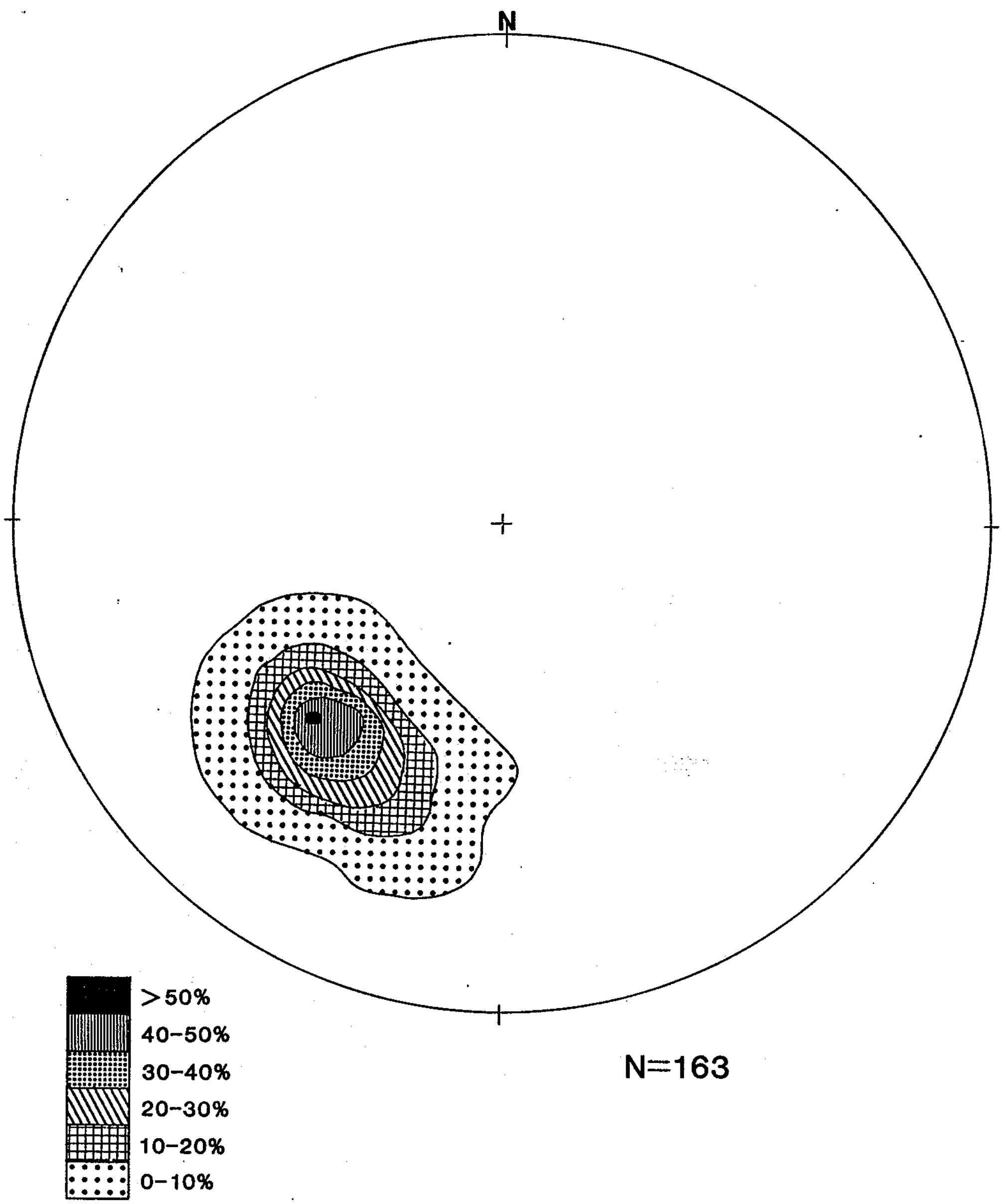

Figure 6: Equal area contour plot of the poles to the hangingwall and footwall contacts of the SAM unit. Twenty five direct measurements underground. One hundred and thirty eight contact measurements were taken from the mine level plans using pairs of successive levels.

However the SAM unit still retains its primary interlocking crystalline texture and has no visible imposed penetrative foliation or lineation. This evidence indicates that the SAM unit was considerably more competent than the surrounding schist. Although the effects of low grade regional metamorphism are not shown by the development of a foliation in the SAM unit, there are other manifestations of this metamorphism in the form of metamorphic assemblages that include variable amounts of Mg-chlorite, actinolite (after pyroxene), albite, epidote (after plagioclase) and sphene (after Fe-Ti oxides).

In addition to the metamorphic effect, there is also evidence of subsequent broad scale progressive alteration in which the actinolite, epidote and sphene assemblage has been partly carbonatized to form chlorite, calcite, rutile and ankerite.

3.2 FOOTWALL AND HANGINGWALL ROCKS

The rocks stratigraphically below and above the SAM unit are felsic and intermediate volcaniclastic and chlorite schists. Immediately adjacent to the SAM unit they have been altered to buff coloured sericite schist (Figure 7). On the footwall side of the SAM unit the sericite schist ranges from 40 m to 120 m thick while on the hangingwall it ranges less than one metre to 20 m.

The schistosity in these schists ($N55^0 - 70^0W/55^0 - 65^0NE$) is generally oblique to the bedding direction ($N49^0W/47^0NE$), but the schistosity increases in intensity and changes in orientation as the contacts of the SAM unit are approached. At the contacts the schistosity in the footwall and hangingwall rocks is parallel to the SAM unit and is so intense that it appears as a shear zone. Folded schistosity occurs commonly in these contact zones (Figure 8).

A

B

Figure 7: Sharp contacts of the SAM unit with the surrounding sericite schist. (A) The contact between the footwall sericite schist (brown) and the SAM unit (dark green) looking northwest. (B) The hangingwall contact of the SAM unit looking southeast. The rule is 15 cm.

Figure 8: Folded schistosity in the hangingwall sericite schist on level 16. The rule is 15 cm.

The intensification of schistosity at the contacts with the SAM unit may be in response to the change in competency across the contact. Alternatively, the explanation may be geochemical control related to alteration.

3.3 ALTERATION

The alteration noted in the SAM unit and in the footwall and hangingwall schist has been studied by Poulsen et al (1986). These authors have interpreted the alteration as hydrothermal carbonatization. Figure 9 shows the distribution of the carbonate mineralogy across the sericite schist and the SAM unit on the 16th level of the mine. The volcaniclastic and chlorite schist rocks (precursors of sericite schists) well away from the footwall contact of the SAM unit are not visibly altered and contain relatively low abundance of carbonate minerals. The transition from volcaniclastic rock to sericite schist is marked by the increased abundance of carbonate minerals and the disappearance of chlorite in the buff coloured sericite schist. Sericitization that occurred in the sericite schist does not involve influx of K_2O, but rather a breakdown of alkali feldspar during carbonatization. Within the SAM unit the abundance of carbonate minerals increases substantially and they are predominantly dolomite and ankerite species. The abundance of the carbonate minerals in the hangingwall sericite schist also decreases away from the contact of the SAM unit.

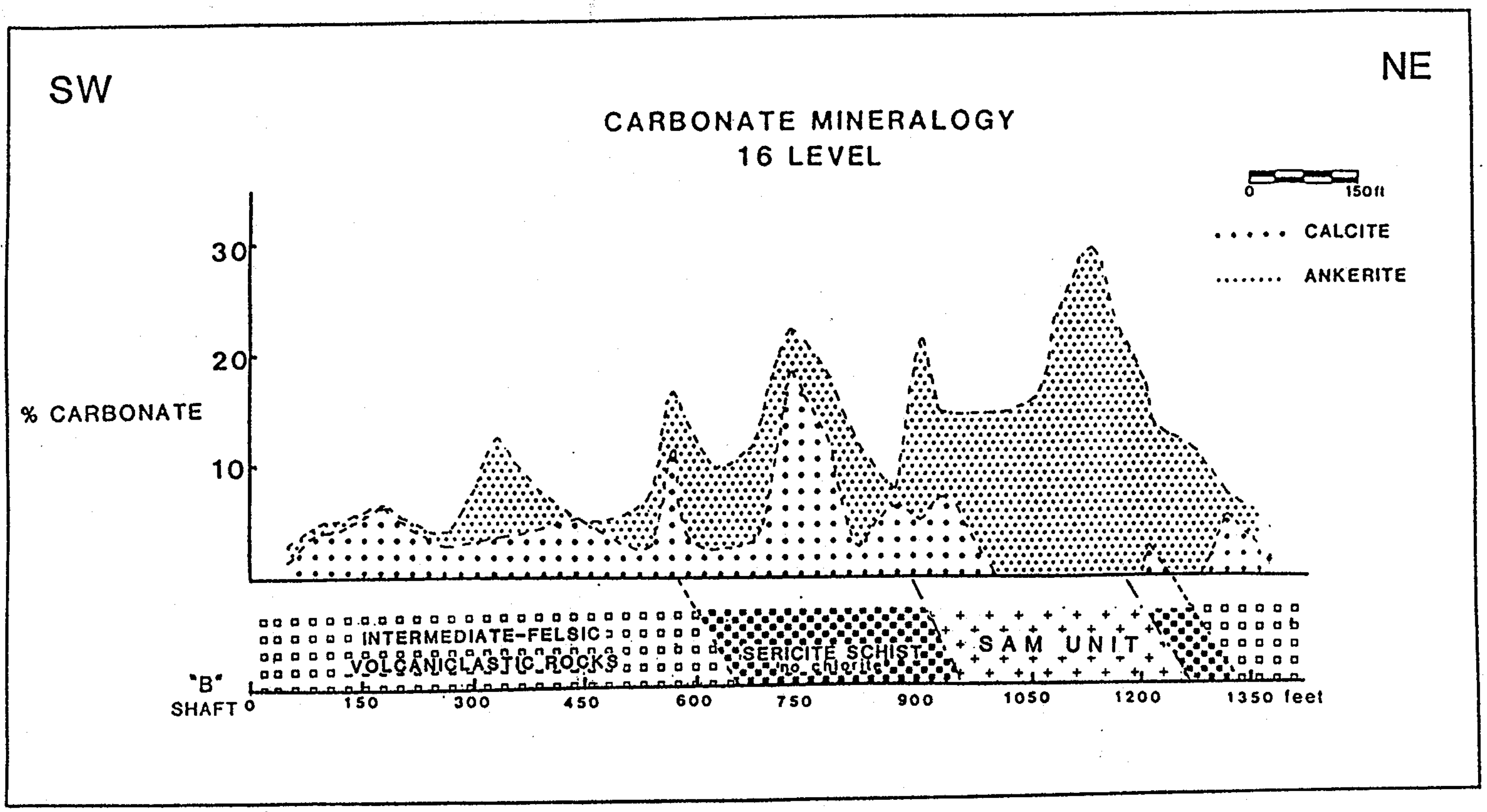

Figure 9: Variations in carbonate mineralogy along a profile through the San Antonio mine along crosscuts on level 16. Note that the total abundance of the carbonate minerals is greatest in a zone adjacent to and nearby the SAM unit. Calcite and chlorite do not coexist in the sericite schist. (From Poulsen et al, 1986).

CHAPTER FOUR

MAJOR FRACTURE SETS WITHIN THE SAM UNIT

Six distinct sets of fractures have developed within the SAM unit. These include: (1) a family of NE-striking, NW-dipping fractures now filled by dikes mostly of quartz porphyry or feldspar porphyry. These dikes are not mineralized. (2) Complex fracture stockworks which contain mineralized quartz veins, (3) shear zones (16-type) which strike NE and dip steeply NW which contain mineralized veins, (4) shear zones which strike NE and dip SE which contain vein material and may be mineralized, (5) fractures which strike NW and dip SW which contain veins and may be mineralized, and (6) a fracture which strikes E-W and dips gently north and which does not contain quartz vein material. The first five of these fracture sets are depicted diagramatically in Figure 10 which is a composite diagram of a portion of the San Antonio mine unit. The diagram shows the geometric relationships between the SAM unit and the fractures as they exist, and the cross-cutting relationships as they have been observed. The displacements shown on the fractures in Figure 10 are apparent and are based on offsets observed in mine plans and cross-sections.

The next four chapters present the description of each of these sets of fractures and the materials that fill them.

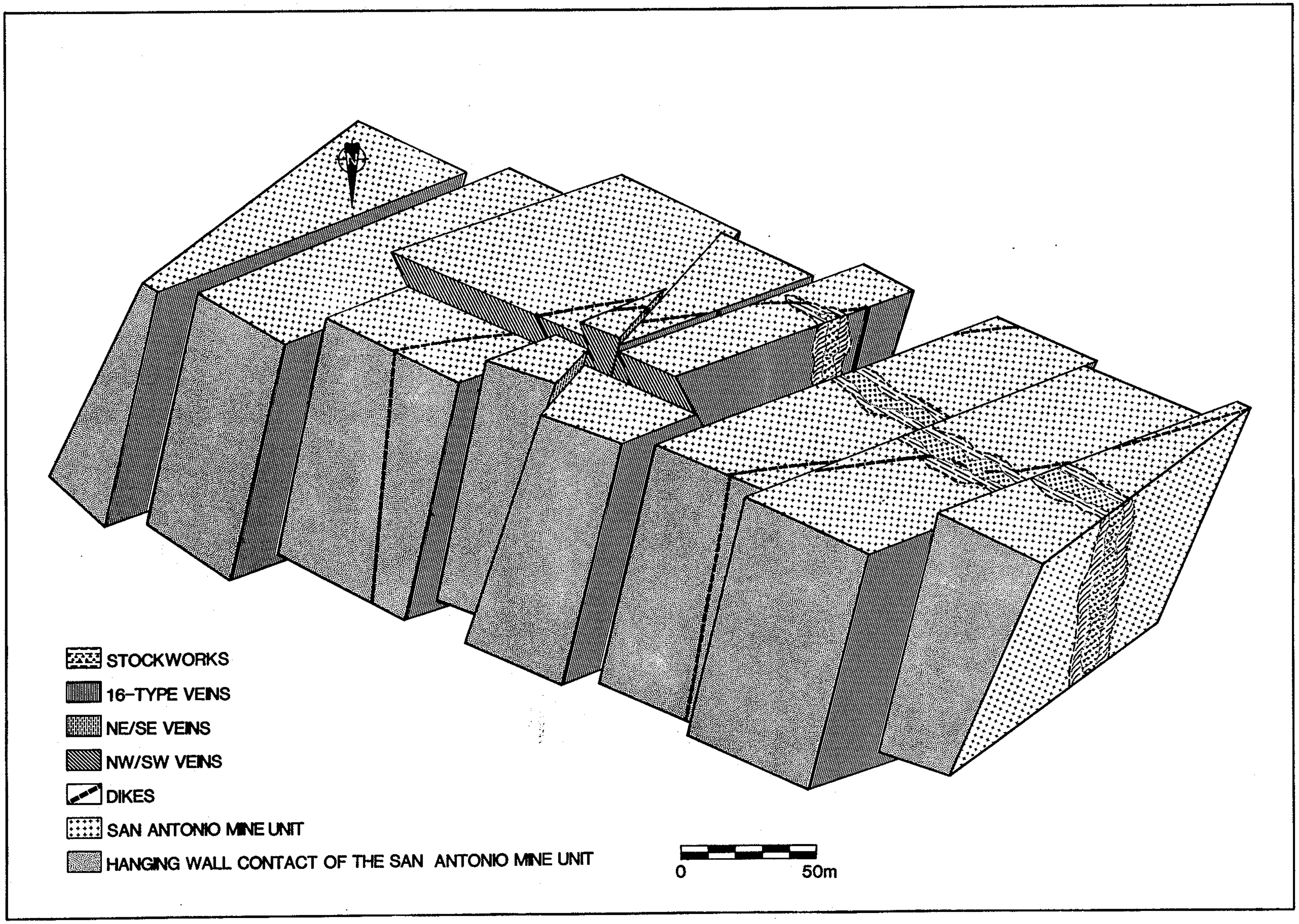

Figure 10: Composite block diagram showing segmentation of the San unit by five fracture sets, now filled by dike and vein materials. Displacements shown on the diagram are apparent only. The diagram is viewed from the north.

CHAPTER FIVE

THE DIKES

5.1 PROPERTIES OF THE DIKES

A set of dikes mostly of quartz or feldspar porphyry filling the early fractures have cut across the SAM unit and the enveloping sericite schist. These dikes range from a few centimetres to 10 m thick and they have length/thickness ratios of greater than 40. The orientation of these dikes is shown in Figure 11 which is an equal area plot of poles to the dikes within the SAM unit. It does not contain dike measurements from outside the SAM unit. Twenty-two data points represent measurements by the author in the mine, the other 180 points were attitudes taken from the mine level plans. The plot shows strong pole concentration at $N88^0E/66^0NW$. Although there is a slight girdle showing in the plot, the strong concentration suggests that the dikes have not been reoriented to a significant degree. Most of these dikes continue into the Rice Lake Group but there is insufficient data to tell whether or not the attitude of these dikes changes as they leave the SAM unit.

The contacts between the dikes and the SAM unit are sharp. The adjacent wall rocks in the SAM unit show no sign of mechanical deformation related to the fractures in which the dikes were emplaced. Some of the dikes terminate within the SAM unit and where this occurs the dikes become progressively thinner and have tapered terminations.

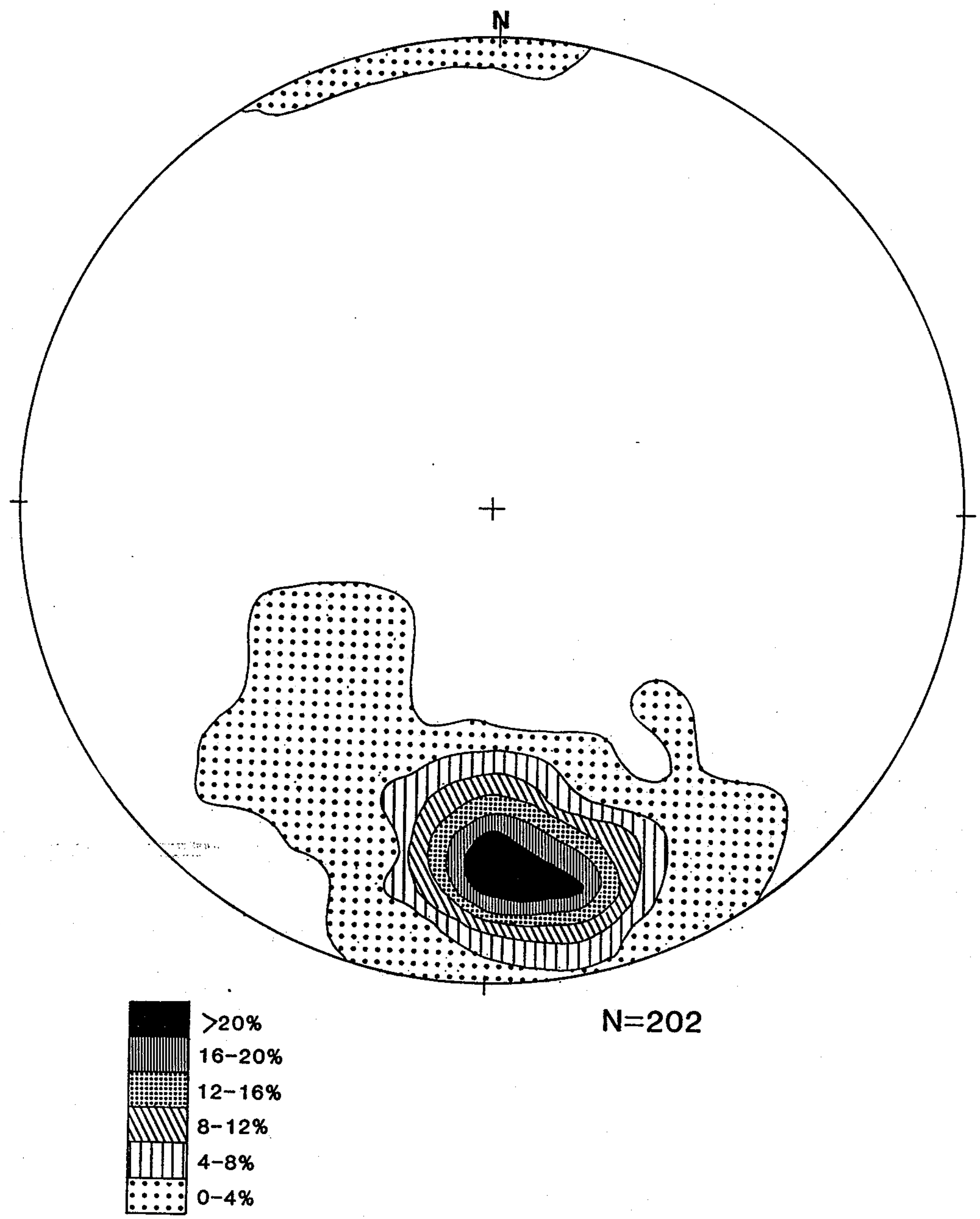

Figure 11: Equal area contour plot of the poles to the early set of dikes. Twenty-two data points represent measurements by the author in the mine. The other 180 data points were taken from the mine level plans.

Most of these dikes have been affected by subsequent deformation and alteration which has caused many of them to resemble the sericite schist that envelope the SAM unit, and thus have often been mistaken for it in the drill cores.

5.2 INTERPRETATION OF DIKE EMPLACEMENT

The early set of dikes which cross-cut the SAM unit have large length-thickness ratios and tapered terminations, and the wall rocks adjacent to them are mechanically undeformed. These properties, according to Pollard (1973), indicate that the dikes were intruded into a homogenous brittle unit by splitting the host rock along extension fractures created by hydraulic "wedging action" of the magma. Such an origin implies that the fracture generation and dike emplacement were coeval.

If the dikes were intruded into homogenous SAM unit by hydraulic fracturing, then the ambient minimum principal stress (σ_3) in the SAM unit at the time of dike emplacement should be as shown in Figure 12. The maximum (σ_1) and intermediate (σ_2) principal stresses could have any orthogonal orientations in the plane of the dikes.

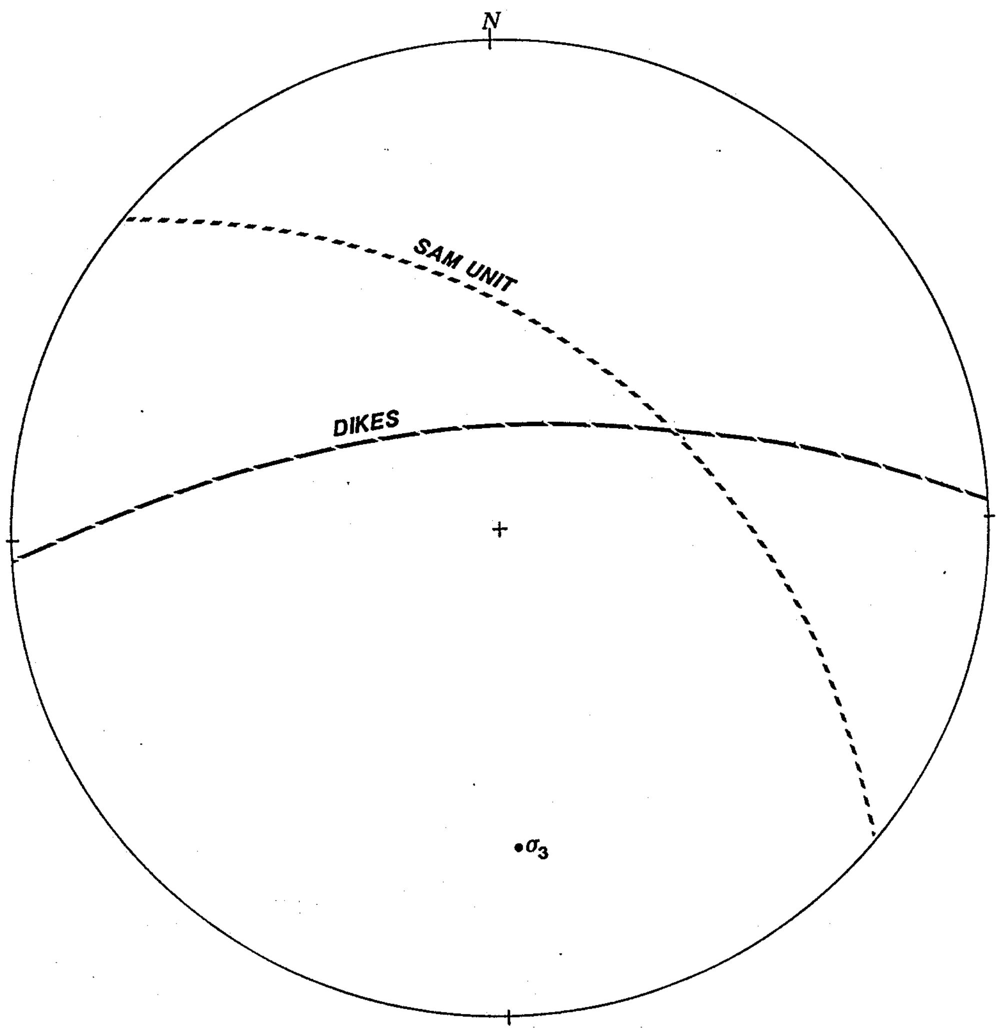

Figure 12: Interpretation of the direction of the ambient minimum principal stress in the SAM unit at time of dike emplacement. ($\sigma_3 = 24^0/S2^0E$). σ_1 and σ_2 can have any orthogonal orientations in the plane of the dikes.

CHAPTER SIX

THE STOCKWORKS

6.1 INTRODUCTION

The set of fractures within the SAM unit which next postdates the development of the dikes is the stockworks. The stockworks cross-cut the dikes and have been intersected and displaced by the four younger sets of fractures. The stockworks have been referred to in previous publications and in the mine records as the 38-type veins. There are at least thirty stockworks of variable size in the San Antonio mine.

6.2 SHAPE, ORIENTATION, SIZE AND CONTINUITY OF THE STOCKWORKS

Stockworks in the San Antonio mine are tabular zones made up of closely spaced veins and altered brecciated SAM unit. The contacts between the stockworks and the SAM unit are gradational. The orientation of each tabular stockwork is similar and the average orientation of all the stockworks within the SAM unit is $N40^0W/78^0NE$ (see sections on central breccia zones and central veins below). Because they strike about 10^0 more northerly and dip more steeply than the SAM unit ($N49^0W/47^0NE$) the stockworks have a long dimension that pitches 19^0NW in the plane of the SAM unit. The long dimension of the stockworks varies from a few metres to about 500 m. The stockworks pinch and swell along their plunge (long dimension) and their thickness varies from one metre to about 10 m. Most stockworks have plunge length/thickness ratios greater than 20.

The stockworks are confined exclusively within the SAM unit. Up dip they pinch out near the hangingwall contact of the SAM unit. Down dip they pinch out at least 20 m from the footwall contact of the SAM unit. Two or three parallel stockworks may occur on the same group of levels within the SAM unit. In such cases the perpendicular distance between the stockworks ranges from 5 m to 20 m.

6.3 INTERNAL COMPONENTS OF STOCKWORKS

Observations at various locations in the mine indicate that every stockwork is made up of two zones: a marginal zone and a central breccia zone. The marginal zone consists of en echelon moderately dipping ladder-veins that gradually pinch out into the SAM unit. The number of ladder-veins increases toward the centres of the stockworks. As the number of ladder-veins increases the wall rocks are increasingly fractured to the point where the fragments are completely separated from each other by vein material, displaced and rotated to form the central breccia cores of stockworks. Figure 13 is a composite diagram of a stockwork which comprises a central breccia zone surrounded by closely spaced ladder-veins in the marginal zone. The thicknesses of the marginal zones and the central breccia zones vary from a couple of metres to about 5 m. Large stockworks, where most of the ores are derived, are made up mostly of central breccia zones. Small stockworks, on the other hand, are made up mostly of ladder-veins (Figure 14).

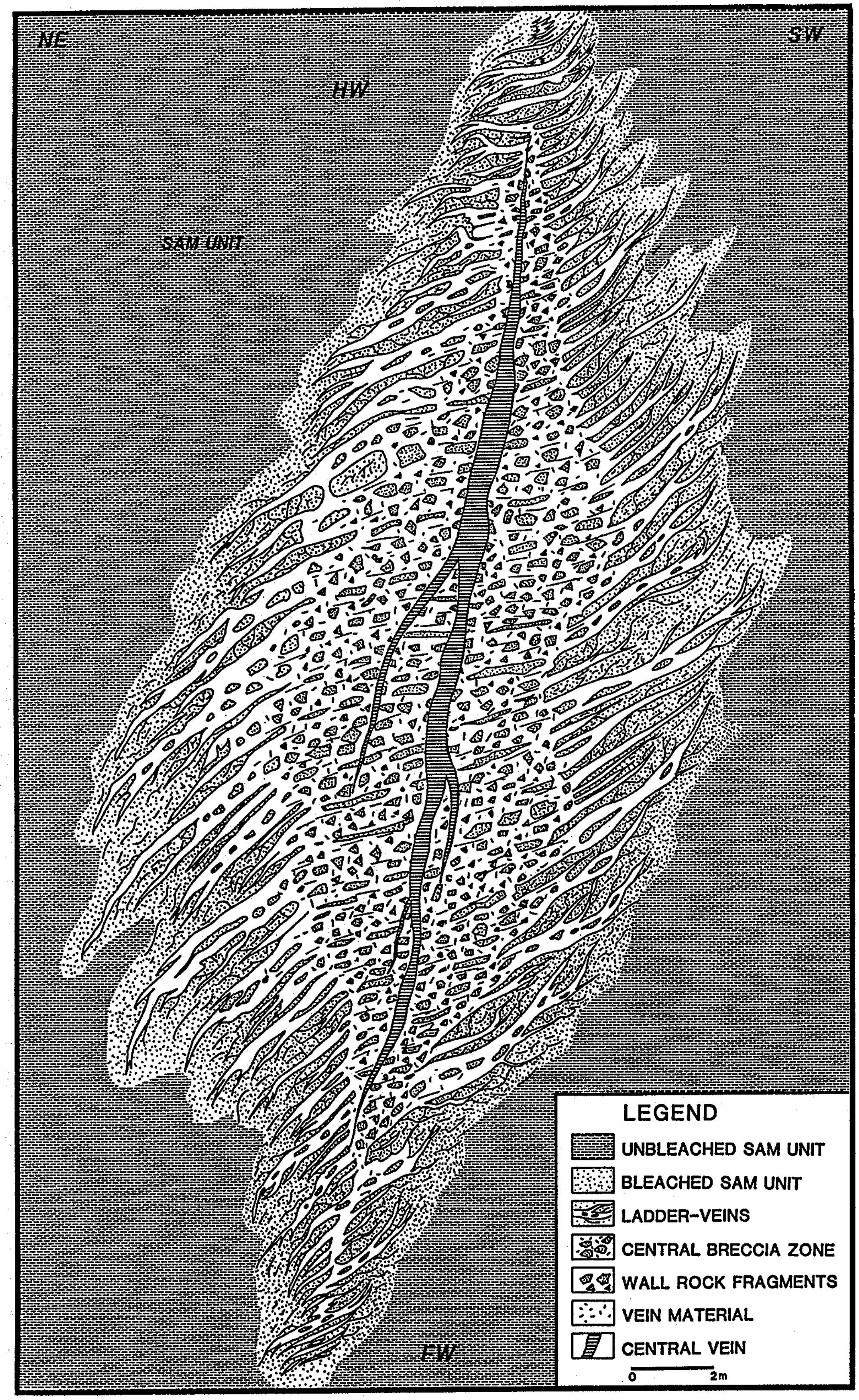

Figure 13: A schematic composite representation showing the marginal and central breccia zones of a stockwork. The diagram is a cross section view of a stockwork, looking southeast.

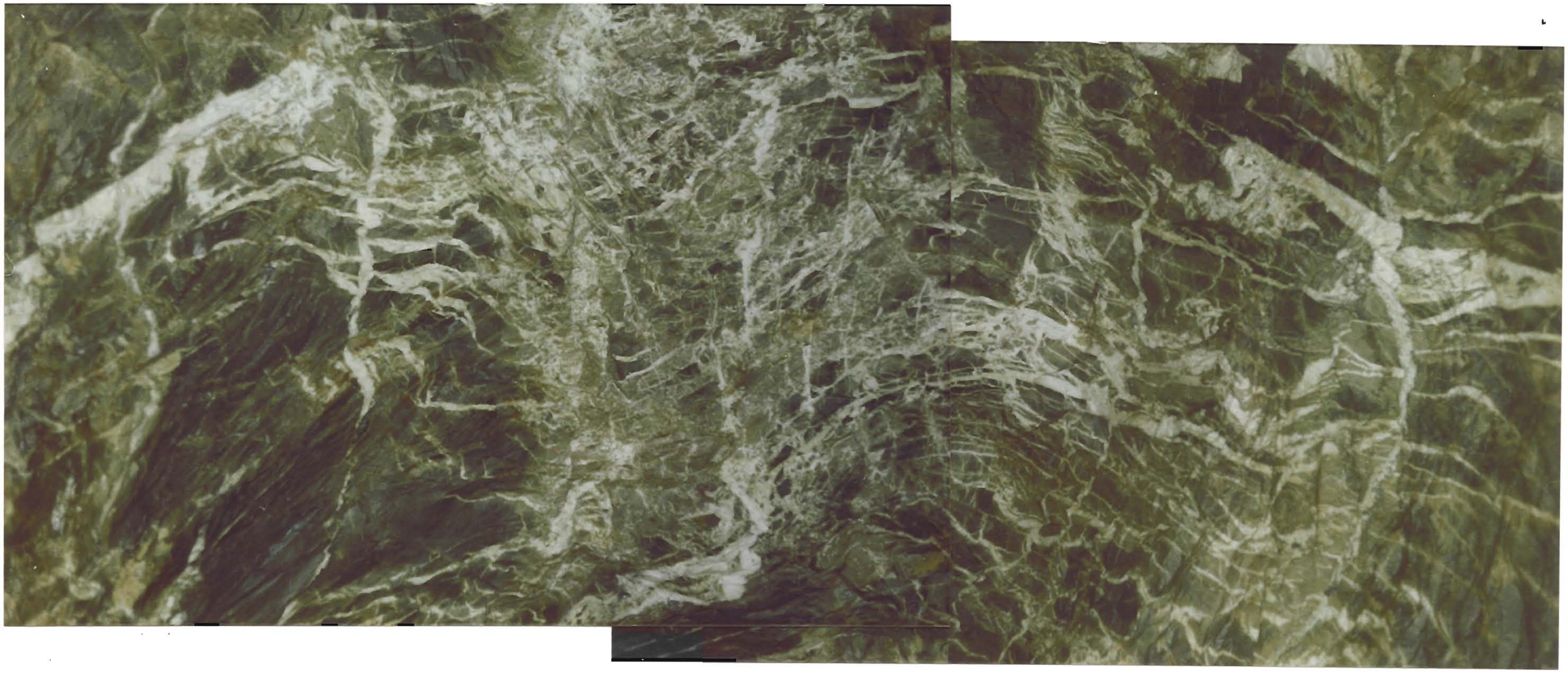

Figure 14: Longitudinal section of a stockwork looking southeast. The stockwork dips steeply towards the viewer. The figure shows a partially developed central breccia zone surrounded by ladder-veins which dip towards the viewer. The wall rocks within the central breccia zone and surrounding the ladder-veins are altered and bleached. Field of view is 7.5 m.

6.3.1 The Marginal Zones

The outer limits of the marginal zones are marked by the disappearance of the ladder-veins. The SAM unit beyond the marginal zones usually shows one to two metres of altered and bleached host rock. The inner limits of the marginal zones are where there are abundant ladder-vein linked to one another by a large number of veinlets branching out at high angles and where the intervening SAM unit shows no major displacement or rotation. The width of the marginal zones varies from one or two metres to about 5 m. The ladder-veins comprise less than 50% of the volume in these zones.

The ladder-veins in the marginal zones are en-echelon moderate dipping vein-filled fractures. They are confined exclusively to, but oriented differently from the tabular stockworks crossing the SAM unit. No single ladder-vein ever continues for the full length of the stockwork. They terminate by pinching out in the SAM unit. Their strike and down dip lengths may vary from a few metres to 10 m. The thickness of veins in these fractures varies from a few millimetres to 40 cm (Figures 15, 16 and 17); they have length/thickness ratios greater than 50. The ladder-veins commonly split and merge along their strike and down dip. They wedge out away from the centres of the stockworks. Many ladder-veins contain small angular or long thin wall rock fragments (Figures 16, 17, 18, and 19). The brecciated wall rocks surrounding the ladder-veins in the marginal zones may be separated from one another by vein material but they show no major displacement or rotation.

Figure 20 is an equal area plot of poles to the ladder-veins within all stockworks. Thirty-five data points represent measurements by the author in the mine, the other 647 points are attitudes of ladder-veins taken from the mine level plans.

Figure 15: Vertical mining face showing ladder-veins in the marginal zone of a stockwork. The ladder-veins have been cut by a set of vertical veinlets. The lense cap on the right for scale.

Figure 16: Vertical mining face showing ladder-veins of variable thickness in the marginal zone of a stockwork. They dip moderately towards the viewer. The ladder-veins show internal compositional zonation. Some thin fragments of wall rock are included in the veins. Field of view equals 1.5 m.

Figure 17: Cross section of a subhorizontal northeasterly dipping ladder-vein looking northwest. The ladder-vein is about 40 cm thick and it includes some wall rock fragments. The ladder-vein has been cut across by a set of vertical veinlets which may/may not contain chlorite (dark green) in addition to quartz, carbonate and albite. Most of the vertical veinlets have lenticular shape. Note that the ladder-vein has been offset with the northwest side up by some vertical veinlets. Field of view equals 1.1 m.

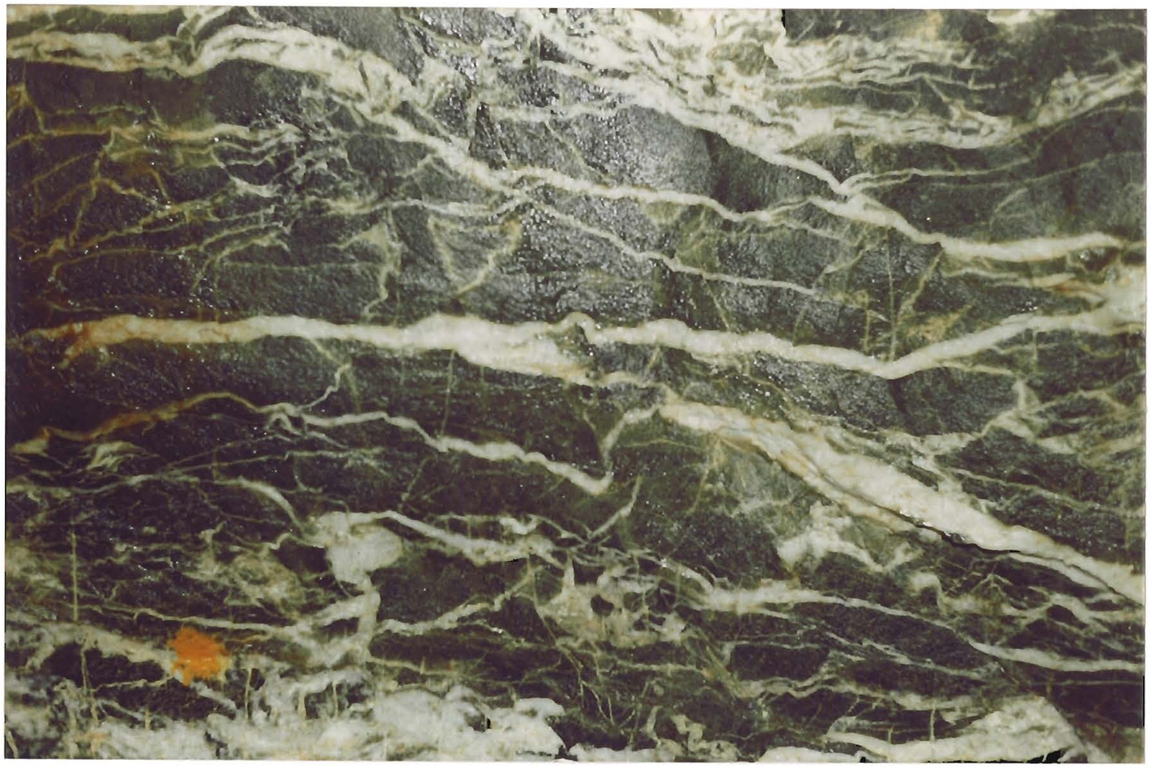

Figure 18: Vertical mining face showing a longitudinal section of ladder-veins in a marginal zone of a stockwork. The ladder-veins are dipping toward the viewer. The figure shows how the ladder-veins split and merge along their strike. Field of view equals 1.5 m.

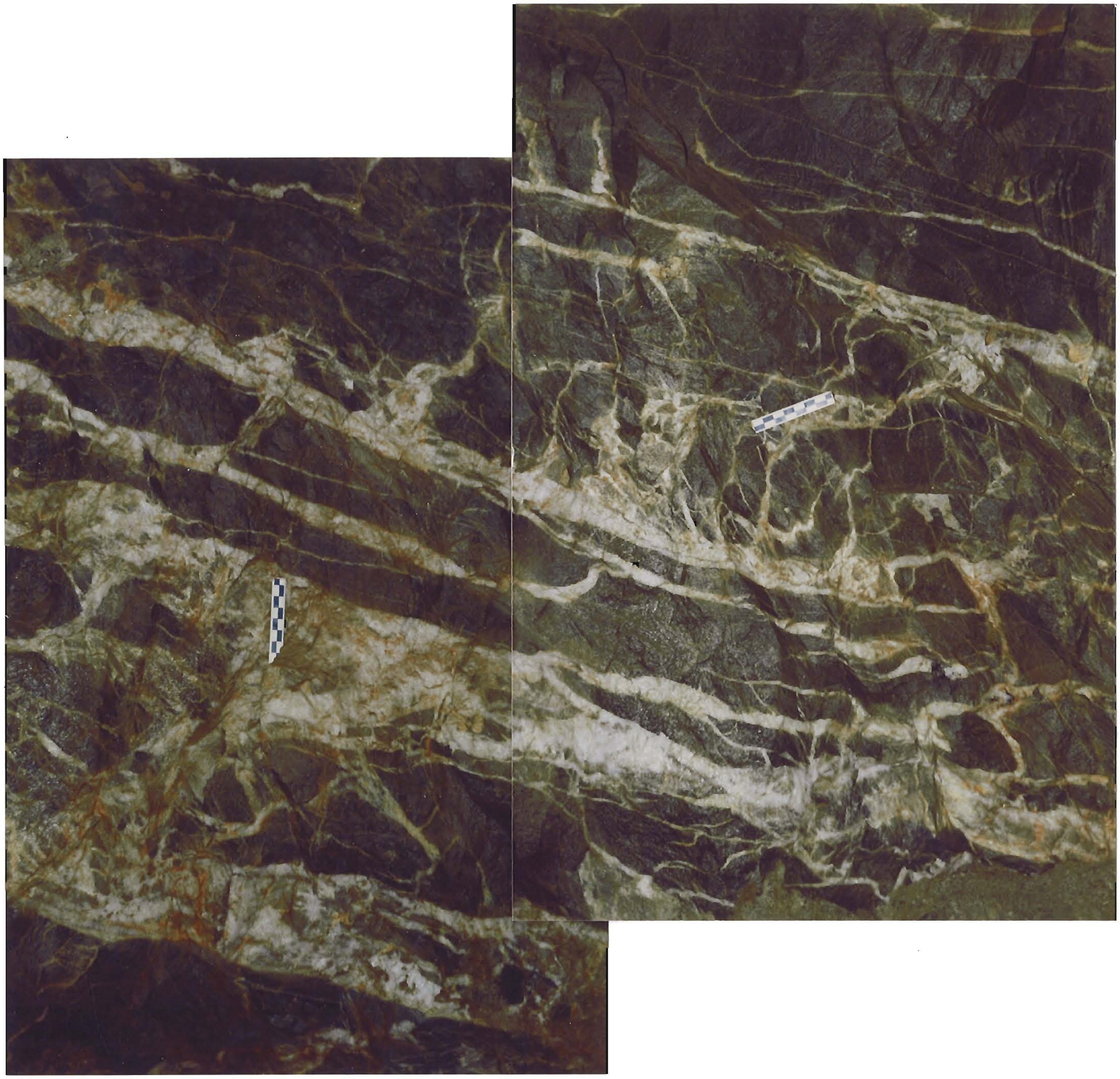

Figure 19: Cross section of ladder-veins in a marginal zone of a stockwork. View northwest. The figure shows how the ladder-veins and branching veinlets isolate blocks of wall rock. Further veining and movement lead to central breccia zone. The rule is 15 cm.

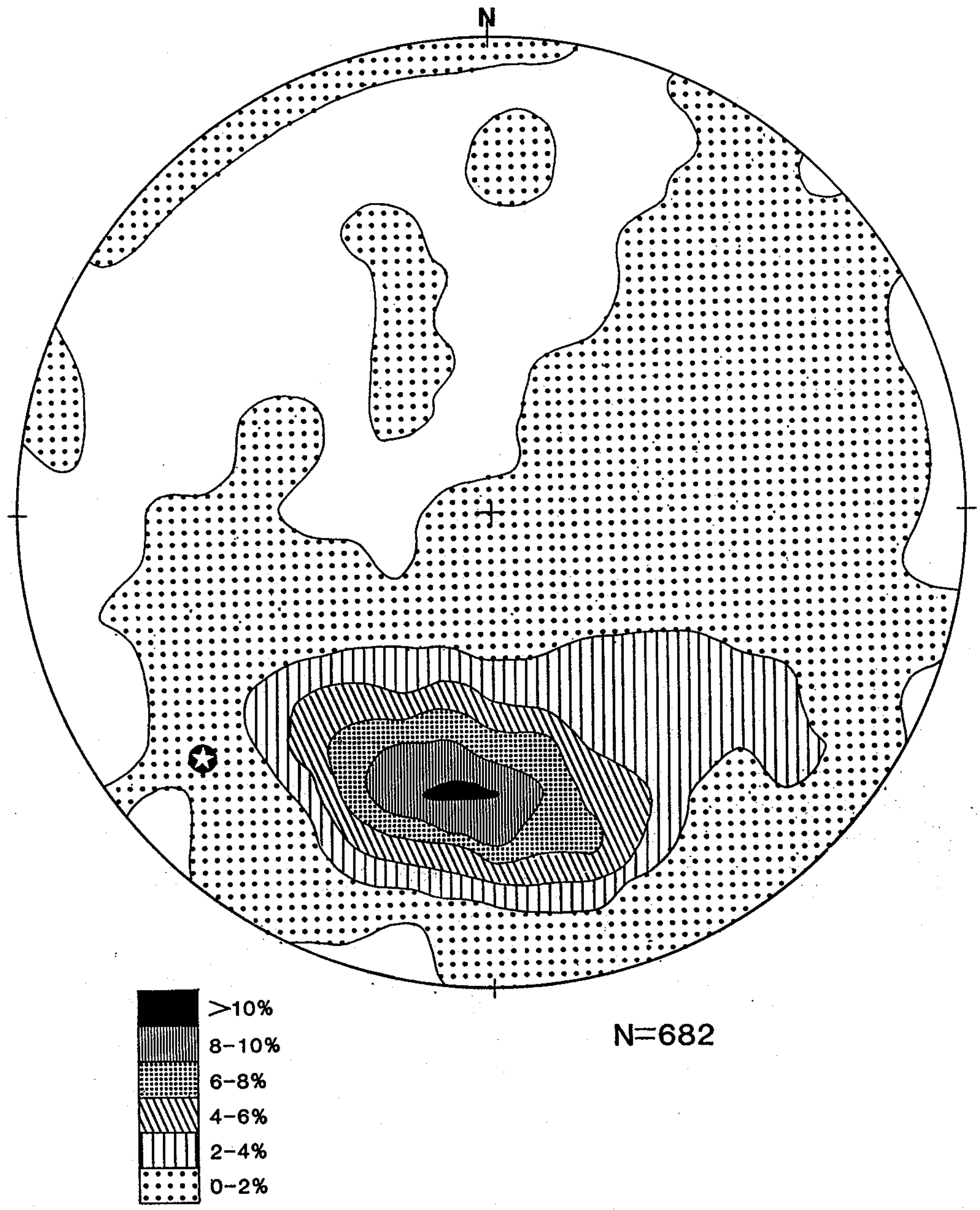

Figure 20: Equal area contour plot of the poles to the ladder-veins within all stockworks. Thirty-five data points represent measurements by the author in the mine. The other 647 data points were taken from the mine level plans. The star represents the mean pole to the plane of the overall stockworks, for comparison.

The greatest concentration of the poles represents an attitude of $N82^0W/50^0NE$. The stereoplot indicates a strong maximum but it also indicates a considerable variation in orientation. Furthermore, Figure 20 indicates that the ladder-veins have a different attitude than that of the tabular stockworks. The attitude of the tabular stockworks taken from section (5.3.2) is also presented in Figure 20 for comparison.

The ladder-veins in the marginal zones in a number of stockworks observed by the author show sigmoidal deformation on either side of the stockworks (Figure 21). Figure 22 is a schematic diagram showing the characteristics of the sigmoidal deformation in the ladder-veins. The veins turn up to steeper dips on the south side of the stockwork and turn down to steeper dips on the north side of the stockwork. The dilational character of the central parts of the ladder-veins coupled with this sigmoidal asymmetry suggest an origin similar to that proposed by Rickard and Rixon (1983) for quartz veins in rotated tension gashes. Such an origin would imply that the relative movement across the stockworks was north side up. The broad distribution of the poles to the ladder-veins shown in Figure 20 could conceivably be related to the sigmoidal shape of the ladder-veins caused by such movements across the stockworks.

The ladder-veins are composed of quartz plus minor amounts of carbonate, albite and pyrite. They are gold bearing. The ladder-veins commonly are internally zoned as shown schematically in Figure 23. They have quartz-carbonate-albite (qtz-cb-alb) fringe near the vein wall and a central core dominantly made up of quartz with few scattered carbonate patches. The qtz-cb-alb fringe near the vein wall may range from a few millimetres to about one centimetre thick (Figure 24) while the central quartz core may range from a few millimetres to about 40 cm thick. The networks of veinlets branching out at high angles from the

Figure 21: The photographs shows sigmoidal shape ladder-veins in a small stockwork. Photograph courtesy of K. H. Poulsen.

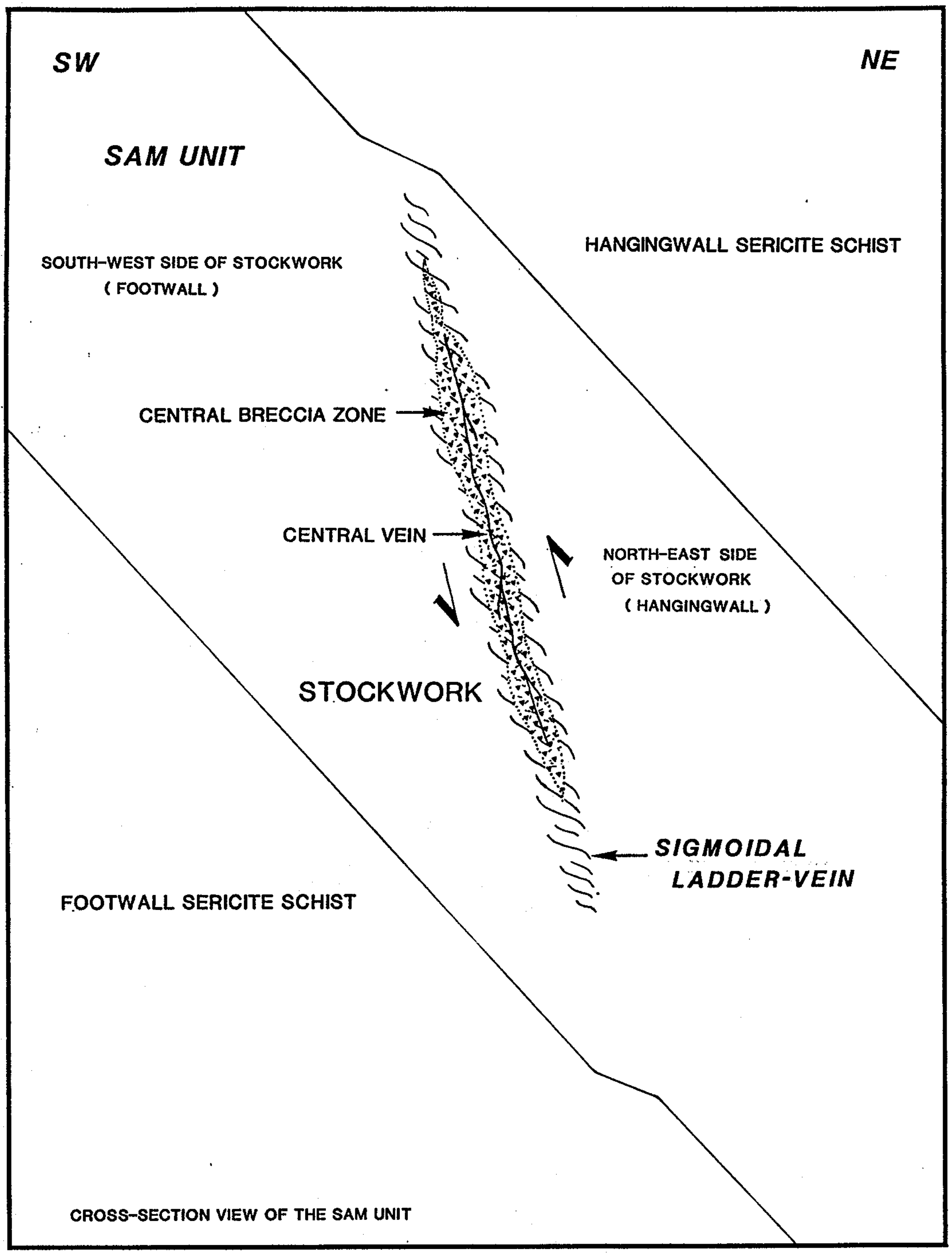

Figure 22: Schematic cross section of the SAM unit showing a stockwork and asymmetry of ladder-veins with sigmoidal change in orientation towards vein tips. Arrows represent interpretation of the couple producing the change in orientation.

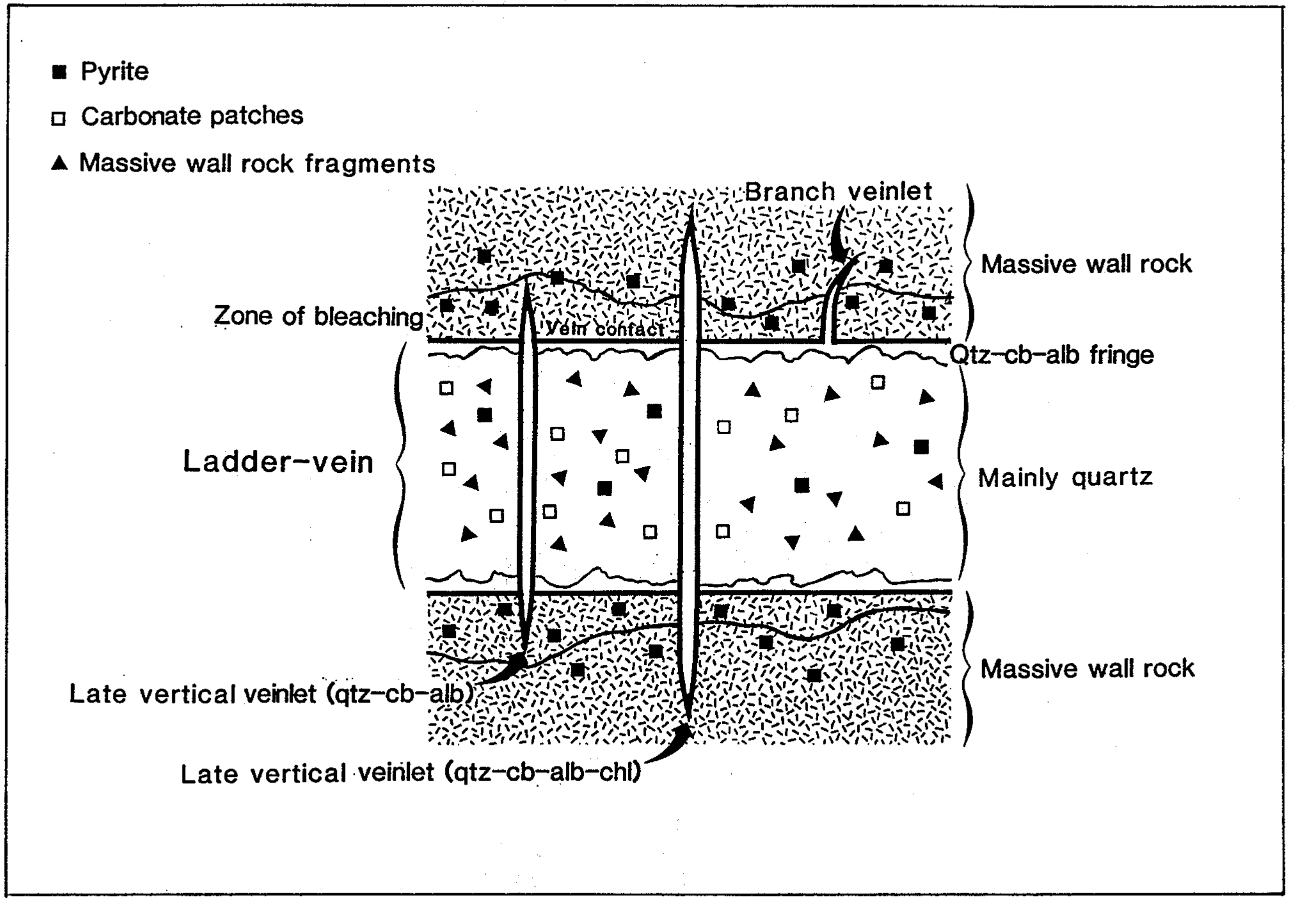

Figure 23: Compositional zonation of a ladder-veins (schematic).

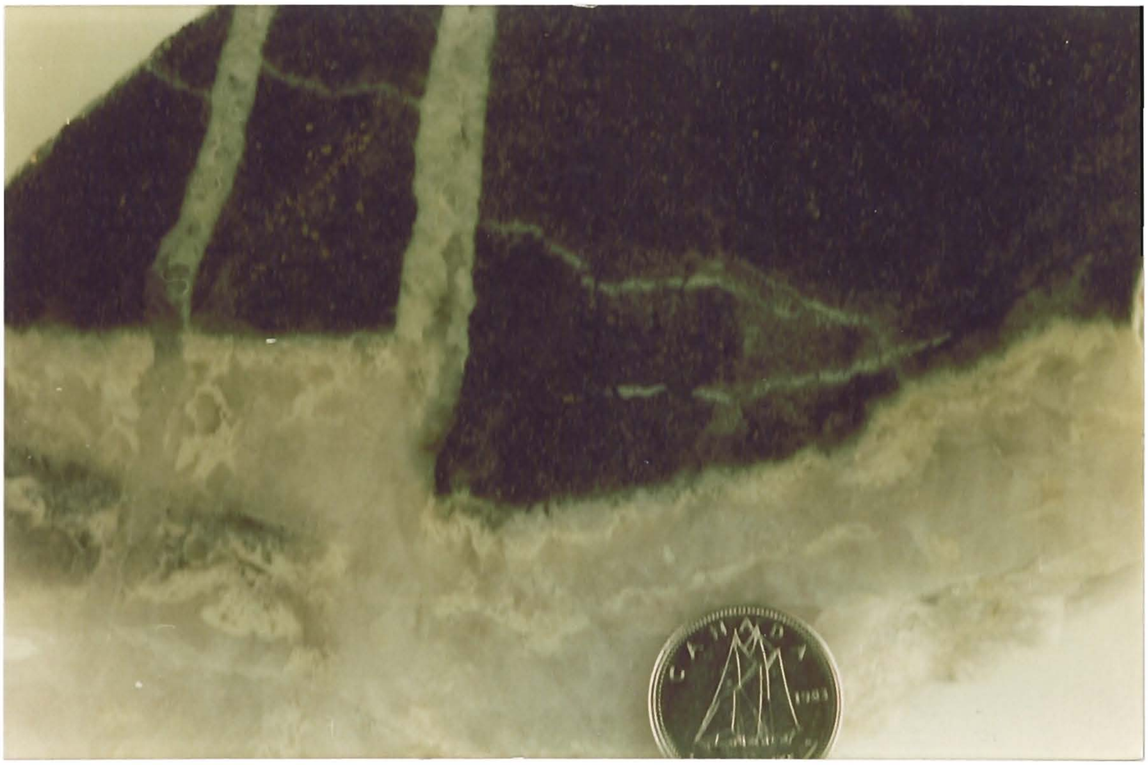

Figure 24: A ladder-veins SAM unit contact cut by vertical veinlets. Both ladder-vein and vertical veinlets show compositional zoning.

ladder-veins have similar compositional zonation. This compositional zonation is interpreted as the result of diffusion of the wall rock constituents into the fractures and crystallization of these constitutents near the vein contacts. Support for this interpretation comes from the fact that the adjacent altered wall rocks contain abundant minerals that make up the outer fringes of these veins.

The wall rocks in the marginal zones and adjacent to the ladder-veins are texturally massive, highly altered and highly bleached to light grey (Figure 25), as compared to normal dark green host rock, because they lack chlorite and are enriched in albite and carbonate. The wall rocks generally are composed mostly of albite, quartz, sericite, carbonate and some disseminated pyrite.

The ladder-veins and the wall rocks in the marginal zones are cut across by a set of distinctly later vertical veinlets (see section 6.3.4 where vertical veinlets are discussed).

6.3.2 The central breccia zones

The central breccia zones are made up of angular wall rock fragments which have been separated from one another, dislocated and rotated by vein materials. The central breccia zones generally contain 50% angular wall rock fragments and 50% vein material (Figure 26). They are roughly tabular in shape. The long dimension of the central breccia zones may range from a few metres (in small stockworks) to about 500 m (in large stockworks). They pinch and swell along their long dimension. Their average thickness is about 3 m, though they may swell from less than a metre to about 10 m. The central breccia zones of most stockworks in the San Antonio mine have plunge length/thickness ratios of greater than 20. The attitude of each individual stockwork is determined by the elongated nature of the central breccia zones.

Figure 25: Stockwork wall rock, showing gradational change caused by depletion of chlorite. Dark green portion is chlorite rich, light grey portion is chlorite poor.

A

B

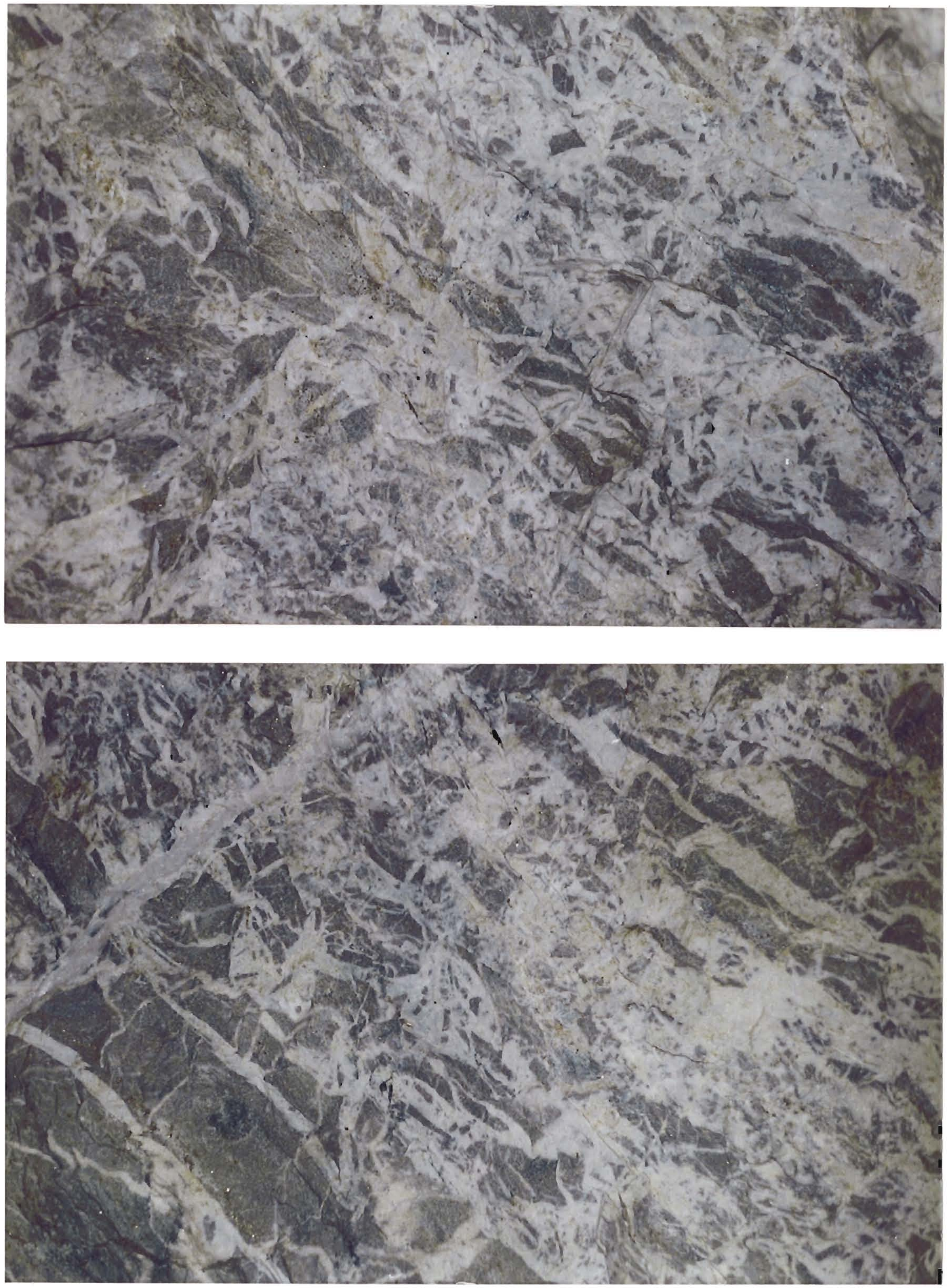

Figure 26: Cross section views of the same central breccia zone of a stockwork, looking northwest. The central breccia zone comprises about 50% wall rock fragments and 50% vein material. Some remnants of ladder-veins can still be seen within (B). Field of view equals 1 m.

Many of the central breccia zones are characterized by younger central veins (see central veins in section 6.3.3).

Figure 27 is an equal area plot of the poles to central breccia zones and central veins of all the stockworks in the San Antonio mine. Fourteen data points represent measurements of the central breccia zones obtained by the author in the mine. One hundred and ninety-two of the data points represent attitudes of the central breccia cores taken from mine level plans; these attitudes were determined by using pairs of successive level plans superimposed one on top of another. The other sixty-eight data points represent measurements of the central veins taken from mine level plans. The attitude indicated by the highest concentration of the poles is $N40^0W/78^0NE$, an attitude that is different from the ladder-veins ($N88^0W/50^0NE$). The central breccia zones and the ladder-veins pitch 19^0NW and 83^0NW in the plane of the SAM unit respectively, and the ladder-veins pitch 45^0NW in the plane of the central breccia zones (Figure 28).

The wall rock fragments engulfed by vein material within the central breccia zones are altered and bleached to light grey. At all except one out of the ten locations examined the wall rock fragments in the central breccia zones are texturally massive. At the other location the wall rock fragments in its central breccia zone show pre-stockwork schistosity.

The vein material in the central breccia zones is made up mainly of quartz (90%) with small amounts of cabonate and albite. The vein material as well as the wall rock fragments are commonly impregnated with small amounts of pyrite.

6.3.3 The Central Veins

Within most central breccia zones there are younger tabular vein-like bodies (see also Reid 1931, Stockwell 1938, DeHuff 1940, Gibson and Stockwell 1948).

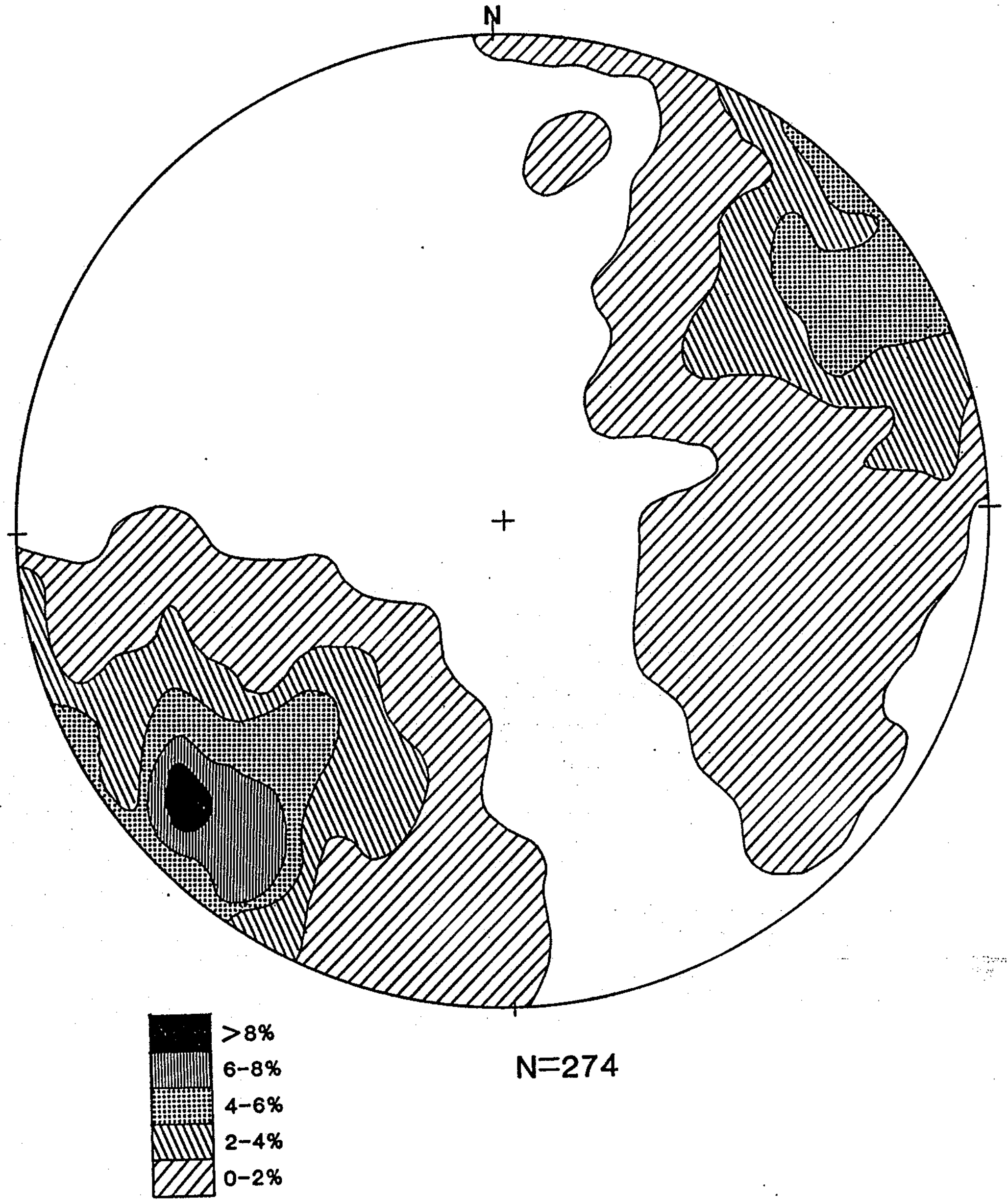

Figure 27: Equal area contour plot of the poles to central breccia zones and central veins of all stockworks. Fourteen data points represent measurements of the central breccia zones obtained by the author in the mine. One hundred and ninety-two data points represent measurements of the central breccia zones taken from the mine level plans. Sixty-eight data points represent measurements of the central veins taken from mine level plans. The attitude indicated by the highest concentration of the poles is $N40^0W/78^0NE$.

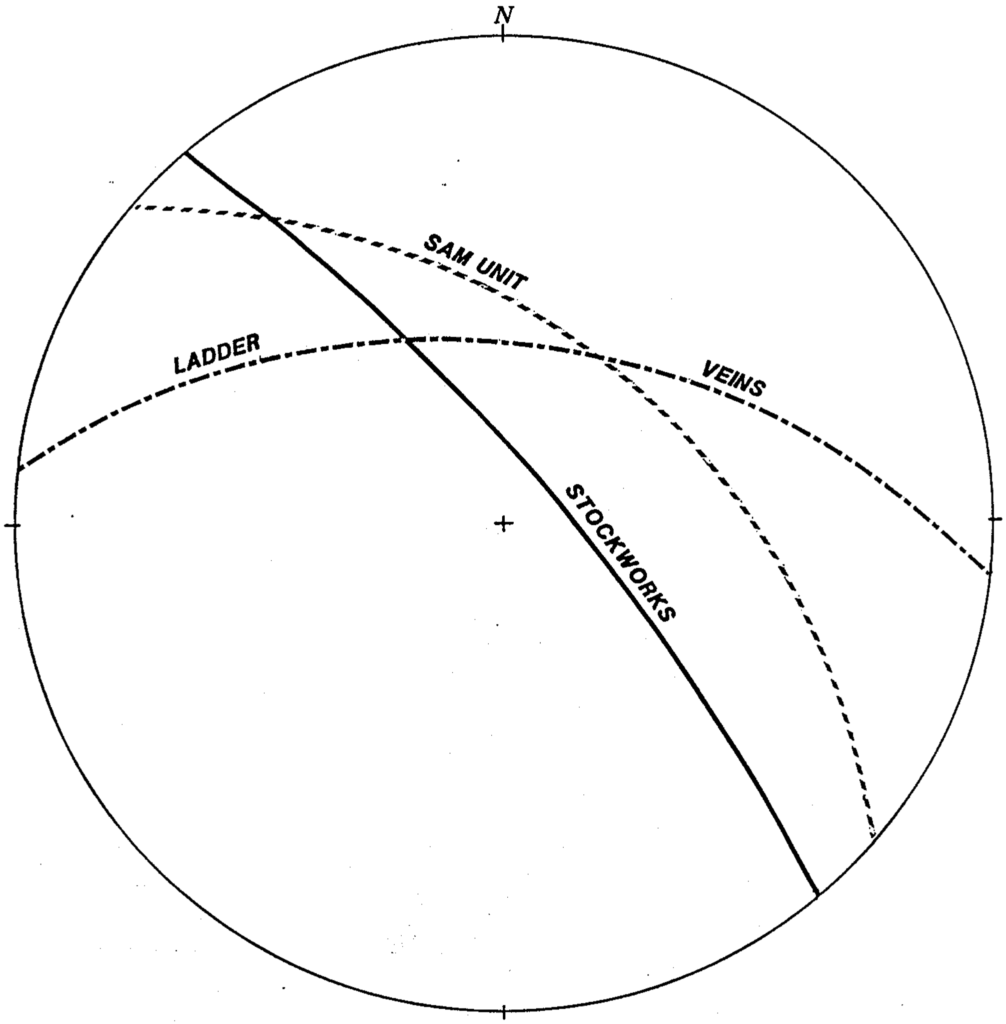

Figure 28: Synoptic projections of the mean orientations of the SAM unit, ladder-veins and overall stockworks. The long dimension of the stockworks pitch $19^0 NW$ in the plane of the SAM unit. The ladder-veins pitch $45^0 NW$ in the plane of the stockworks and $83^0 NW$ in the plane of the SAM unit.

These are known as central veins and they have sharp contacts with the wall rock fragments and vein material of the breccia cores (Figures 29 and 30). The central veins have similar attitudes as the enclosing central breccia zones and they are also used to determine the orientation of the stockworks. The thickness of these central veins ranges from a few centimetres to about one metre. Their strike and down plunge lengths may range up to 200 m and 100 m, respectively. They are not as continuous as the central breccia zones and they frequently branch out within the central breccia zones.

The central veins are mainly made up of quartz (Reid 1933, Stockwell 1938, DeHuff 1940, Gibson and Stockwell 1948). Narrow streaks of fine-grained pyrite are commonly found adjacent to most of these central veins.

6.3.4 The Vertical Veinlets

The ladder-veins, the central breccia zones and the central veins have been cut by younger vertical veinlets (Figures 14, 15, 16, 24 and 31). They strike $N45^0E$ to $N65^0E$ (10^0 to 30^0 more to the north than the 16-type veins (see 16-type veins in Chapter 7)). The average strike and down dip lengths of these vertical veinlets are about a metre, though some may range up to 10 m, and their thickness may range from a few millimetres to 5 cm. Most of them have lenticular shape (Figures 17 and 31). They terminate by tapering down in width in the wall rock.

The vertical veinlets are most abundant in the parts of the stockworks cross-cut by the 16-type veins or shear zones. Apparent vertical offsets of up to 5 cm and usually with the northwest side up are common in these vertical veinlets (Figures 17, 24 and 31).

The vertical veinlets are composed of variable proportions of quartz, carbonate, albite and dolomite. They are commonly internally zoned, with

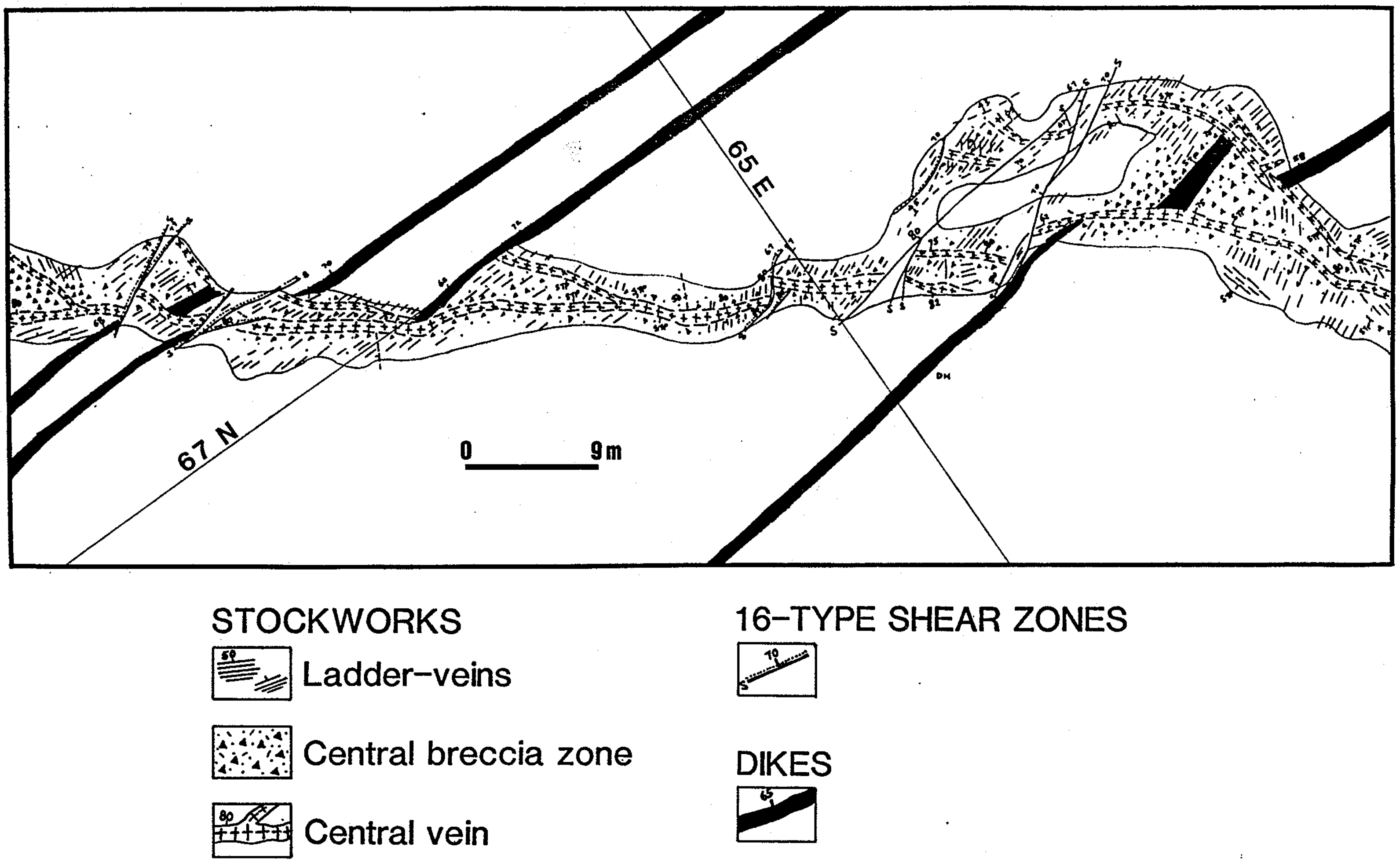

Figure 29: Level 9 plan showing ladder-veins, central breccia zone and central veins of a stockwork. The early set of dikes have been offset by the stockwork.

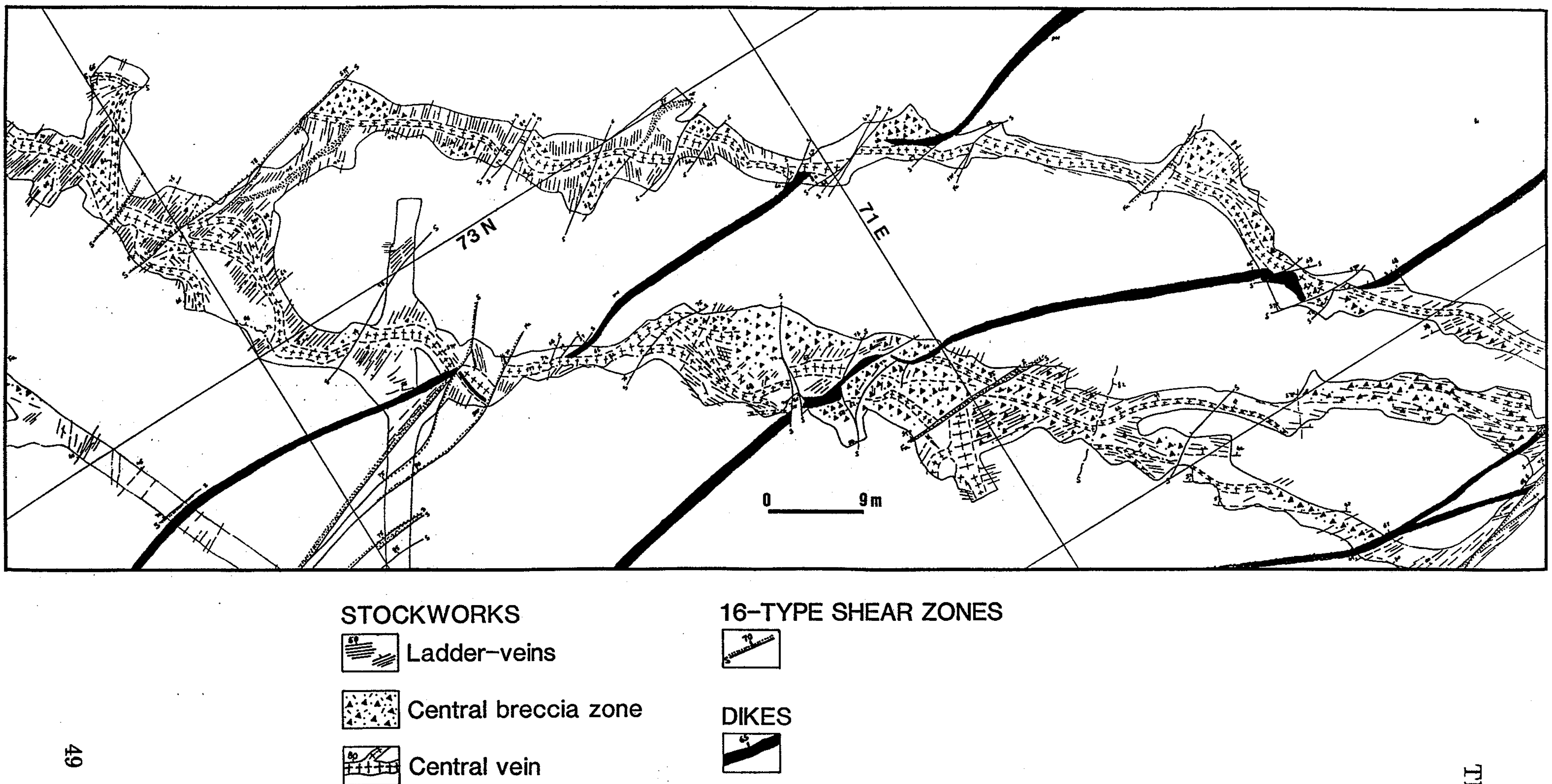

Figure 30: Level 15 plan showing two stockworks arranged subparallel to one another. The early set of dikes have been offset by the stockworks.

Figure 31: Vertical veinlets cross cutting and offsetting a ladder-vein. View northwest. The vertical veinlets have tapered termination and drusy texture.

quartz-carbonate-albite (qtz-cb-alb) fringe near the vein wall and dominantly coarse-grained quartz in the centre (Figures 24 and 31). The qtz-cb-alb fringe and qtz-cb-alb fills near the tips of th veinlets (Figure 31) often show drusy texture. Chlorite is usually only present in large vertical veinlets.

The wall rocks adjacent to the vertical veinlets are texturally massive, altered and variably bleached.

6.3.5 Offset of the early dikes by stockworks

The early set of dikes have been cut by, and offset by the stockworks. The offset of these dikes in plan view is right-lateral. Evidence of such offsets are shown in Figures 29 and 30. The amount of horizontal offsets may range up to 20 m.

6.4 DISTRIBUTION OF STOCKWORKS IN THE SAM UNIT

Detailed examination of the mine level plans and sections for the distribution of the stockworks within the SAM unit has revealed three conditions. (1) The stockworks occur exclusively within the 700 m strike length of the SAM unit near the mine site (Figure 32 (in pocket)) where its average apparent thickness is 140 m. (2) Over 90% of the stockworks occur in the area where the apparent thickness of the SAM unit is greater than 110 m, and (3) the "inflated" zone of the SAM unit in which all the stockworks occur pitches $80^0 SE$ on the plane of the SAM unit (or plunges $46^0/N55^0$). Within the inflated zone of the SAM unit where all the stockworks are confined there is local variation in apparent thickness of the SAM unit and in distribution of the stockworks. For instance, between levels 23 and 27 where the apparent thickness of the SAM unit has dropped by 30% to 70% compared to the apparent thickness of the SAM unit in the upper levels where most of the stockworks occur there is hardly any stockwork. This is also true for the SAM unit on either side of the mine. These observations suggest the possibility that the increased thickness of the SAM unit may be somehow related to the emplacement of the stockworks.

6.5 INTERPRETATION OF STOCKWORK DEVELOPMENT

Age relationships between the different components that make up the stockorks indicate that there are four stages in the development of the stockworks. The four stages are: (1) the development of ladder-veins, (2) the development of central breccia zones, (3) the development of central veins within central breccia zones, and finally (4) the development of the vertical veinlets which cross-cut the ladder-veins, central breccia zones and central veins. The following sections give interpretation of these four stages based on evidence from only the stockworks themselves.

6.5.1 Stage 1: Development of ladder-veins

The ladder-veins have different orientations from the whole tabular stockwork of which they are a part. Figures 33 and 34 are plan and cross-section views showing the relationship between the ladder-veins, tabular stockworks, the SAM unit, and the early dikes. The characteristics of the ladder-veins suggest that they are hydraulically generated according to the work of Phillips (1972) and Sibson (1981). The have en echelon arrangement, dilational characteristics, wedge-like terminations and high length/thickness ratios. Such an origin would have yielded an orientation normal to the ambient least principal stress (σ_3) within the SAM unit at the time of their formation (Figure 35). The orientations of the maximum (σ_1) and intermediate (σ_2) principal stresses in Figure 35 can be anywhere within the plane of the ladder-veins.

The arrangement of ladder-veins, produced by hydraulic fracturing, in discrete

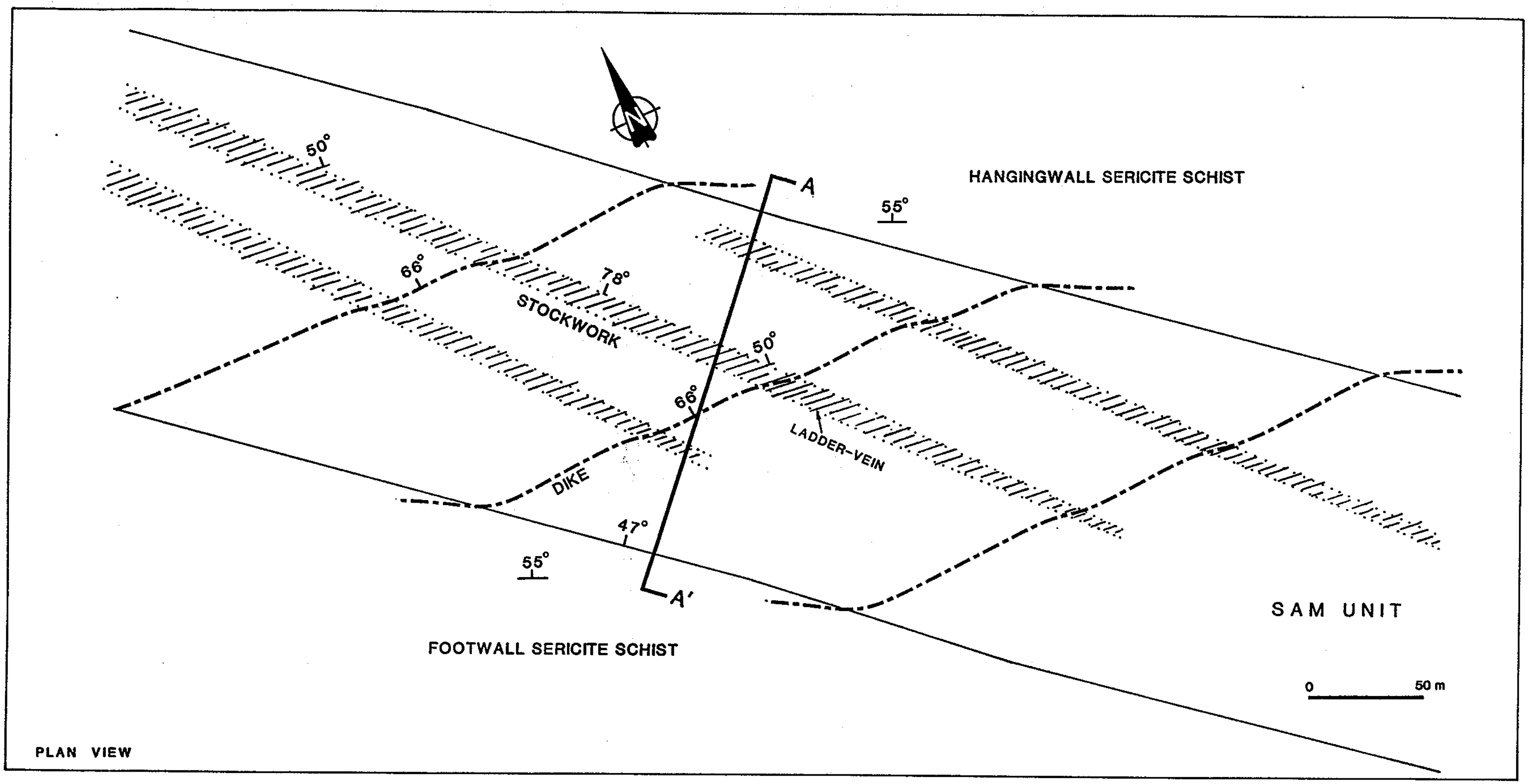

Figure 33: Schematic plan view showing the ladder-vein stage of stockwork development. Whether or not the dikes were offset during this stage is uncertain. Vertical cross section A-A' is shown in Figure 34.

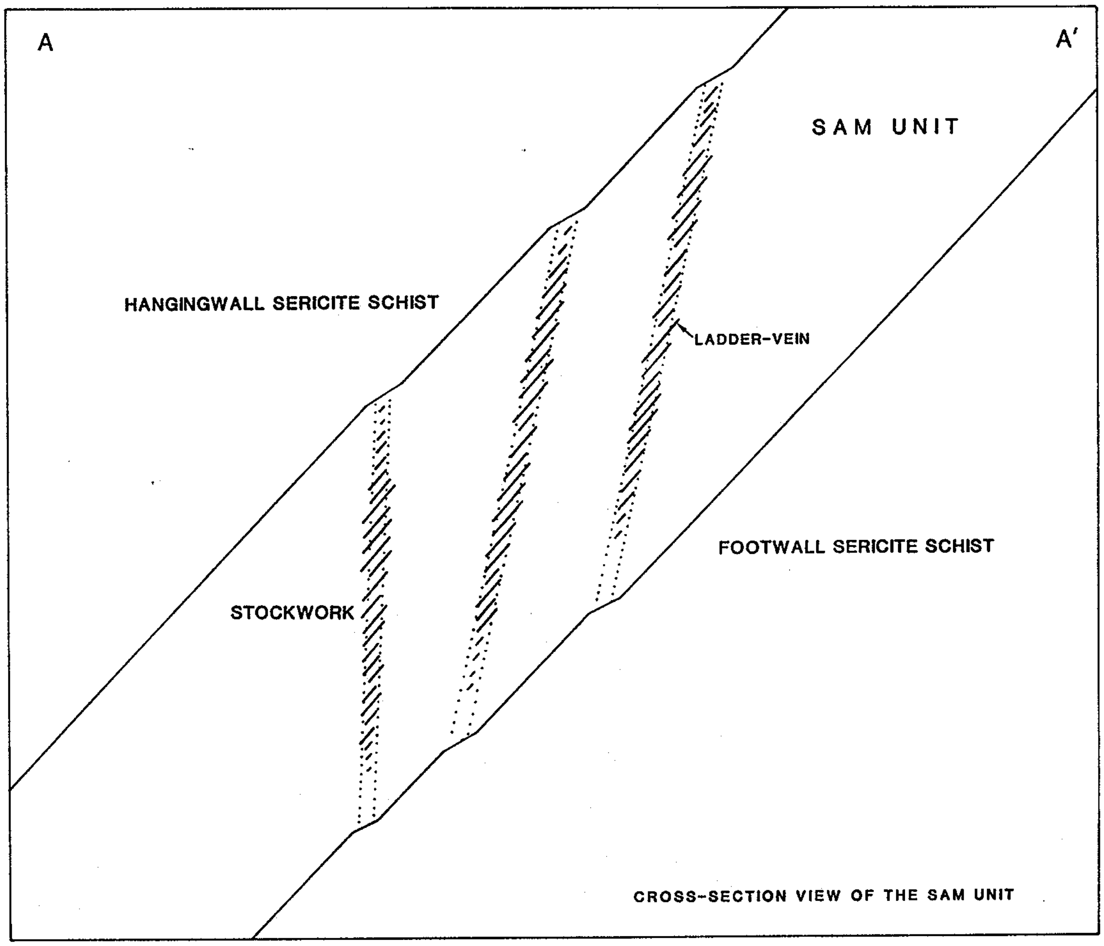

Figure 34: Schematic cross section view of the SAM unit showing the ladder-vein stage of stockwork development.

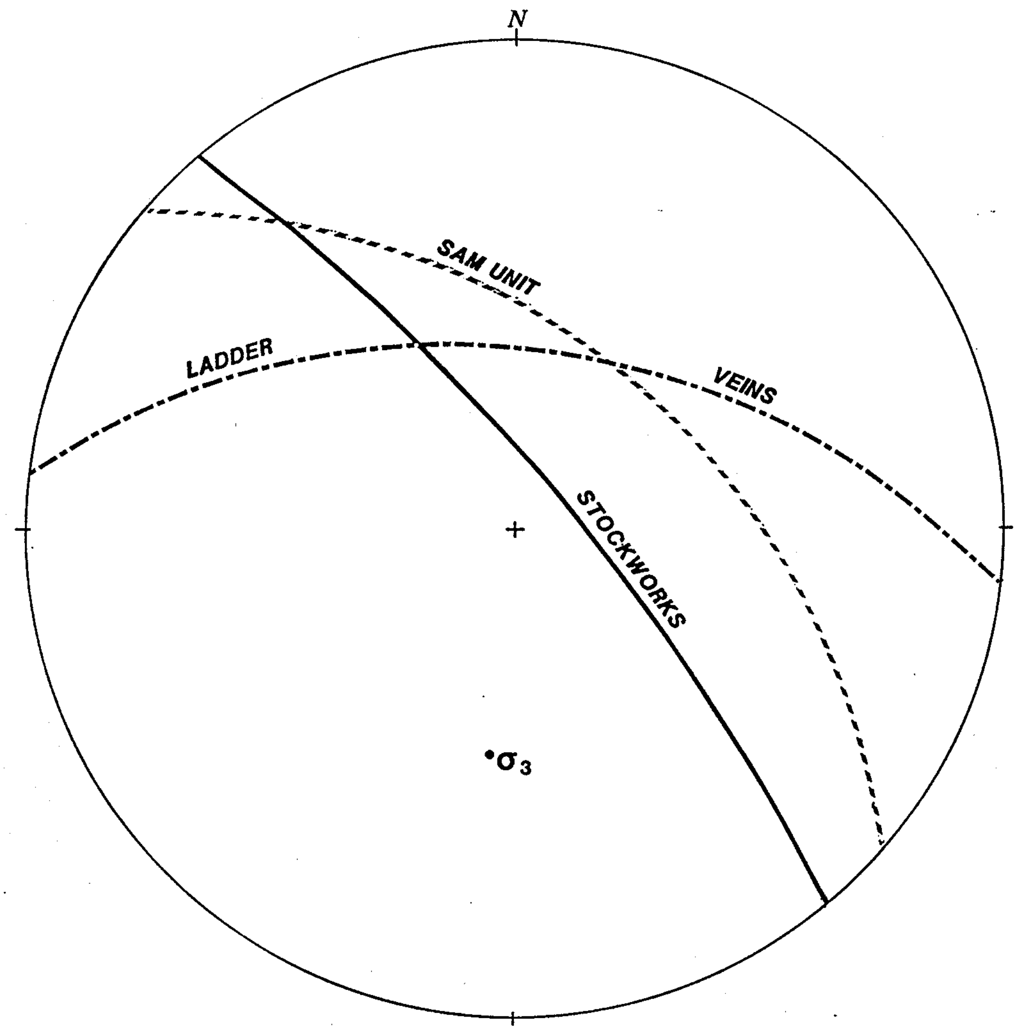

Figure 35: Interpretation of the ambient minimum principal stress in the SAM unit during ladder-vein development stage of stockworks. (σ_3 is $40^0/S7^0W$).

tabular zones cross the SAM unit is problematic. Two explanations are possible. (1) There might have been some kind of pre-existing structures in the SAM unit which controlled the introduction of fluids into discrete tabular zones. In support of this idea there is one stockwork which shows evidence of a pre-ladder-vein schistosity in wall rock fragments within its central breccia zones. Otherwise, there is no evidence of such a condition. (2) The tabular zones might represent incipient shear zones where tension fractures, produced hydraulically, were starting to link up. This explanation is similar to a method proposed by Johnson (1970) for the initiation of shear fractures, although the scale of tension fracture development is quite different. This possibility is tested later in section 6.6.2.2 where translational movement within the stockworks is discussed.

6.5.2 Stage 2: Development of the central breccia zones

The growth of the central breccia zones from a simple ladder-vein condition may be accounted for by one or other of the two possible mechanisms: (1) excessive branching and dilation of individual ladder-veins at the advanced stage of hydraulic fracturing results in dislocation and rotation of fragments of the SAM unit in the matrix of vein material, (2) shear movement in the tabular zones laden with ladder-veins linking up followed by rotation of the ladder-veins that produced sigmoidal shape and brecciation of the SAM unit. Either one of these mechanisms could have produced the central breccia zones. Figures 36 and 37 are plan and cross-section view schematically showing the central breccia zone stage of the stockwork development.

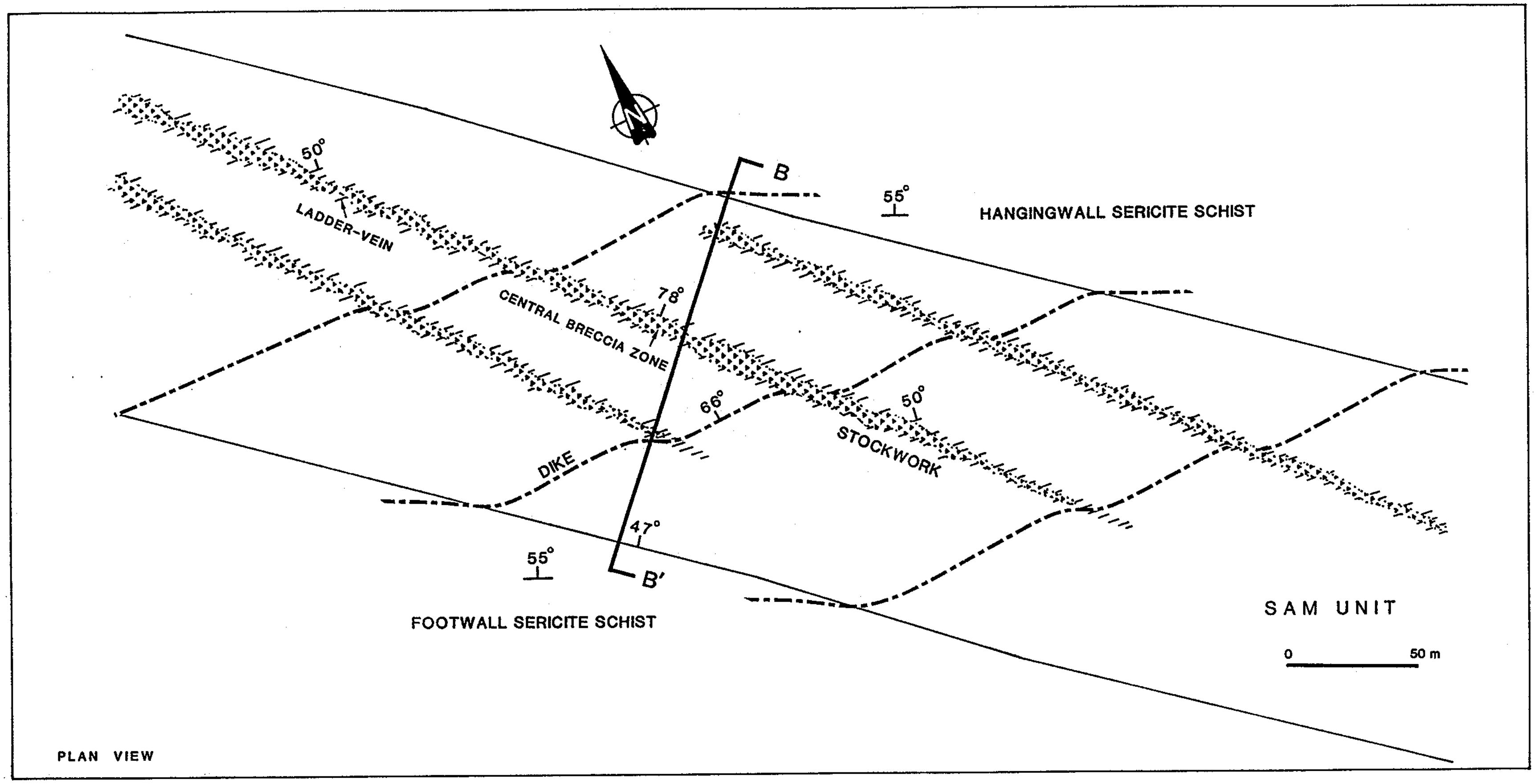

Figure 36: Schematic plan view showing the central breccia zone stage of stockwork development. Vertical cross section B-B' is shown in Figure 37.

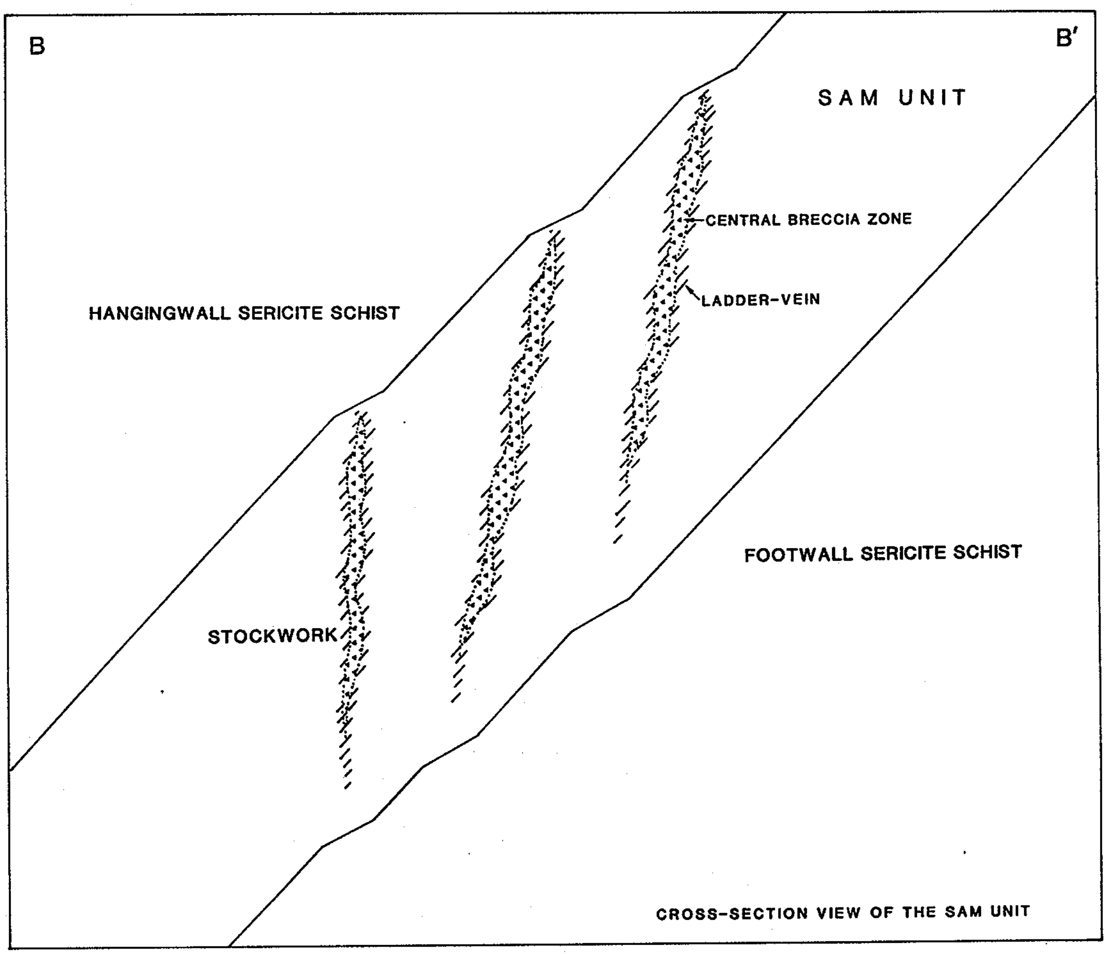

Figure 37: Schematic cross section view of the SAM unit showing the central breccia zone stage of stockwork development.

6.5.3 Stage 3: Development of Central Veins

The tabular central veins are distinctly younger than the wall rock fragments and vein material of the central breccia zones. This, coupled with evidence of right-lateral offset of the earlier dikes on these central veins suggest that the central veins are probably vein-filled, brittle shear fractures developed only after the central breccia zones had consolidated and solidified. The central breccia zones probably caused a strength anisotropy within the SAM unit which controlled the position of the fractures in which central veins were emplaced. Figures 38 and 39 are plan and cross-section views showing further development of the central breccia zones with the emplacement of central veins.

6.5.4 Stage 4: Development of Vertical Veinlets

The vertical veinlets which cut across the ladder-veins, central breccia zones and central veins are the last component of the stockworks to develop. The lenticular shape, internal zonation and drusy texture of these structures are characterstics typical of vein-filled tension fractures (Beach 1980, Rickard and Rixon 1983, Etheridge 1983, Engelder 1987). The fact that they are most abundant in the parts of the stockwork cross-cut by the 16-type shear zones suggest that they are related to the development of the 16-type fracture set. Furthermore, it will be shown in chapter 7 on the 16-type shear zones that the orientation of these structures may be accounted for through the same stress configuration as that proposed for the 16-type shear zones.

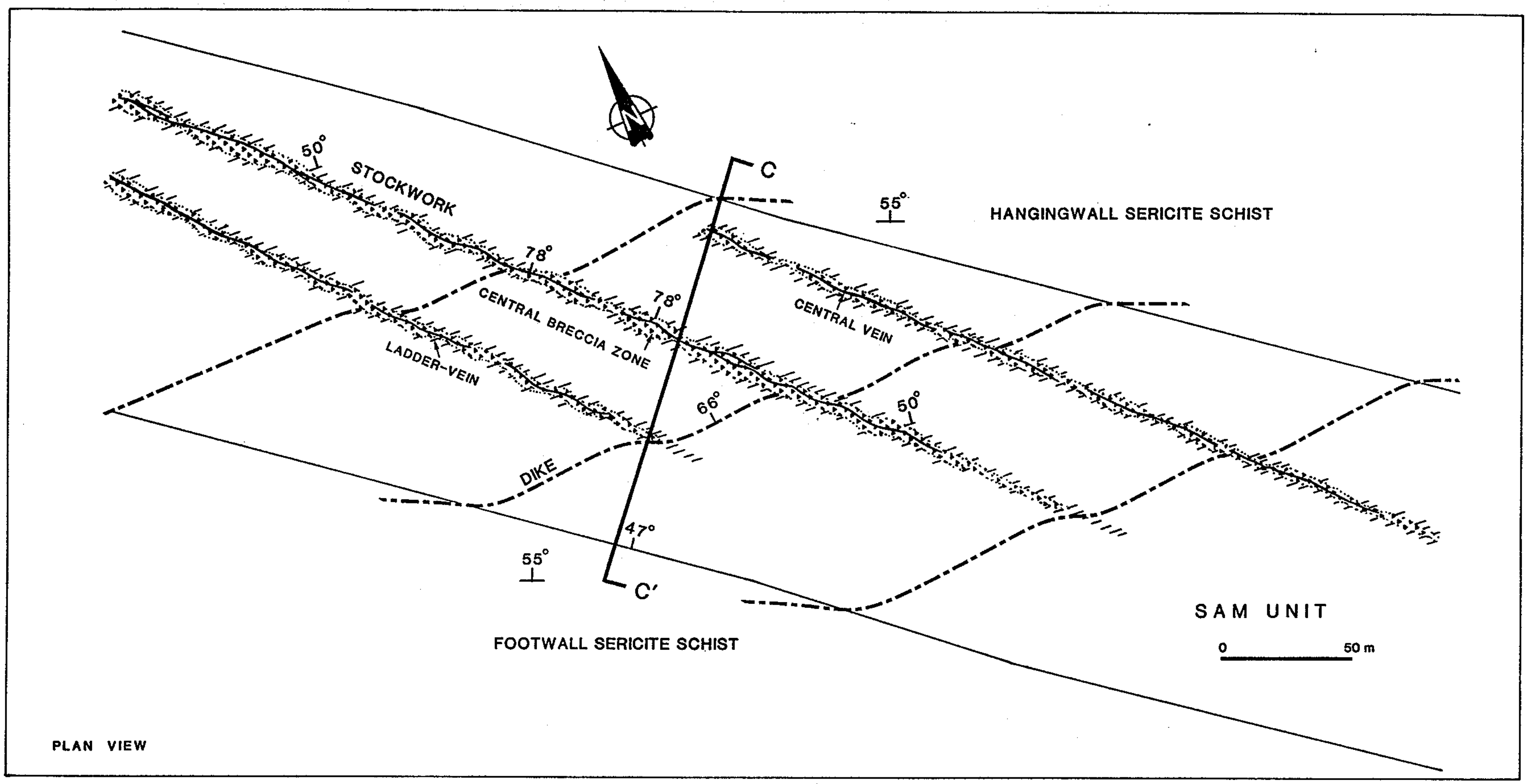

Figure 38: Schematic plan view showing the central vein stage of stockwork development. The early set of dikes have been apparently displaced dextrally by the stockworks. Vertical cross section C-C' is shown in Figure 39.

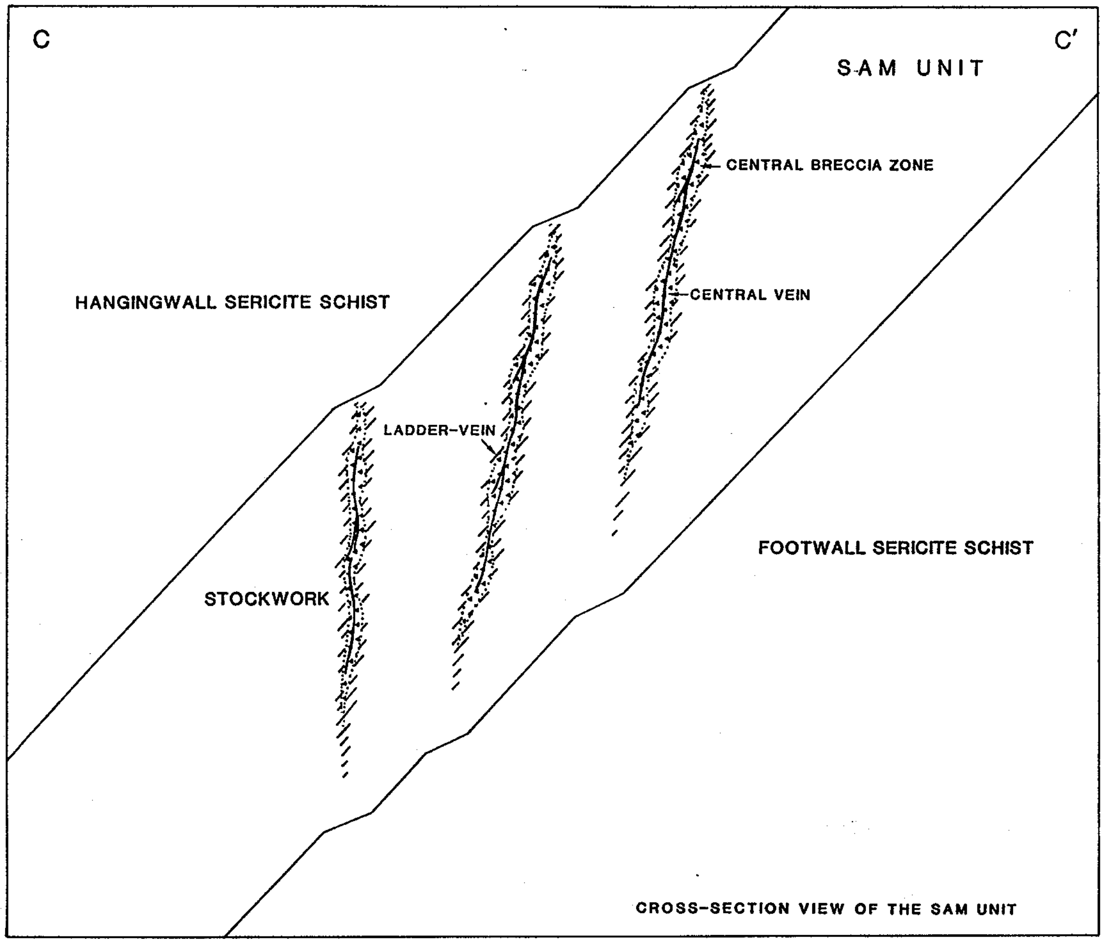

Figure 39: Schematic cross section view of the SAM unit showing the central vein stage of stockwork development.

6.6 MOVEMENTS RELATED TO DEVELOPMENT OF STOCKWORKS

The stockworks show evidence of both dilational and translational movements.

6.6.1 Dilational movements

There are three sources of dilational movements during stockwork development. These are dilational movements normal to the planes of (1) the hydraulically generated ladder-veins, (2) the tabular stockworks caused by inundation of vein material into the central breccia zones, and (3) the tabular stockworks caused by the emplacement of the central veins within the central breccia zones. All these dilational movements should have offset the early set of dikes in a left-lateral fashion in plan view. Such an offset contradicts the observed right-lateral offset of these dikes by the stockworks in the mine. Consequently it is necessary to appeal to separate translational movements within the stockworks during their development. The sigmoidal shape of the ladder-veins is further evidence of translational movements.

6.6.2 Translational movements

Translational movements may have occurred in the central vein stage alone or in both the central breccia and central vein stage of the stockwork development.

6.6.2.1 A single translational movement event in the central vein stage

If all the translational movement in the stockworks is attributed to the central vein stage, the offsets of the dikes and the sigmoidal asymmetry of the ladder-veins can be used to determine the range of slip directions as shown in Figure 40. This figure shows the movement directions that pitch from $45^0 NW$ to $69^0 NW$ on the stockworks.

If translational movements had occurred within the stockworks and assuming that the internal angle of friction (ϕ) of the SAM unit is 30^0 the range of principal stress directions that could produce the above range of slip directions have also been determined as shown in Figure 40.

6.6.2.2 Two translational movement events in the central breccia stage and central vein stage

If the central breccia zones were the result of rotation and linking up of ladder-veins caused by shear translational movement in the tabular zones, then the asymmetry of the ladder-veins indicates that only a single slip direction has occurred in the stockworks as shown in Figure 41. This interpretation is consistant with the possibility considered earlier in section 6.5.1 where the stockworks were interpreted as incipient shear zones linking up the tension fractures (ladder-veins). The effect of this translational movement, however, would produce left-lateral offset of the earlier dikes which contradicts to that observed in the mine. Inorder to remove the effect of this left-lateral offset it was necessary for a large right-lateral translational movement to occur in one of the subsequent stages of the stockwork development. The only later stage at which right-lateral translational movement perceivably could occur was the development of the central fractures that preceded the emplacement of the central veins. The range of slip directions that could produce this right-lateral translational movement are as shown in Figure 42.

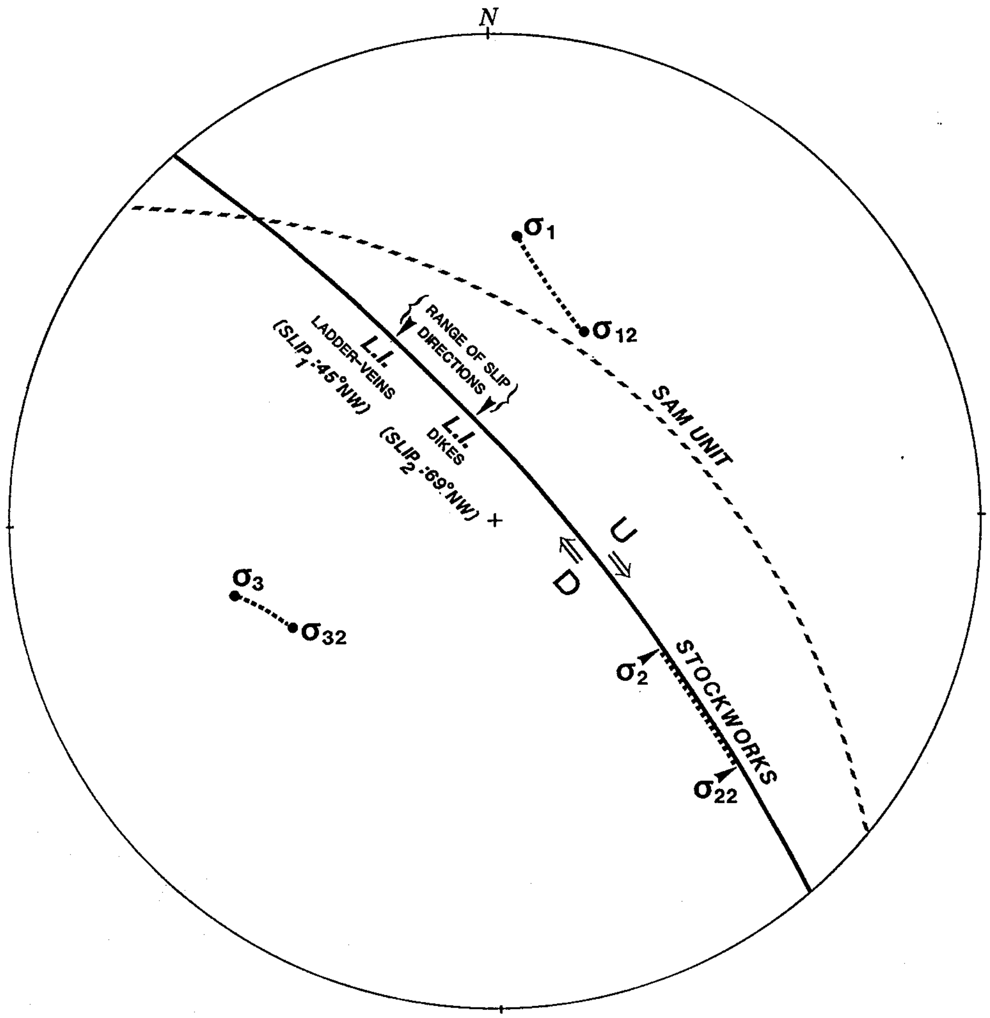

Figure 40: Range of orientations of slip directions on stockworks based on displaced dikes and sigmoidal ladder-veins. The range is restricted to the lines of intersection (L.I.) between the stockworks and the ladder-veins and dikes. For slip $(S_1) = 45^0 NW : \sigma_1 = 40^0/N5^0, \sigma_2 = 44^0/S51^0E$ and $\sigma_3 = 32^0/S75^0W$. For slip $(S_2) = 69^0 NW : \sigma_{12} = 44^0/N36^0E$, $\sigma_{22} = 19^0/S44^0E$ and $\sigma_{32} = 39^0/S63^0W$.

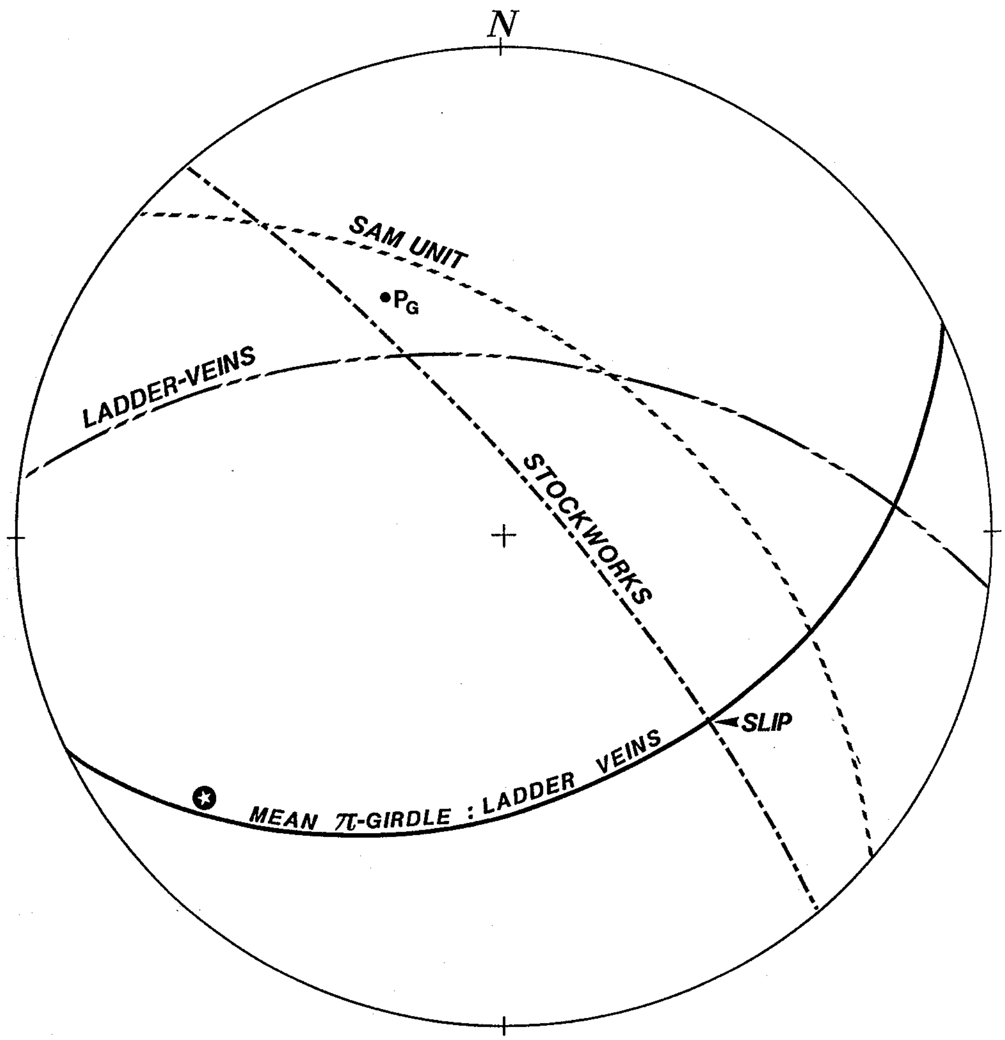

Figure 41: The slip direction of the translational movement at the central breccia zone stage. If the sigmoidal shape ladder-veins and the central breccia zones were the result of the same translational movement then the pitch of the slip direction (SLIP) on the stockworks is $43^0 SE$. P_G represents the pole to the π−girdle. The star represents the pole to the mean stockwork plane.

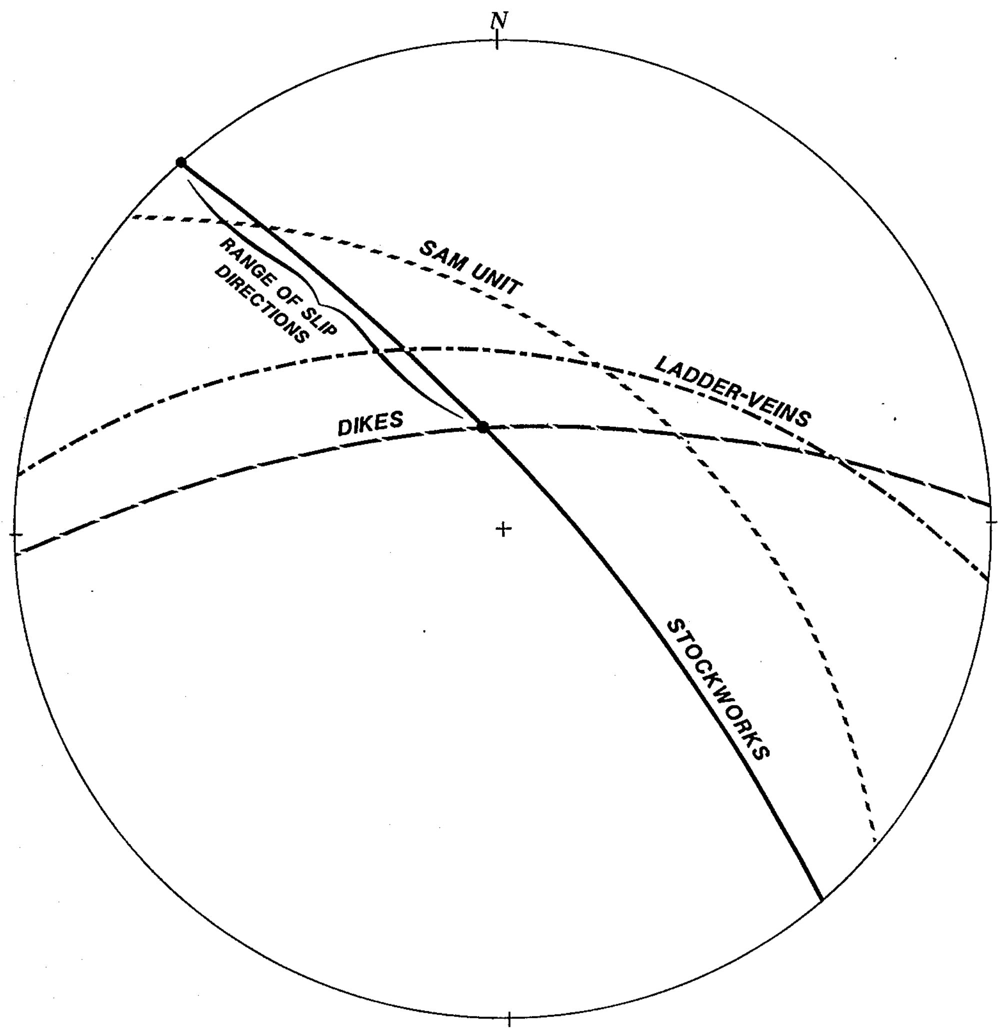

Figure 42: The range of the slip directions on the stockworks that would right-lateral offset of the dikes.

CHAPTER SEVEN

THE 16-TYPE VEINS

7.1 THE 16-TYPE VEINS

The 16-type veins occur within a set of well defined parallel tabular shear zones within the SAM unit called the 16-type shear zones. These structures are oblique to the SAM unit, consequently when viewed in plan or section they appear to be arranged in an en echelon pattern. The 16-type shear zones always offset the dikes, stockworks and the footwall and hangingwall contacts of the SAM unit.

Not all the 16-type shear zones contain 16-type veins. Some are completely without vein material while others contain only thin, discontinuous stringers.

Where present in the shear zones, the veins are made up predominantly of quartz and contain limited numbers of wall rock fragments. Most of the included fragments have well developed schistosity indicating that the shearing pre-dated the vein emplacement. The veins are characterized also by younger cross-cutting discordant veinlets and by post-vein movement. Figure 43 is a photograph of a typical 16-type vein. Figure 44 presents several composite sketches of 16-type veins in which the above and other properties still to be discussed are shown.

The 16-type veins will be discussed in detail under the following headings: (1) 16-type shear zones, (2) the characteristics of the 16-type veins, (3) cross-cutting discordant veinlets, and (4) post-vein movement.

Figure 43: A 16-type vein, exposed on back and on wall of drift, number 3 level. Wall rock adjacent to the vein shows typical zone of schistosity related to the shearing of the SAM unit. A narrow streak of fine-grained pyrite is located in the centre of the vein. A late shear fracture characterized by a rusty band is oriented subparallel to the vein contact. The wall rock adjacent to the vein is altered but remains minimally bleached. The width of the vein is 30 cm.

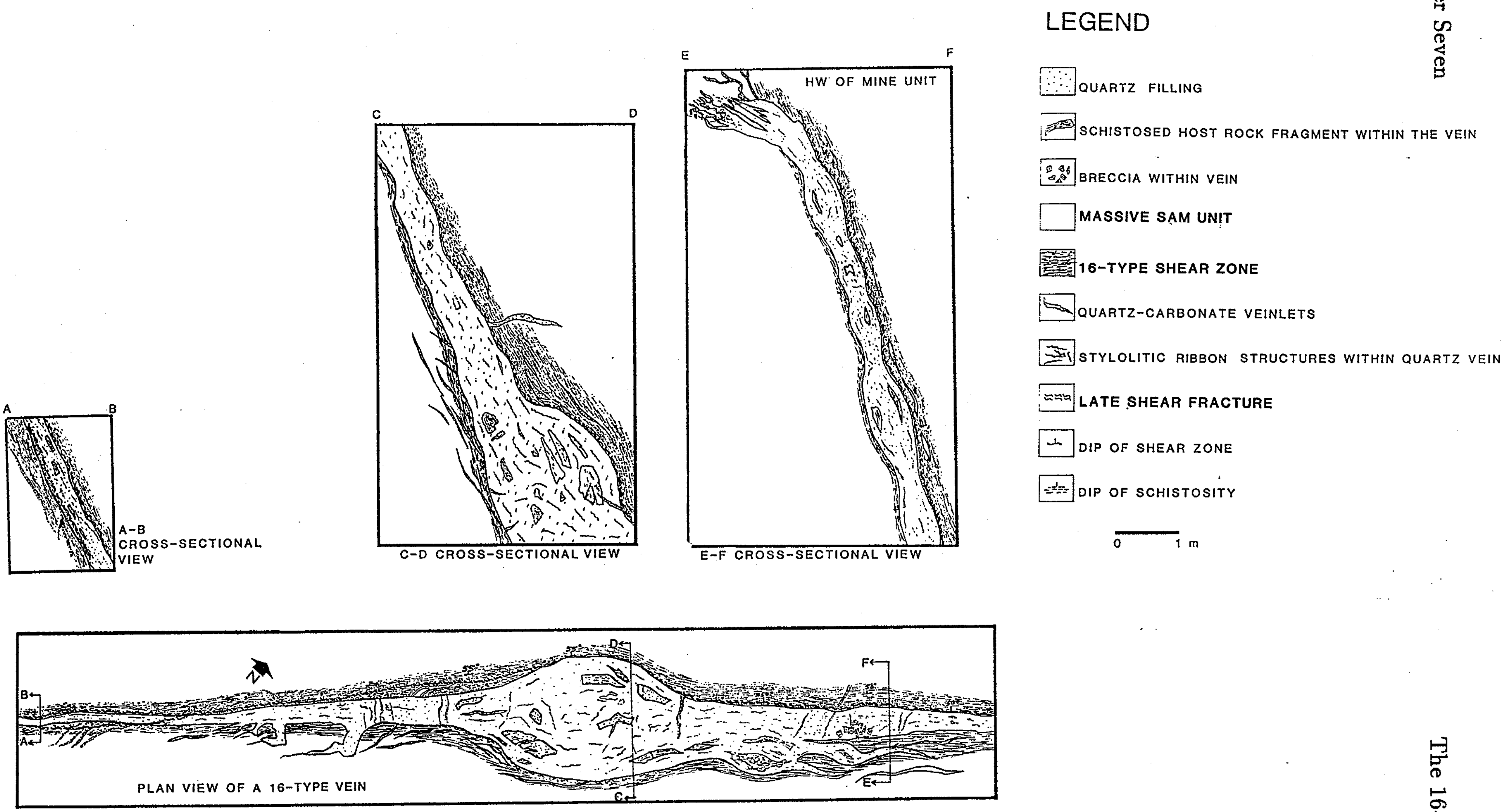

Figure 44: Plan and cross section sketches of a 16-type vein on 3 level.

7.1 THE 16-TYPE SHEAR ZONES

7.2.1 Attitude

Figure 45 is a plot of the poles to the 16-type shear zones. Seventy-five of the attitudes were measured by the author in the mine. The other 1429 attitudes were taken from the mine level plans. The average attitude reflected by the greatest concentration of the poles is $N74^0E/68^0NW$. The orientation of the long dimension of these shear zones within the SAM unit coincide with the line of intersection between the shear zones and the SAM unit. This orientation expressed as a pitch in the SAM unit is 85^0SE (Figure 46).

7.2.2 Spacing

The average perpendicular distance between strikes of the 16-type shear zones in the SAM unit is about 10 m. However, at some locations the 16-type shear zones may be spaced only a few metres apart. At other locations they may be spaced more than 40 m apart. There is an observed quantitative correlation between the spacing of the 16-type shear zones and the thickness of the SAM unit. Between levels 23 and 27 the SAM unit is considerably thinner than other levels and the average spacing of the 16-type shear zones is reduced to one or two metres. This correlation is similar to that observed for joints (Harris et al 1960, McQuillan 1973, Narr and Lerchie 1984, Williams 1985, Suppe 1985), however, it is not clear that the explanation for joints applies here.

7.2.3 Continuity and Thickness

The 16-type shear zones often branch and merge along their strike and down their plunge. In plan view most of the 16-type shear zones cut across the SAM unit completely and most of their strike lengths range up to 250 m. Along their

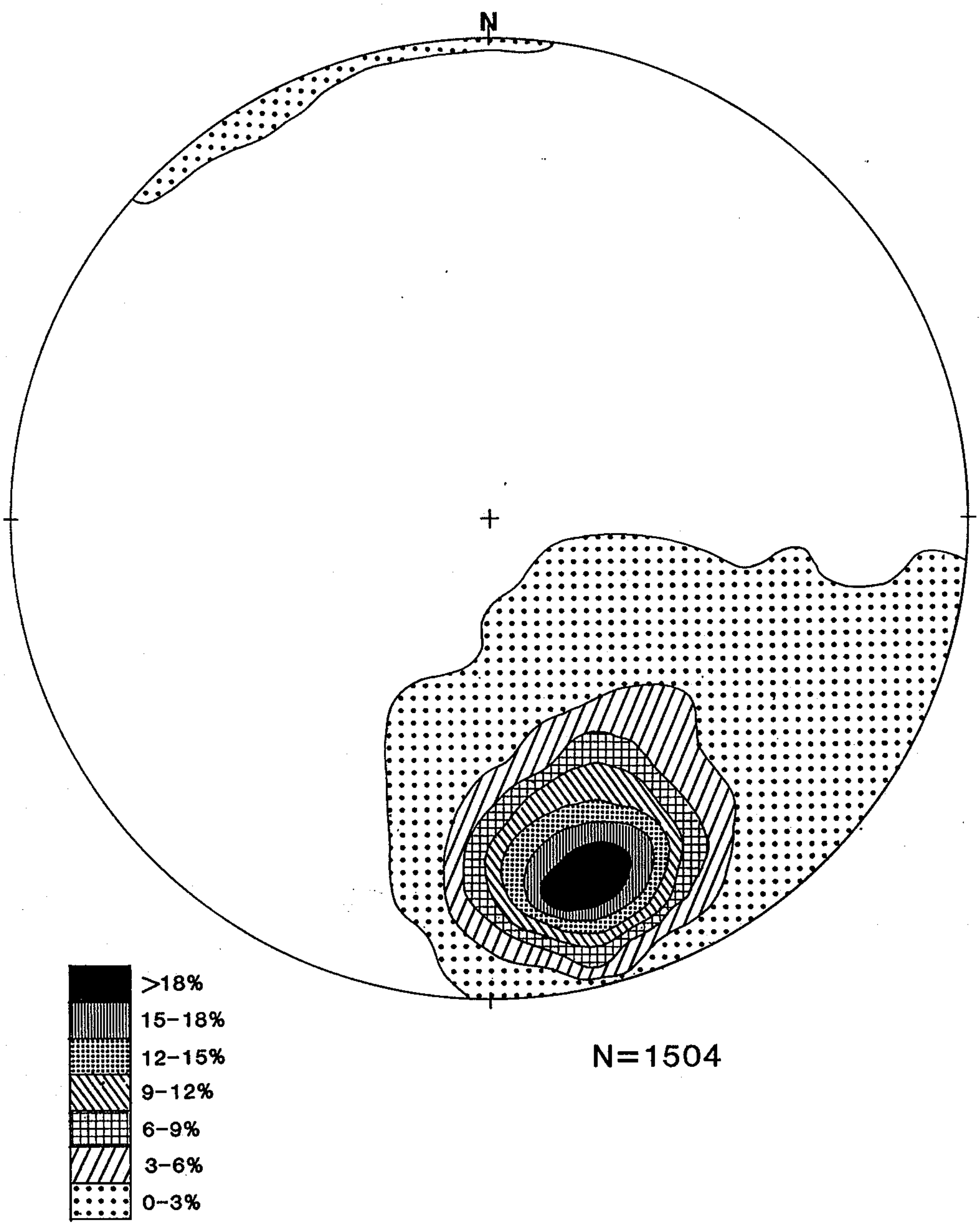

Figure 45: Equal area contour plot of the poles to the 16-type shear zones. Seventy-five data points represent measurements taken by the author in the mine. One thousand four hundred and twenty-nine data points were taken from the mine level plans.

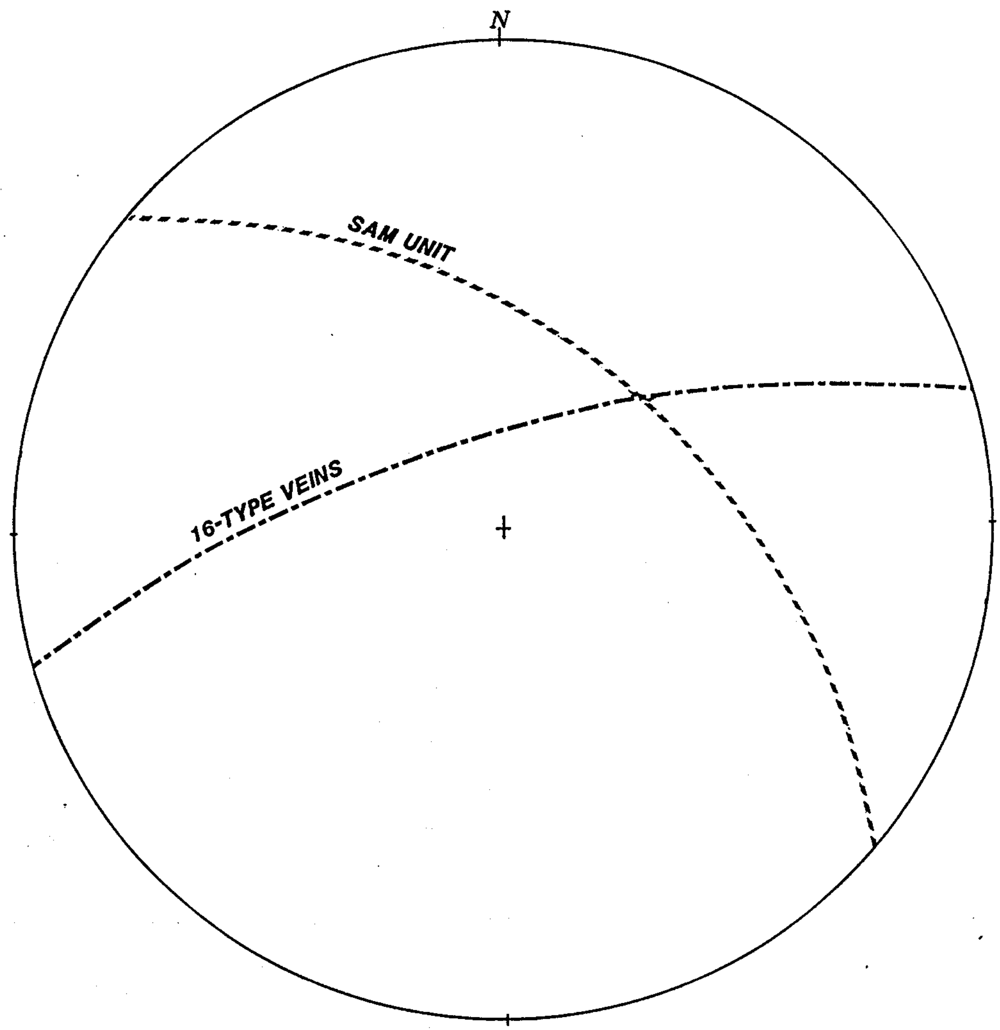

Figure 46: Synoptic projections of the mean orientations of the 16-type shear zones and the SAM unit. The pitch of the long dimension of the 16-type shear zones in the SAM unit is $85^0 SE$.

strike these shear zones usually branch into numerous smaller splay shears as they approach the footwall contact of the SAM unit.

The lengths of the long dimension of these shear zones (plunge $47^0/N50^0E$ in the SAM unit) may vary from a few of metres to over 1200 m. In down plunge they always terminate within the SAM unit by branching into numerous smaller shears. The thickness of the 16-type shear zones (excluding vein material) vary from one or two centimetres to about 2 m. Generally shear zones which have large strike and down plunge lengths are thicker than those which have shorter strike and down plunge lengths.

The thickness of many 16-type shear zones are greatly reduced where they intersect the stockworks. Where this occurs the stockwork adjacent to the cross-cutting 16-type shear zone always contain abundant vertical veinlets which strike $10^0 - 30^0$ more northerly than the 16-type shear zones (Figure 47). There is a physical association between the vertical veinlets and the 16-type shear zones, and it is apparent that the character of strain in the stockworks is different than the character of strain in the 16-type shear zones. The relationship between the vertical veinlets and the 16-type shear zones will be discussed further in section 7.5 where the principal stresses at the time of the formation of the 16-type shear zones is discussed.

7.3 OFFSET ON 16-TYPE SHEAR ZONES

The SAM unit has been greatly dissected by the family of 16-type shear zones. The footwall and hangingwall contacts of the SAM unit, the dikes and the stockworks all have been variably displaced by this set of shear zones. The offsets of these features observed in plan view is almost always left-lateral. Figures 48, 49 and 50 reveal these conditions. The amount of horizontal offsets of these 30 m.

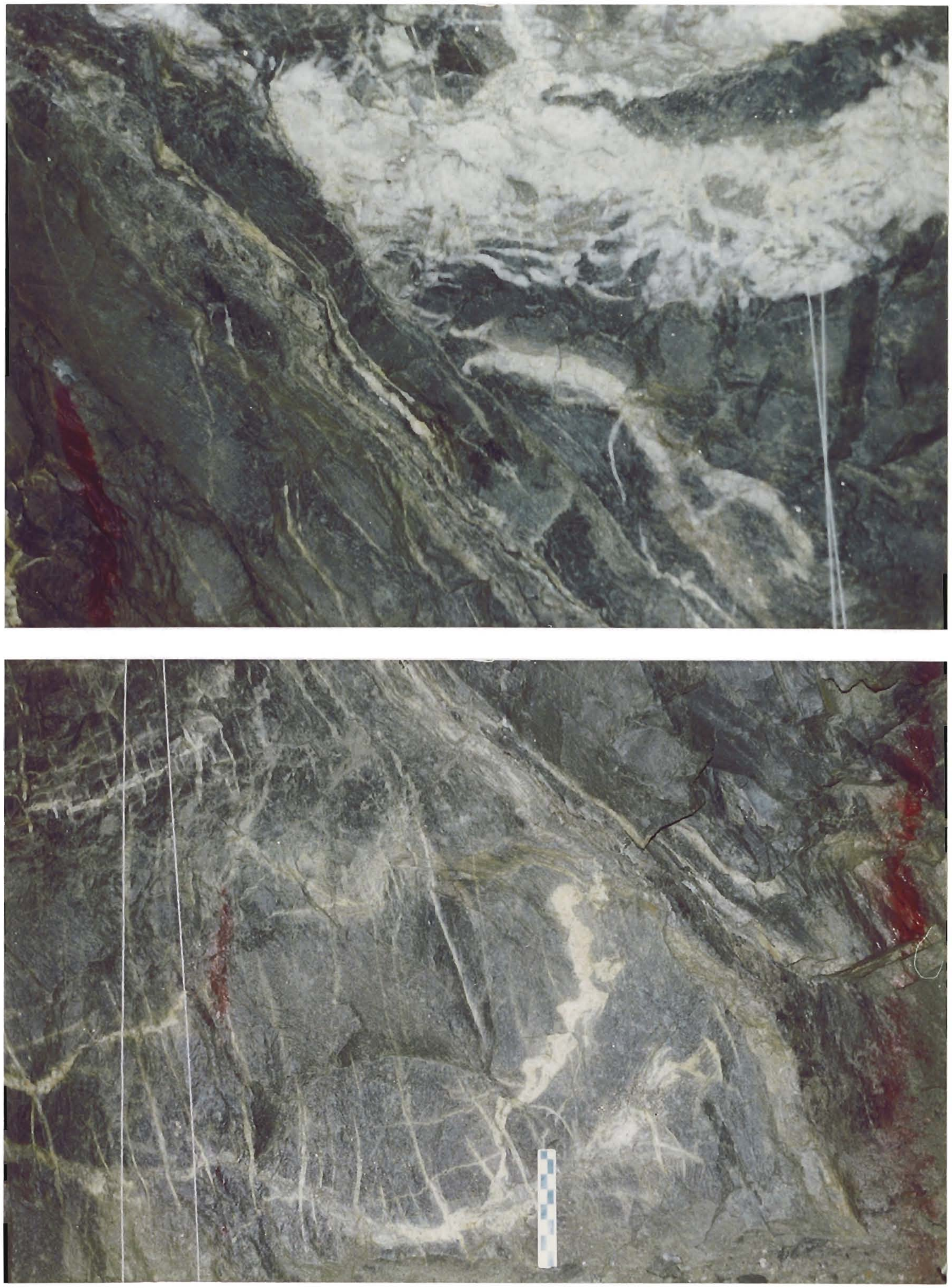

Figure 47: Two photographs showing a 16-type shear zone cross-cutting and offsetting a stockwork. The stockwork contains abundant vertical veinlets oriented oblique to the cross-cutting shear zones. Field of view in both photographs is 1.2 m.

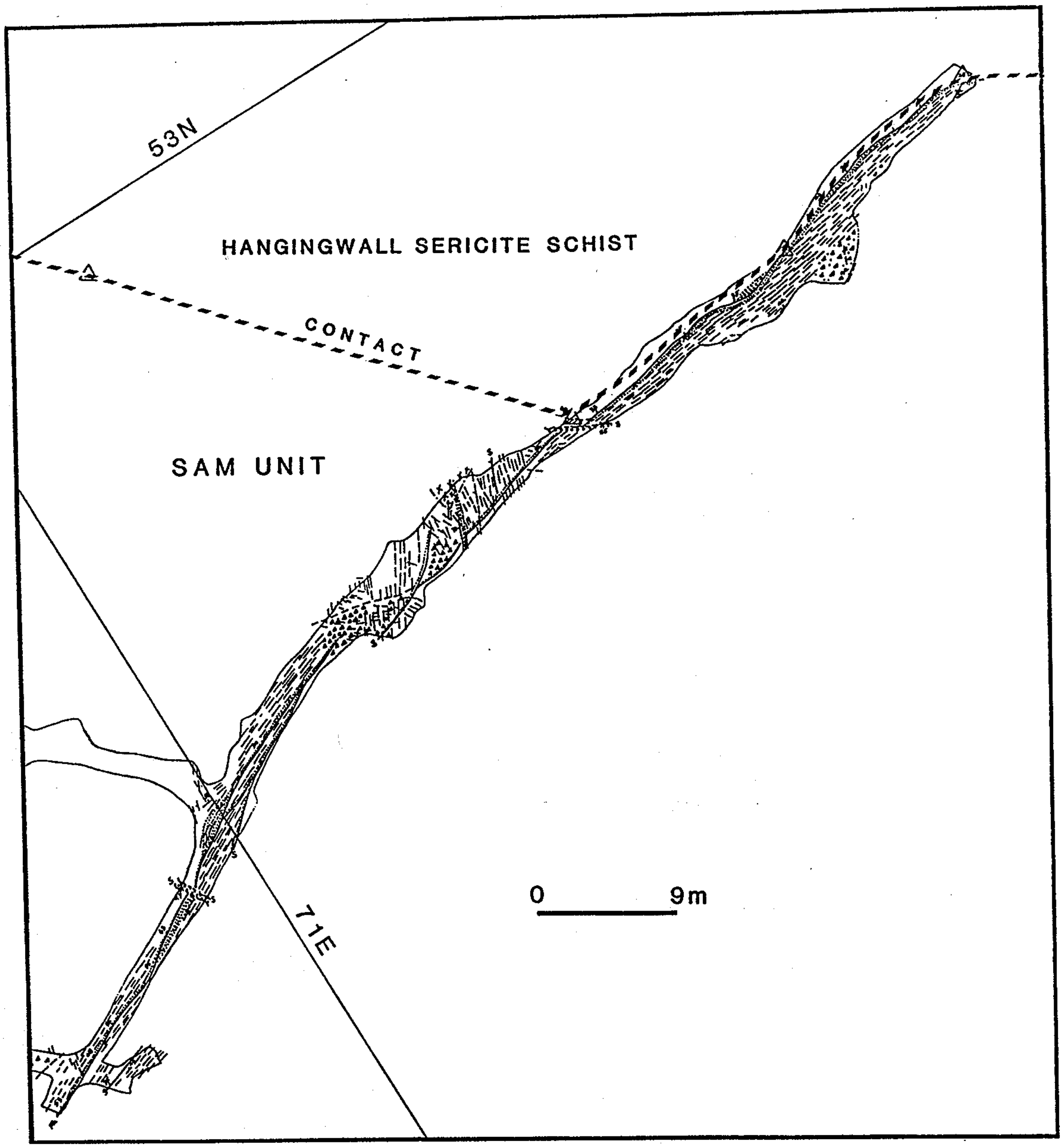

Figure 48: Level 3 mine plan showing left-lateral displacement of the hangingwall contact of the SAM unit by a 16-type shear zone.

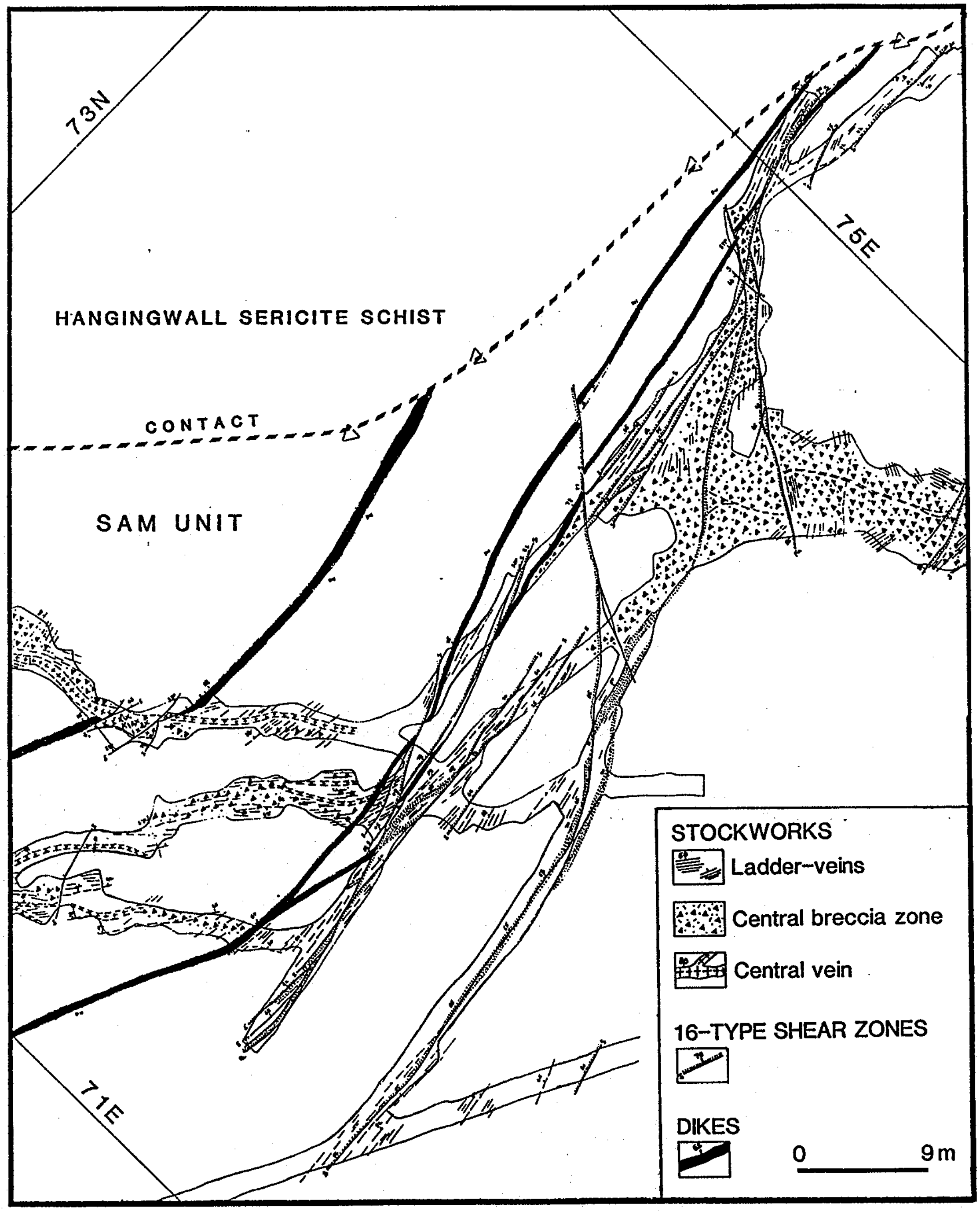

Figure 49: Level 15 plan showing left-lateral displacement of dikes and stockworks by 16-type shear zones. Although the hangingwall contact of the SAM unit is displaced in a similar fashion, the particulars of the displacements are uncertain.

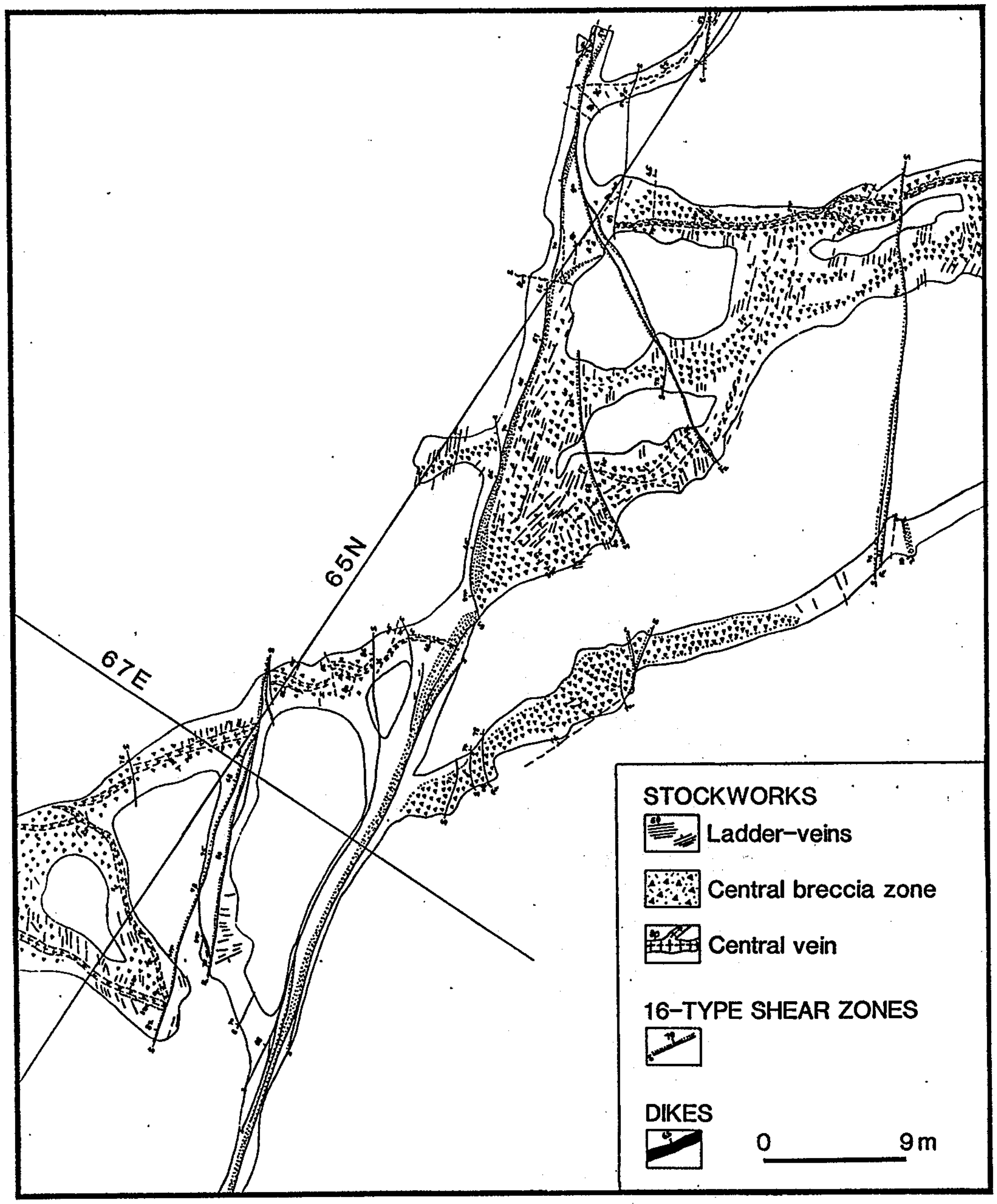

Figure 50: Level 9 plan showing left-lateral displacements of stockworks by 16-type shear zones.

features may range up to There are a few smaller 16-type shear zones, on the other hand, which show small amounts of horizontal offsets right-lateral.

7.4 FABRICS AND MINERALOGY WITHIN THE 16-TYPE SHEAR ZONES

The 16-type shear zones are localized zones of intensely deformed SAM unit. The deformed rocks within the shear zones are texturally and mineralogically different from the adjacent SAM unit outside the shear zones. Mesoscopically, the schistose rocks within the shear zones form sharp contacts within the undeformed SAM unit. Microscopically, however, there is a gradational transition across the contacts. The gradation is characterized by intensification of schistosity development and of grain size reduction toward the centres of the shear zones; characteristics that are typical of mylonitic shear zones (Sibson 1977, Ramsay 1980, White 1979, Simpson and Schmid 1983, Bell and Hammond 1984, Lister and Snoke 1984).

Figures 51 through 55 show the stages in progressive deformation from least to most deformed SAM unit in a 16-type shear zone. They are photomicrographs of oriented thin sections cut parallel to the direction of slickensides and mineral lineations and normal to the schistose surfaces. Figure 51 shows the least deformed SAM unit which is massive and is composed mainly of coarse-grained plagioclase mineral. Figure 52 shows SAM unit that has been partly deformed near the contact of the shear zone. On one side the SAM unit remains intact. On the other side the SAM unit has been sheared and the grain size has been reduced. The schistosity has developed as the result of the preferred crystallographic alignment of the fine-grained minerals. Figure 53 shows the deformed SAM unit inside the boundary of a 16-type shear zone. The grain size of all the original plagioclase minerals has been reduced greatly with increase in intensity of schistosity development. Figure 54 shows further reduction of grain size with further increase in intensity of schistosity toward the centre of the shear zone. Figure 55 shows the most deformed SAM unit found in the centre of the shear zone, which is composed mainly of fine-grained quartz- mica-chlorite rich minerals and which contains two sets of schistosity: c-surfaces and s-surfaces. Microstructurally, the c-surfaces appear as thin layers of crystallized, polymineralic aggregates of quartz, mica, chlorite, and plagioclase with reduced grain size and which are aligned parallel to the main shear zone boundary (parallel to the long dimension of the photograph). The s-surfaces, on the other hand, are defined by the preferred crystallographic orientation of the larger grains of quartz, mica, feldspar and chlorite between the c-surfaces. The s-surfaces are oriented oblique to and curve into the c-surfaces. The angular relationships between the c-surfaces and s-surfaces define the sense of shear in the rock (Simpson and Schmid 1983, Lister and Snoke 1984). In Figure 55 the angular relationships between the two surfaces indicate that the material in the upper parts of the photograph moved left with respect to that in the bottom. Reoriented into its natural position, this indicates reverse sinistral shear on this particular shear zone.

The 16-type shear zones contain two linear fabrics: slickenlines and mineral lineations. The smooth, polished slickensided surfaces are parallel to the c-surfaces. Mineral lineations which also occur within the s- and c-surfaces are comprised of elongated aggregates or single crystals of calcite, leucoxene, feldspar and quartz.

Figure 51: Photomicrograph of the SAM unit unaffected by a 16-type shear zone. Horizontal field of view is 5 mm.

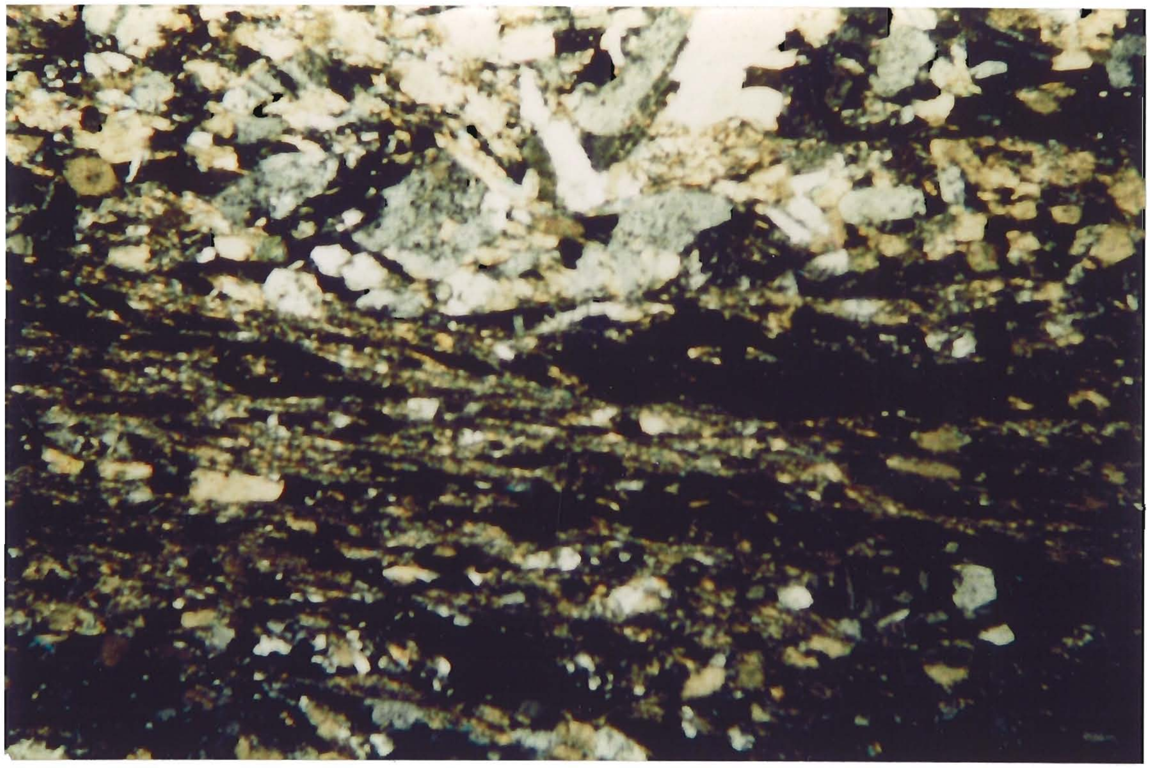

Figure 52: Photomicrograph of the boundary of a 16-type shear zone. The SAM unit on the top part of the photograph is undeformed. The SAM unit on the bottom part of the photograph shows reduced grain-size and schistosity related to shearing. Horizontal field of view is 5 mm.

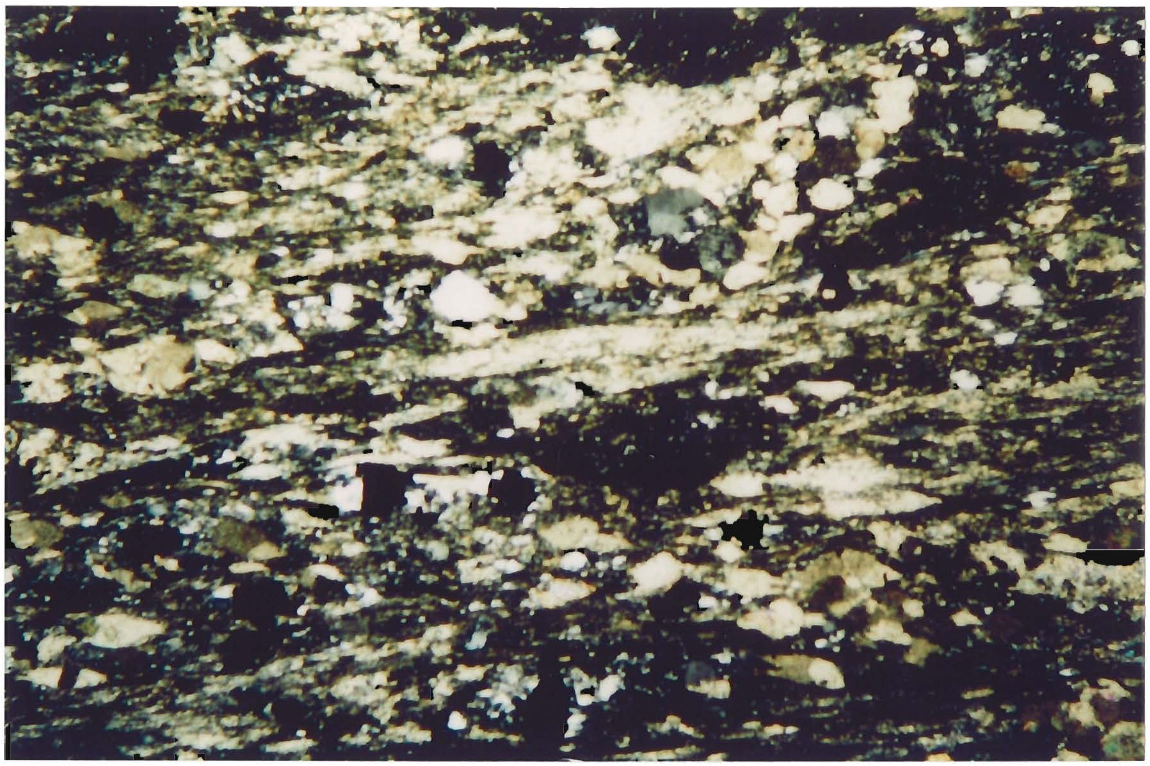

Figure 53: Photomicrograph showing sheared SAM unit inside the boundary of a 16-type shear zone. The reduced grain-size and intensification of schistosity reflect more intense shearing. Horizontal field of view is 5 mm.

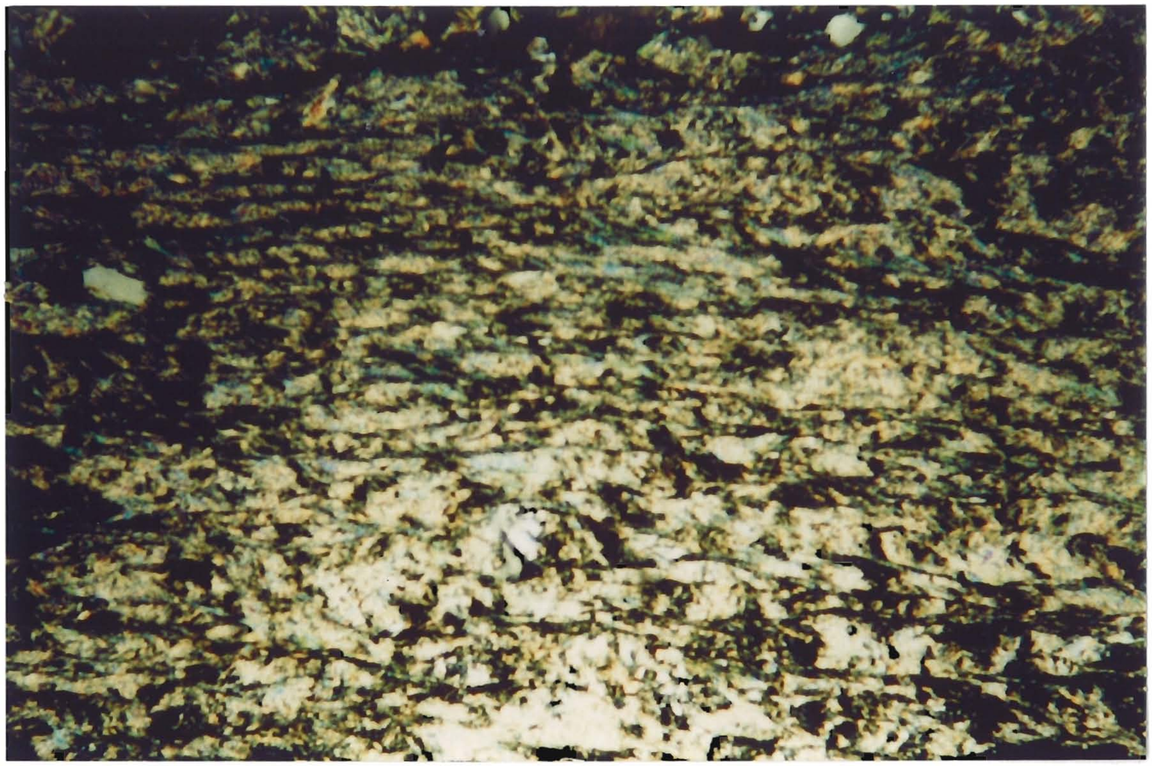

Figure 54: Photomicrograph of sheared SAM unit close to the centre of a 16-type shear zone. Horizontal field of view is 5 mm.

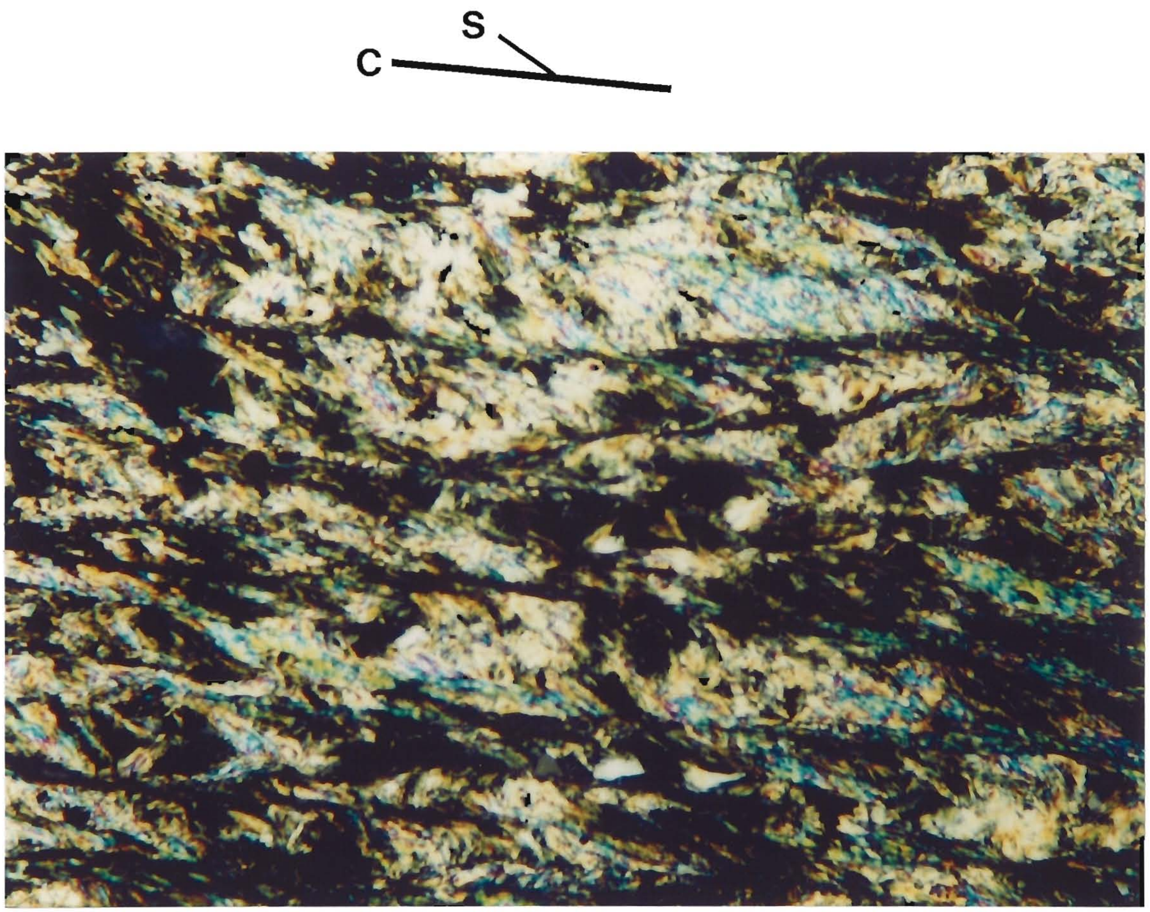

Figure 55: Photomicrograph of sheared SAM unit at the centre of a 16-type shear zone. Where shearing is most intense well developed s- and c-surfaces are present. Horizontal field of view is 5 mm.

Figure 56 is an equal area plot of the slickenlines and mineral lineation directions collected by the author from several 16-type shear zones in the mine. Sixty-six of the data points represent slickenlines and the other 40 data points represent mineral lineations. The maximum concentration of these points is centred on the direction $33^0/N45^0E$. This centre of maximum makes an angle within 10^0 of the mean plane of the shear zone and therefore it is pressumed that the point is on the plane. Relocation of this point on the plane is done by choosing the smallest angle between the point and the mean plane of the shear zone. The new attitude of this point on the plane is $39^0/N54^0E$ (Figure 56). The difference is probably due to (1) the contouring of the two sets of data (i e, the 16-type shear zones and, slickenlines and mineral lineations) and (2) that some of the mineral lineations might have been collected from the s-surfaces.

All the above fabric elements of the 16-type shear zones suggest that they were developed as the result of simple ductile shear deformation.

7.5 INTERPRETATION OF DIRECTION AND SENSE OF MOVEMENT ON THE 16-TYPE SHEAR ZONES

If the slickenlines and mineral lineations that occur within the 16-type shear zones are the products of shear movement, then the general direction of motion indicated by the plunge of these features is $39^0/N54^0E$. In order to account for the left-lateral offsets of the hangingwall and footwall contacts of the SAM unit, of the dikes and of the stockworks by the 16-type shear zones in plan view, it is necessary for the movement on the 16-type shear zones to have been thrust and left-lateral. This interpretation is supported by the s- and c-fabrics in an oriented thin section from a 16-type shear zone (Figure 55).

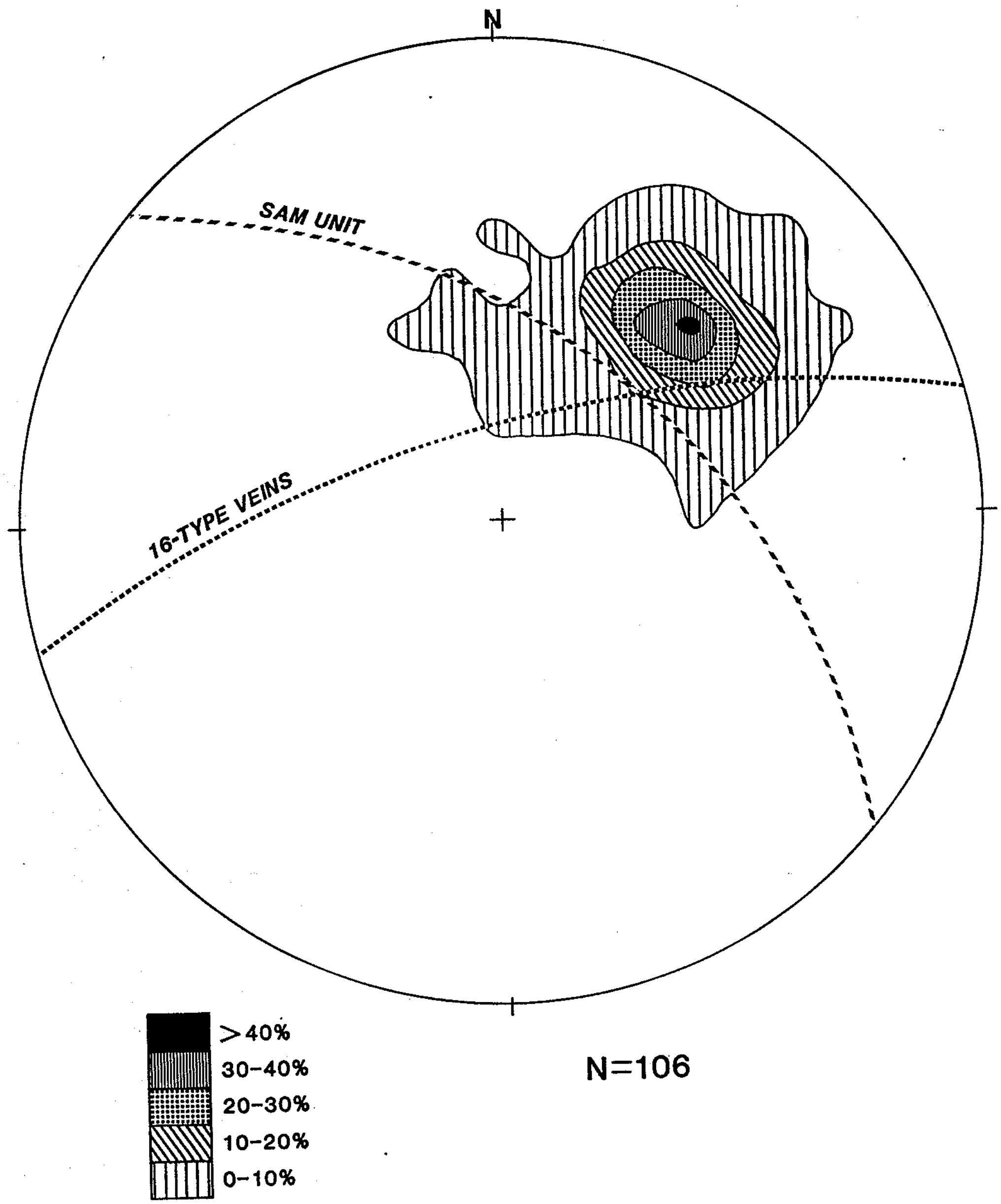

Figure 56: Equal area contour plot of the direction of slickenlines and mineral lineations from 16-type shear zones. Sixty-six data points are slickenlines. Forty data points are mineral lineations. The mean 16-type shear zone orientation is shown for comparison.

Figure 57 is the plot of the mean planes of the SAM unit, the dikes, the stockworks and the 16-type shear zones, and the direction of the slip on the 16-type shear zones. The pitch angles of the mean planes of the SAM unit ($52^0 NE$), dike ($73^0 NE$) and stockworks ($86^0 NE$) on the 16-type shear zones are larger than the pitch of the slip ($43^0 NE$) and thus this may account for most of the left-lateral offsets of the above features on the 16-type shear zones. The fact that there are a few right-lateral offsets of the hangingwall and footwall contacts of the SAM unit may be due to the slip direction of some 16-type shear zones is pitching greater than the line of intersection of the SAM unit and the 16-type shear zones.

The configuration of the principal stress directions at the time of the development of the 16-type shear zones has been determined (Figure 58). The determination of this configuration is based on: (1) the orientation of the 16-type shear zones, (2) the slip direction indicated by slickenlines and mineral lineations, (3) the interpreted sense of slip (hangingwall up and to the left), and (4) the assumption that the 16-type shear zones are shear fractures formed at approximately 30^0 to the direction of the maximum compressive principal stress (σ_1) and 60^0 to the direction of the minimum principal stress (σ_3). If the above observations and assumption are valid, then the directions of the principal stresses at the time of the 16-type shear zones development are: $\sigma_1 = 21^0/N27^0E$, $\sigma_2 = 41^0/N84^0W$ and $\sigma_3 = 41^0/S44^0E$.

The vertical veinlets most abundant in the parts of the stockworks cross-cut by the 16-type shear zones have been interpreted earlier as vein-filled tension fractures which might be related to the same stress configuration that developed the 16-type shear zones. If this is the case, the tension fractures should be

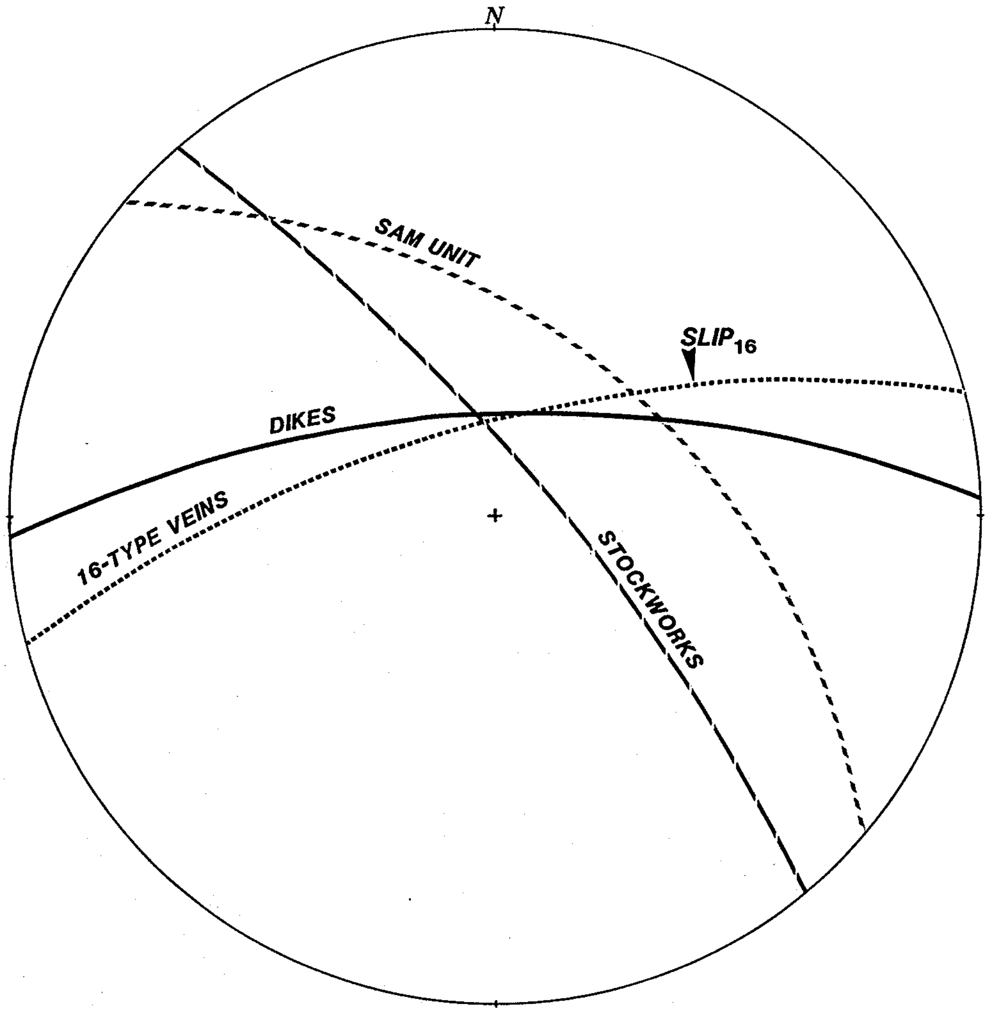

Figure 57: Synoptic projections of mean orientations, including SAM unit, dikes, stockworks, 16-type shear zones and shear zone lineations ($SLIP_{16}$).

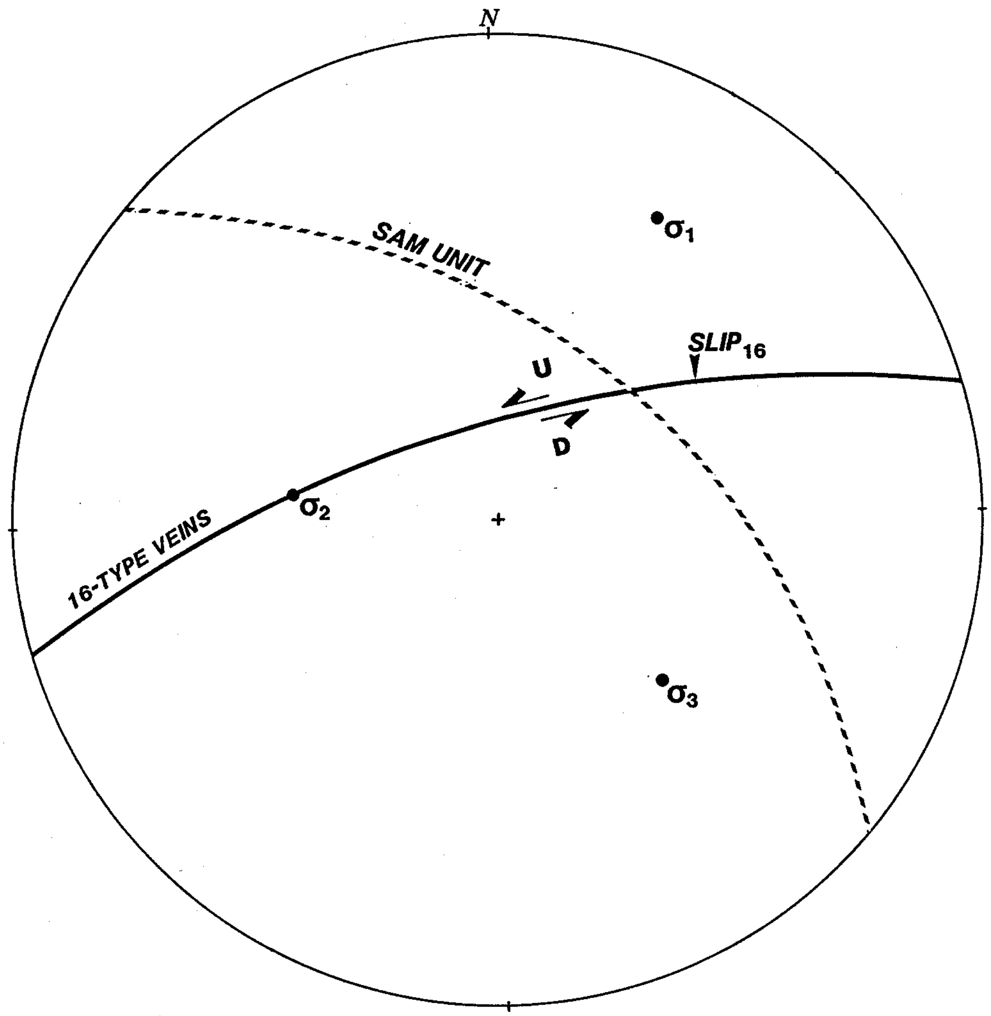

Figure 58: Interpretation of the principal stress directions in the SAM unit at the time of the 16-type shear zone formation.

oriented ideally at $N46^0E/50^0NW$ (the $\sigma_1 - \sigma_2$ plane in Figure 58). The limited number of observations of the real attitudes of these features indicates a strike similar to the ideal situation but much steeper dips. Although the vertical veinlets appear to have developed along with the 16-type shear zones, the problem of the stresses responsible for these features remain unresolved.

7.6 RELATIONSHIPS OF THE 16-TYPE SHEAR ZONES TO HANGINGWALL AND FOOTWALL CONTACTS AND SERICITE SCHIST

The 16-type shear zones occur as discrete zones in the SAM unit spaced at distinct intervals (Figure 59). Otherwise, the SAM unit does not contain a schistosity. The shear zones never extend into the surrounding sericite schist. In contrast, the sericite schist contains a strong penetrative foliation. Although the angles that the 16-type shear zones and the penetrative foliation make with the SAM unit contacts are different, they have a common line of intersection (Figure 60). These relationships are similar to those produced by a refracted cleavage in a rigid tabular unit (the SAM unit) surrounded by a more ductile unit (sericite schist). Wilson (1982), Ramsay and Huber (1983), and Suppe (1985) have dealt with the problem of refracted cleavage, however, their spaced cleavage within the brittle unit does not occur as shear zones. Shearing could be promoted later by the rotation of the brittle unit fragments. In the case of the SAM unit the slip direction interpreted for the 16-type shear zones does not appear to be consistent with such rotation.

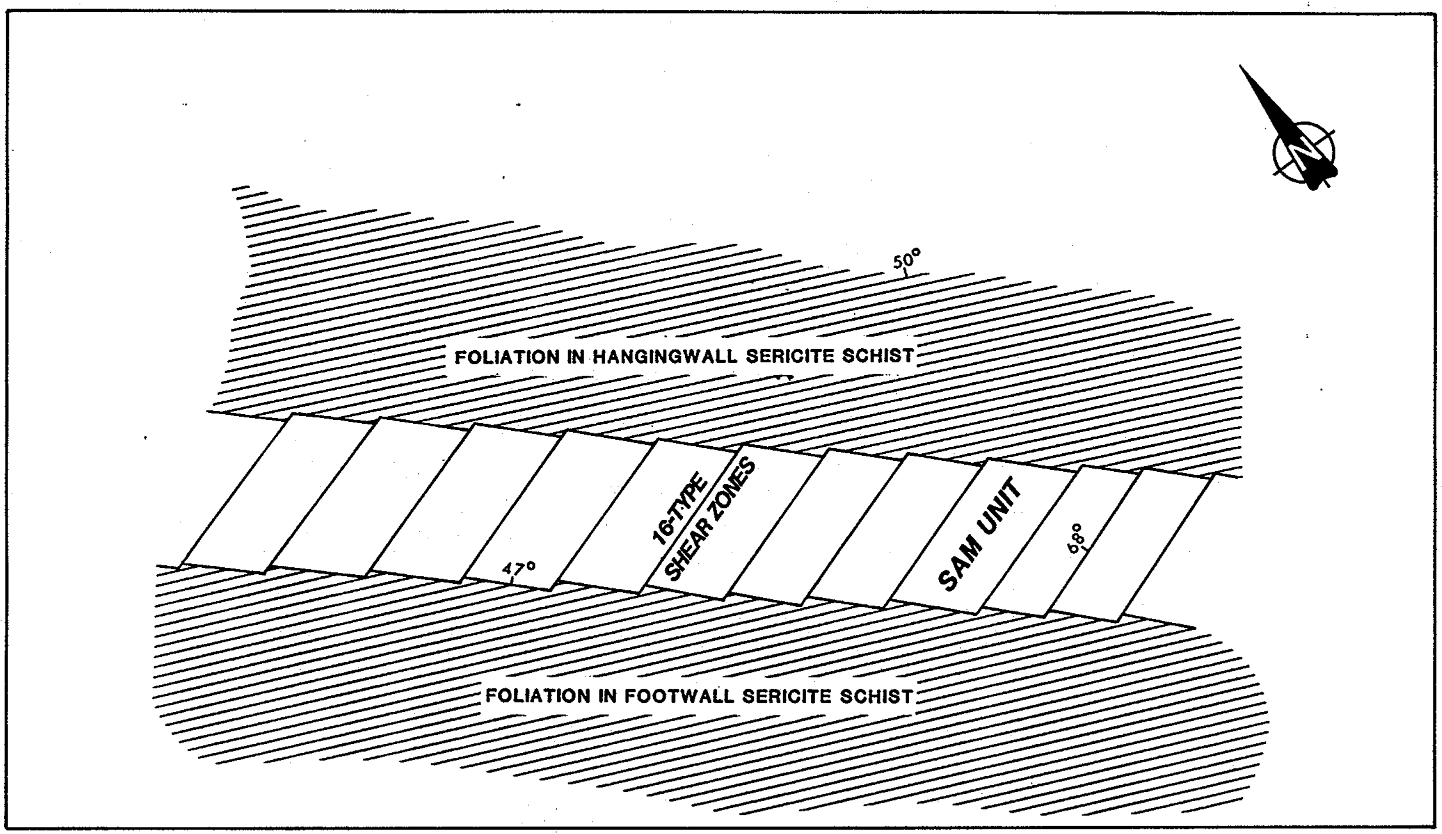

Figure 59: Schematic plan view showing orientation of spaced 16-type shear zones in the SAM unit and penetrative foliation in the sericite schist.

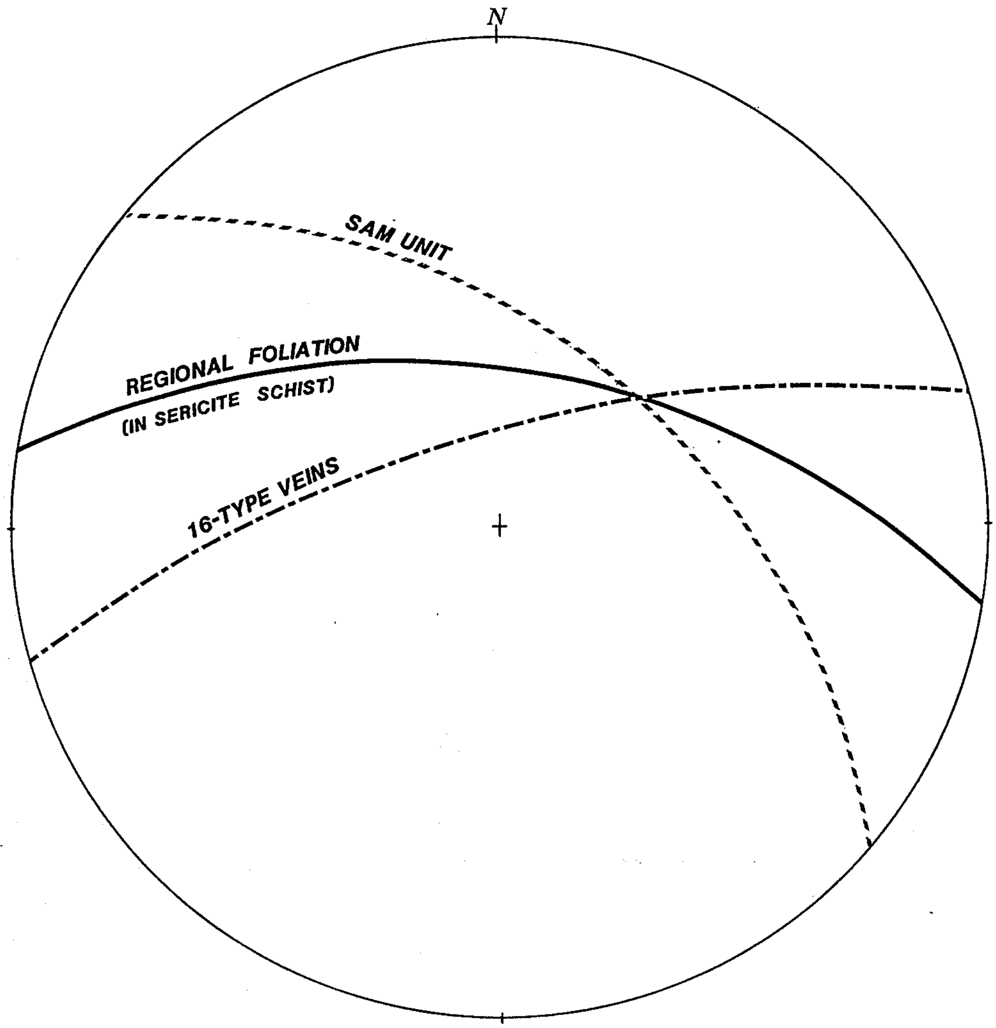

Figure 60: Synoptic projections of the mean orientations of the SAM unit, 16-type shear zones and hangingwall and footwall schistosity.

7.7 THE CHARACTERSTICS OF THE 16-TYPE VEINS

7.7.1 Occurences

The 16-type veins occur within the 16-type shear zones. About 95% of the total number of the 16-type shear zones contain only small amounts of vein material or are completely without vein material. Approximately only 5% of the total number of the 16-type shear zones contained sufficient amount of vein material to constitute ore bodies. Figure 61 (in pocket) is a mine plan which shows those 16-type veins that were large enough to be mined.

7.7.2 Vein Spacing

The average perpendicular distance between strikes of the 16-type veins in plan view is about 15 m, but they can range from a few metres to over 40 m apart. The large veins which have been mined, however, are much wider spaced and their average spacing is about 90 m (Figure 61).

7.7.3 Vein Continuity and Thickness

The strike and down plunge lengths of the 16-type veins are always less extensive than the 16-type shear zones which contain them. Their strike lengths may range from a few metres to about 200 m. Their down plunge dimensions are usually longer than their strike lengths and these may range from a few metres to over 1200 m. The 16-type veins terminate along their strike and up and down plunge by pinching out within the shear zones. There are some 16-type veins, however, which terminate in their up plunge by branching into stringers which cut across the wallrock schistosity and terminate a short distance from the hangingwall contact of the SAM unit.

The 16-type veins commonly pinch and swell (Figure 62). Their thickness

Figure 62: Pinching and swelling of a 16-type vein. The rule is 15 cm.

may range from one or two centimetres to about 2 m (Figures 63 and 64). The thicker parts of most 16-type veins are located closer to the hangingwall than the footwall contacts of the SAM unit. Many 16-type veins diminish in size or terminate near the stockworks even though the shear zones which contain them may cut across the stockworks completely (Figure 47).

The 16-type veins also commonly branch and merge following shear zones which do the same. The most notable of these is the #16 vein (Figure 61) which is joined by numerous smaller veins from adjacent shear zones at varous depths. Locally, stringers may branch out from the main 16-type veins at low angles. These stringers have "wedging" characteristics common to hydraulic fractures (Figures 65 and 66). Dilation of these stringers have wedged out pieces of schistose rock fragments from the adjacent walls.

7.7.4 Vein Composition

The 16-type veins are made up of greater than 95% quartz plus less than 5% combined carbonates, chlorite, albite and pyrite. They are characterized by internal compositional zonation consisting of irregular fringes of coarse-grained quartz-carbonate-albite-chlorite (qtz-cb-alb-chl) surrounding the central core made up dominantly of coarse-grained quartz. These features are depicted schematically in Figure 67. The coarse-grained qtz-cb-alb-chl fringes which form next to the vein walls may range from less than a millimetre to about a centimetre thick. The central quartz cores are the dominant component of the 16-type veins and they may range from a centimetre to about 2 m thick. The central quartz cores also contain patches of carbonates, albite, minor amounts of disseminated pyrite and locally flakes of visible gold.

The compositional zonation of these veins is interpreted to be the result of the diffusion of wall rock consitutents into the shear zones and crystallization of these constituents near the vein contacts. Support for this interpretation comes from the fact that the composition of the adjacent altered wall rocks contain abundant minerals that make up the outer fringes of the veins.

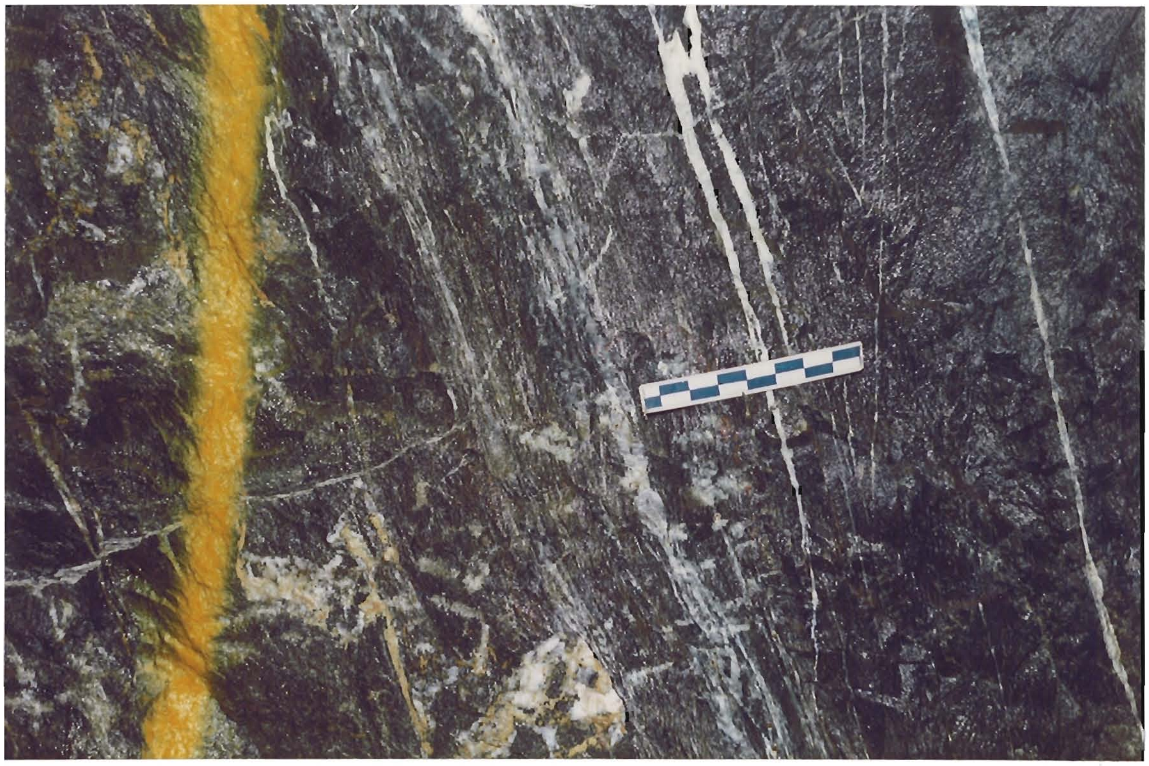

Figure 63: A 16-type shear zone containing thin discontinous veins which follow shear foliation. The rule is 15 cm.

Figure 64: A thick 16-type vein containing schistose wall rock fragments and ribbon structures. The exposure is the face of a take down back. The rule is 15 cm.

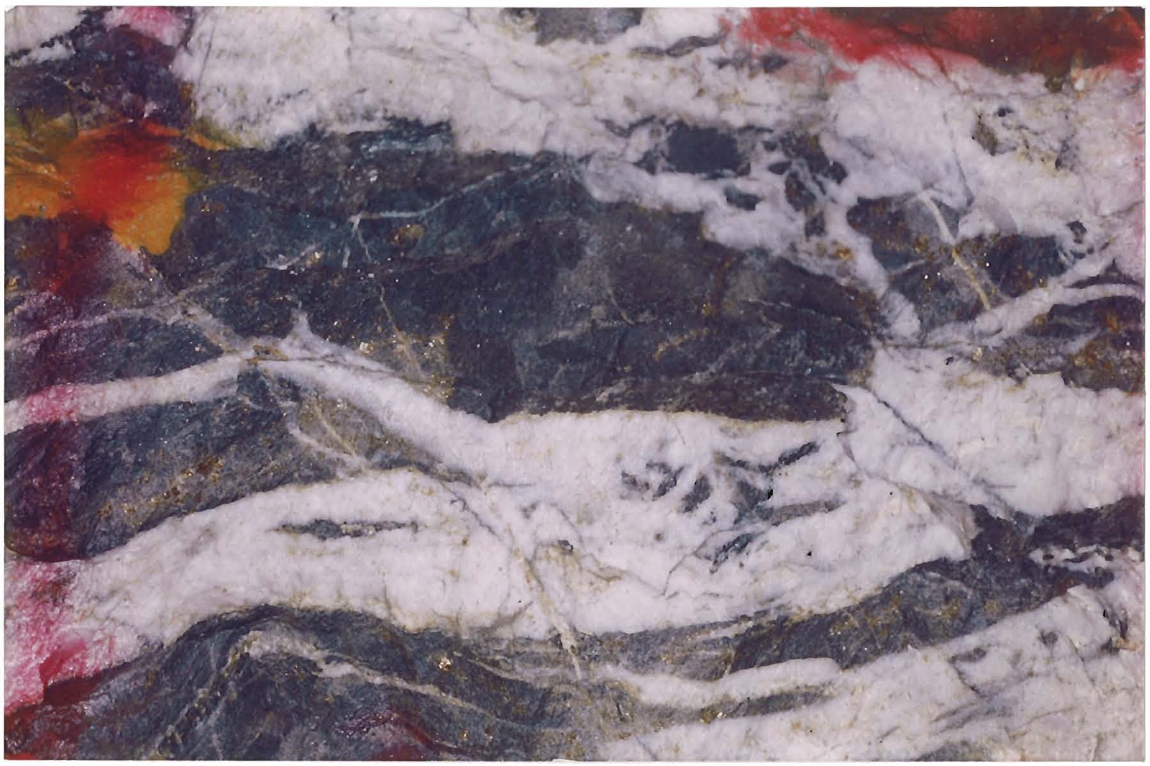

Figure 65: Stringers branch out from a main 16-type vein at a low angle. The stringers have "wedging" characteristics of hydraulic fractures. The exposure is in a drift face. Field of view equals 1.0 m.

Figure 66: Stringers branching out at high angles from a 16-type veins. The stringers have "wedging" characteristics of hydraulic fractures. The vein is exposed in a drift back. Field of view equals 1.0 m.

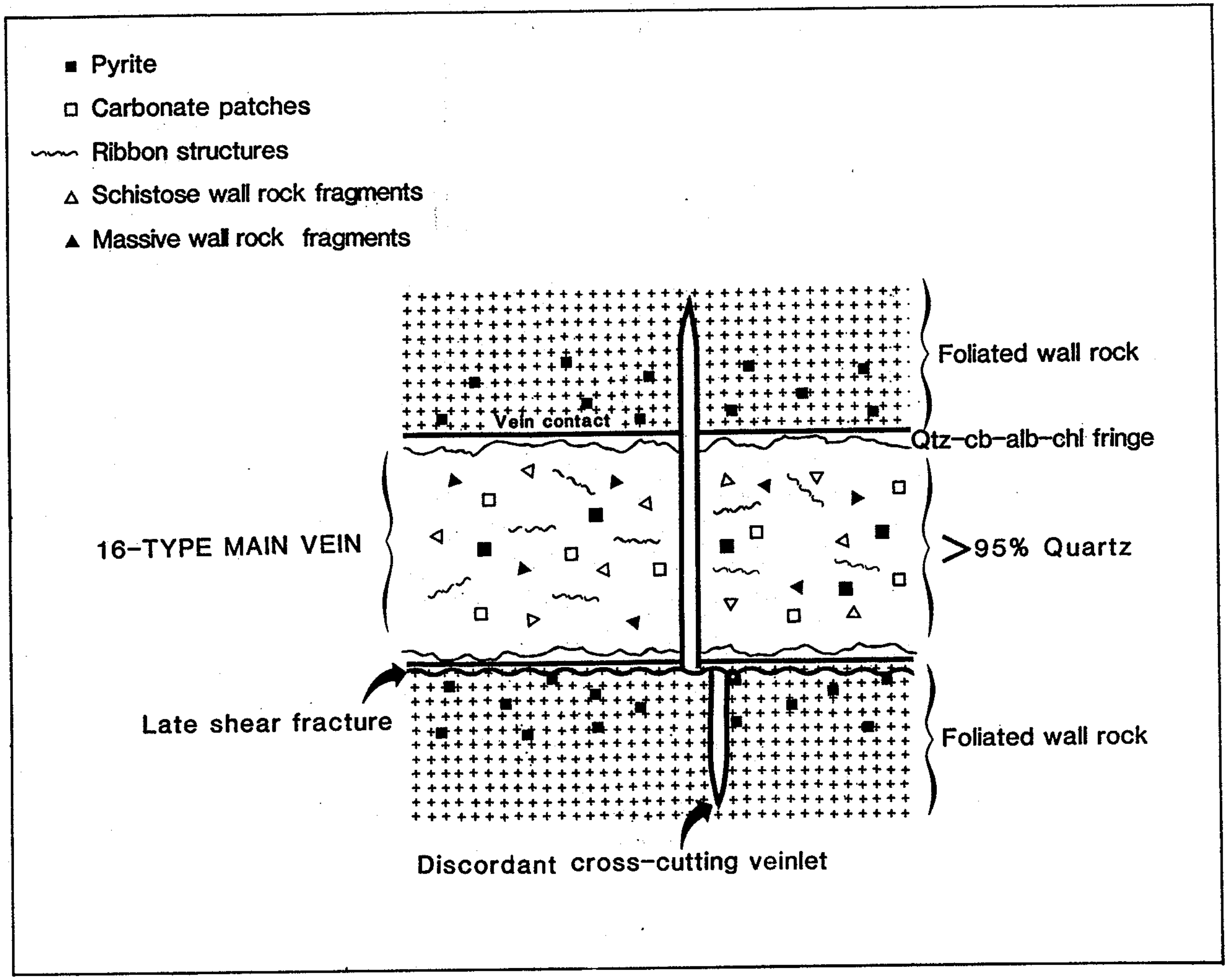

Figure 67: Schematic illustration of the composition zoning and structures of a 16-type vein.

7.7.5 Structures within the 16-type Veins

The 16-type veins contain many internal structures including wall rock fragments, streaks of fine- grained pyrite and stylolitic ribbon structures.

7.7.5.1 Wall Rock Fragments

Most of the wall rock fragments within the veins are schistose and are commonly arranged subparallel to the vein contacts (Figure 68). They may range from a few millimetres by a few centimetres to about 15 cm by a metre. A few angular, massive wall rock fragments which appear to have been derived from shattering of larger fragments have also been found in the 16-type veins (Figure 69).

7.7.5.2 Pyrite Streaks

Many 16-type veins also include solid streaks of fine-grained pyrite arranged subparallel to the vein contacts (Figure 43). They are typically discontinuous within the vein. Their length ranges from a few metres to over 100 m and their thickness varies from a few millimetres to about 2 cm.

There are two possible explanations for the origin of these pyrite streaks. They could have been introduced into fractures within the veins by pyrite-rich fluid, and alternatively, they were the result of mobilization and concentration of pyrite mineral into streaks before vein consolidation. It seems the second alternative is more plausible from the fact that these pyrite streaks are discontinuous within the veins and that there are no evidence of fractures around them in the veins.

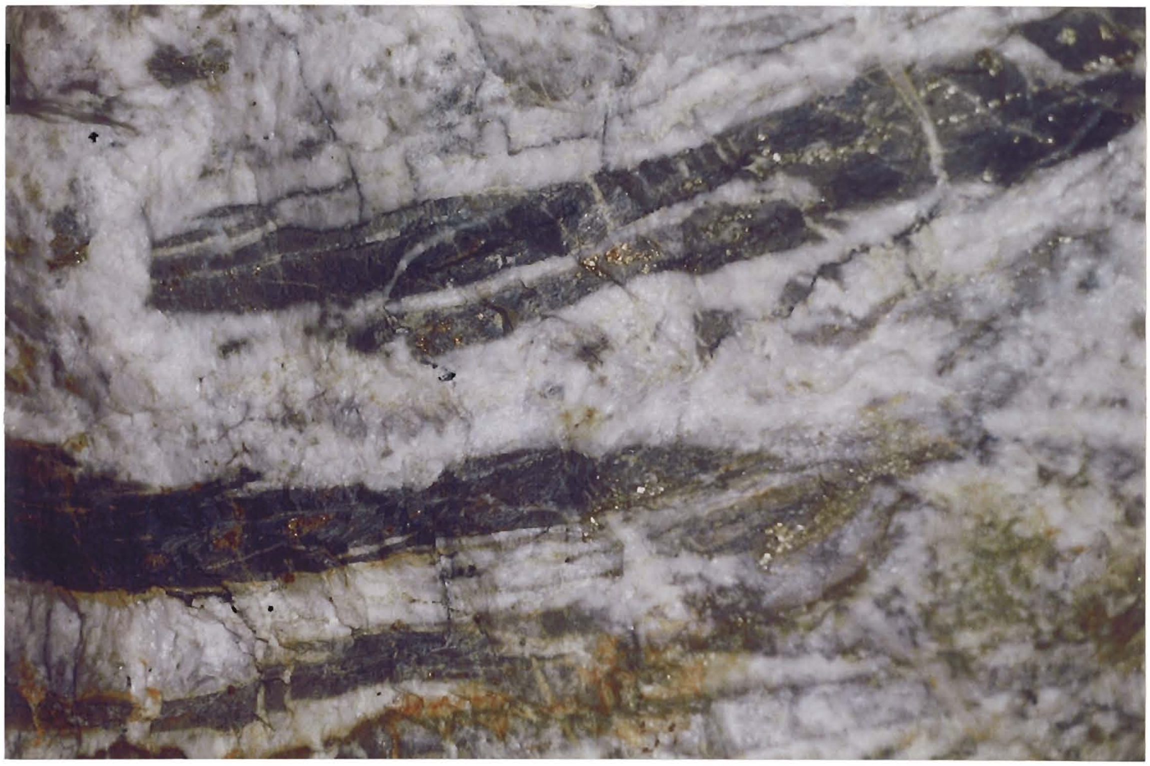

Figure 68: Schistose wall rock fragments and ribbon structures within a 16-type vein. Field of view equals 50 cm.

Figure 69: Wall fragmentation within a 16-type vein.

7.7.5.3 The Stylolitic Ribbon Structures

The 16-type veins contain abundant stylolitic ribbon-like structures (Figures 62, 64, and 68). These structures range from a few millimetres to about 50 cm long and from less than a millimetre to about 5 mm thick. They are oriented randomly within the veins. They are found dominantly in the regions of the veins where abundant wall rock fragments have been incorporated (Figure 68). Examination of a polished slab (Figure 70) and thin sections of these structures reveal that they consist mainly of opaque carbonaceous-like material plus small amounts of fine-grained carbonate, chlorite, sericite and pyrite. The irregular grain boundaries along which this material is concentrated may represent solution boundaries, and the stylolite ribbon structures may represent insoluble residue of the vein material.

7.8 CROSS-CUTTING DISCORDANT VEINLETS

A few laterally discontinuous subsidiary veinlets cut sharply across some 16-type veins (Figure 71). They are vertical and strike 50^0 to 90^0 more to the north than the 16-type shear zones and main veins. Their horizontal and vertical lengths may range from a couple of centimetres to about a metre, and their thickness from a few millimetres to about 2 cm. They have wedge-like terminations. These veinlets are also characterized by internal zonation similar to that of the main 16-type veins.

The fact that these veinlets reveal wedge terminations and internal zonation and are dilational suggest that they are vein-filled tension fractures developed in the already consolidated 16-type main vein possibly related to the late stages of movement on the 16-type structures.

Figure 70: A polished section showing a close up view of a black stylolitic ribbon structures in a 16-type vein.

Figure 71: Subsidiary veinlets cross-cutting a 16-type vein, and late shear fractures. The subsidiary veinlets are approximately normal to the 16-type vein. The late shear fractures are parallel to the 16-type vein and are characterized by rusty bands. They offset the subsidiary veinlets. Field of view is 1.0 m.

7.9 POST-VEIN MOVEMENT

Subsequent to the emplacement of the cross-cutting subsidiary veinlets, most of the 16-type veins have undergone renewed movement along their contacts (Figures 43, 63 and 71). These late shear fractures are characterized by 1-5 cm wide rusty bands of gouge-like material. At places the late fractures may cut across the schistosity of the wall rocks and the veins. They have produced left-lateral horizontal offset of the cross-cutting veinlets measuring 5-10 cm. The amount and sense of true slip on these fractures are unknown. No vein has been emplaced in these late fractures.

The brittle nature of the late shear fractures suggests that the veins in the shear zones had solidified and that the ductility in the adjacent wall rock had been greatly reduced at the time they were developed.

7.10 TIMING OF THE DEVELOPMENT OF BARREN 16-TYPE SHEAR ZONES

Not all the 16-type shear zones in the SAM unit contain 16-type veins. Some are completely without vein material. There are two possible explanations that may account for the presence or absence of vein material in the 16-type shear zones. (1) All the 16-type shear zones were developed simultaneously but only some of them were dilated preferentially by the vein fluid because of the variation in effective pressure in different parts of the shear zones. Support for this idea comes from the fact that some of the shear zones are only partially filled by vein material, and where they are present the veins usually pinch and swell along their strike and down plunge within the shear zones. (2) Alternatively, the family of 16-type shear zones and veins might have been developed over a long period of time and the barren 16-type shear zones were developed after the availability of vein fluid had dropped or disappeared. If this alternative applies, the barren shear zones and the late shear fractures in the vein-filled shear zones might have developed contemporaneously.

7.11 SUMMARY OF THE 16-TYPE VEINS

In summary, the events producing all the structures in the 16-type veins are as follows: (1) Development of spaced ductile shear zones in the SAM unit (possibly at the same time as the development of the regional schistosity in the Rice Lake Group). This produced spaced strength anisotropies in the SAM unit. (2) Hydraulic tensile fracturing, by pressurized vein fluids, of strength anisotropies in the SAM unit followed by variable dilation producing 16-type veins. (3) Consolidation of the main vein precipitates yielded brittle vein mass. Development of cross-cutting fractures and introduction of late vein fluids. (4) Development of late shear fractures along main vein contacts.

The way the SAM unit looks after the development of the dikes, the stockworks and the 16-type structures is portrayed in Figures 72 and 73. Figure 72 is a schematic diagram in plan veiw depicting the SAM unit after it has been extensively cross-cut and segmented into blocks by the family of the 16-type shear zones and veins. Figure 73 is an isometric block diagram made from the level plans of the 14th, 15th and 16th levels portraying the real situation of the San Antonio mine on these levels.

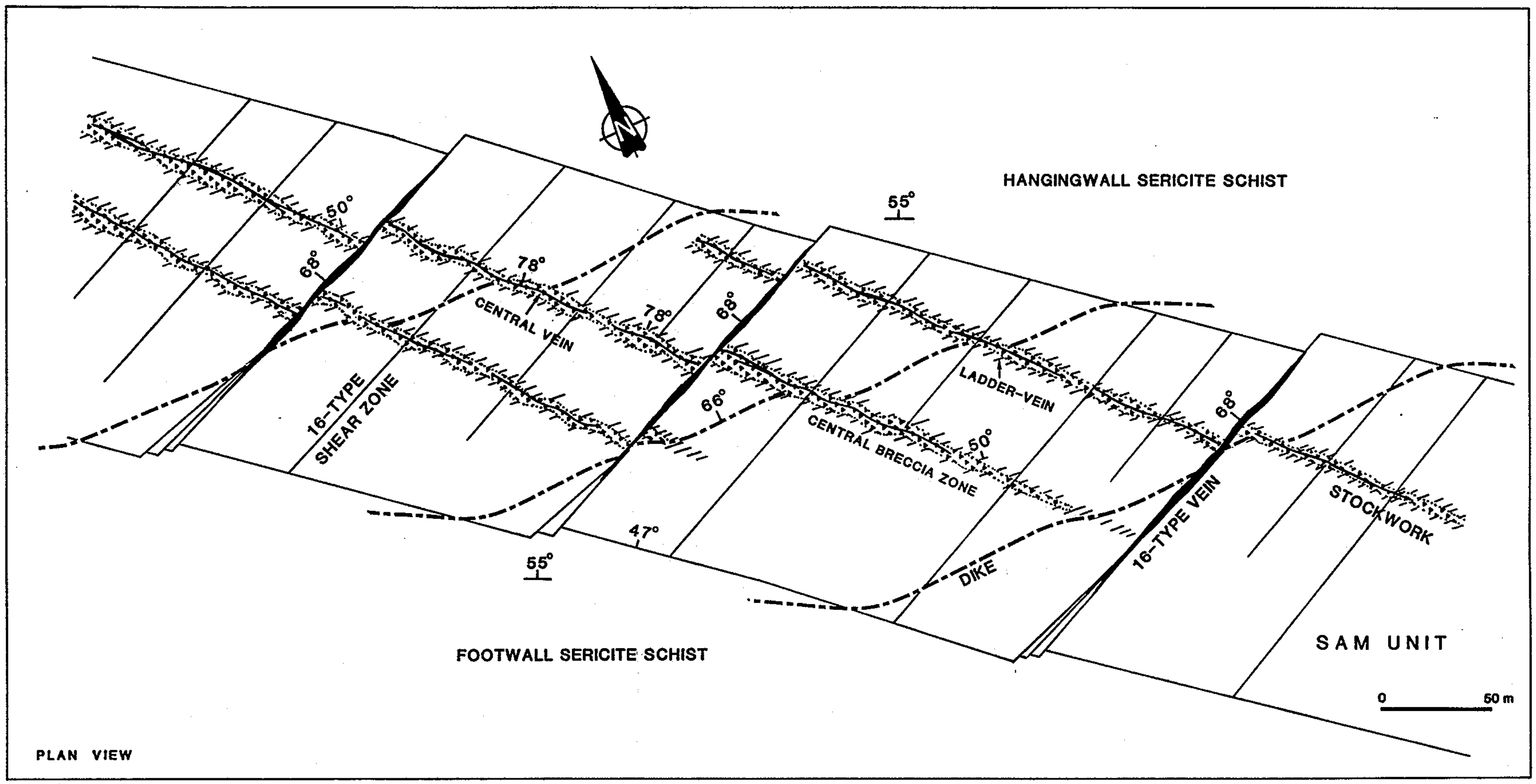

Figure 72: Schematic plan view of the SAM unit after the development of the 16-type shear zones and veins. The SAM unit has been extensively segmented into blocks by the family of the 16-type structures. The hangingwall and footwall contacts of the SAM unit, the dikes and the stockworks all have been displaced in an apparent left-handed direction by 16-type structures.

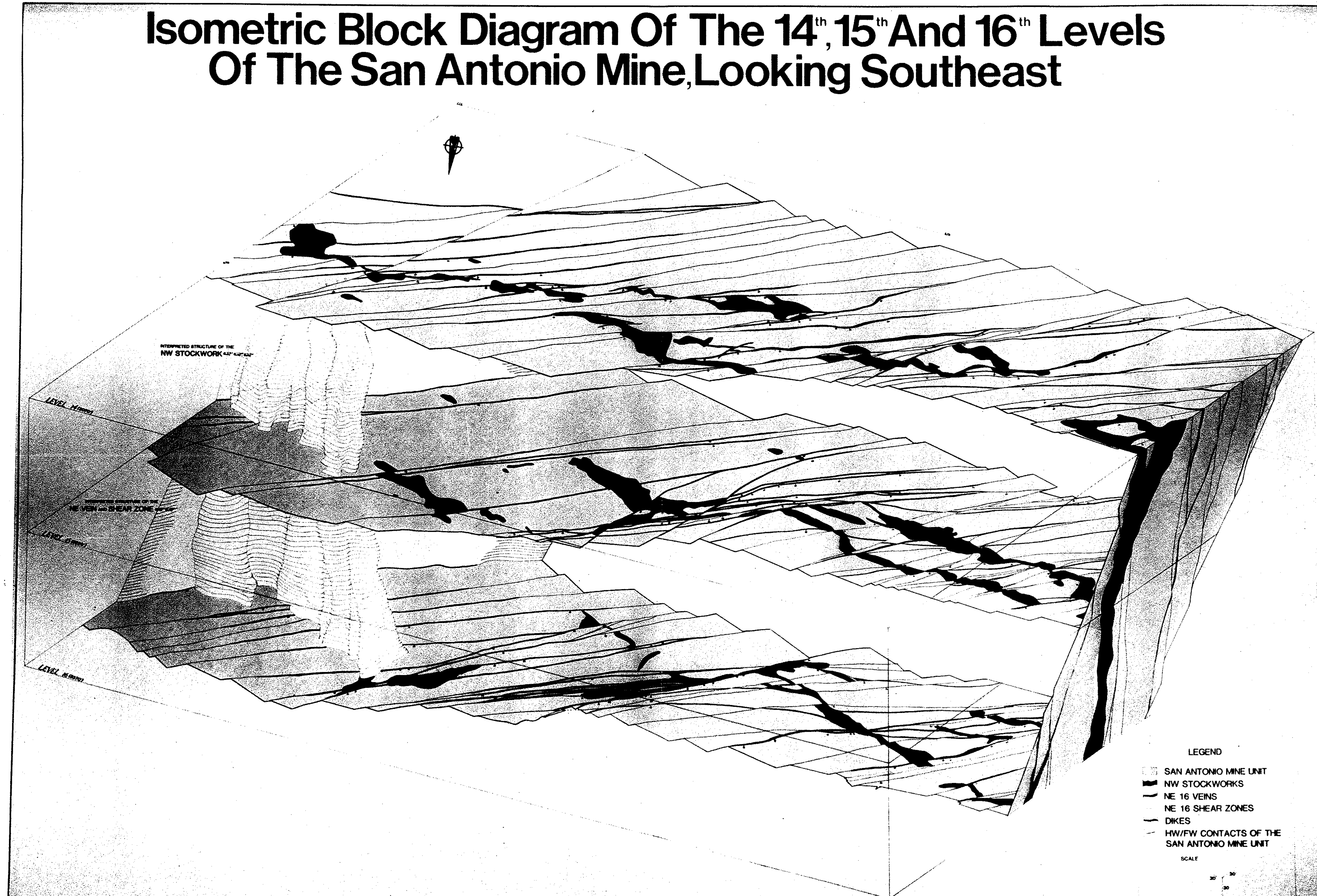

Figure 73: An isometric block diagram of levels 14, 15 and 16 of the San Antonio Mine.

CHAPTER EIGHT

OTHER SETS OF STRUCTURES IN THE SAN ANTONIO MINE

8.1 THE NE/SE VEINS

The NE-striking SE dipping veins occur within narrow tabular shear zones in the SAM unit called NE/SE shear zones. They are not significant from the mineralization point of view and they have been reported rarely in the previous studies. Not all the NE/SE shear zones contain vein material. Some are completely without vein material while others contain only thin, discontinuous stringers. The contacts between the veins and the surrounding schistose wall rocks are always sharp.

Where present in the shear zones, the veins cut across the schistosity of the wall in some locations and the wall rock fragments included in the veins are schistose. Consequently, there are good evidence to suggest that the shear zones were formed before the introduction of the vein material. Figure 74 is a photograph of a typical NE/SE vein.

8.1.1 The NE/SE Shear Zone

There are less than a hundred members of this set of shear zones that have been observed in the mine. Figure 75 is the plot of the poles to all of these NE/SE shear zones. Twenty data points are measurements taken by the author in the mine. The other 118 data points were taken from the mine level plans. The greatest concentration of the poles represents an attitude of $N36^0E/70^0SE$.

Figure 74: A folded NE/SE vein occurs within sheared SAM unit and contains numerous seams of schistose wall rock fragments arranged parallel to the vein contact. Stylolitic ribbon structures are present also. The exposure is a mining face looking northwest. Folding of the vein is rare. The rule is 15 cm.

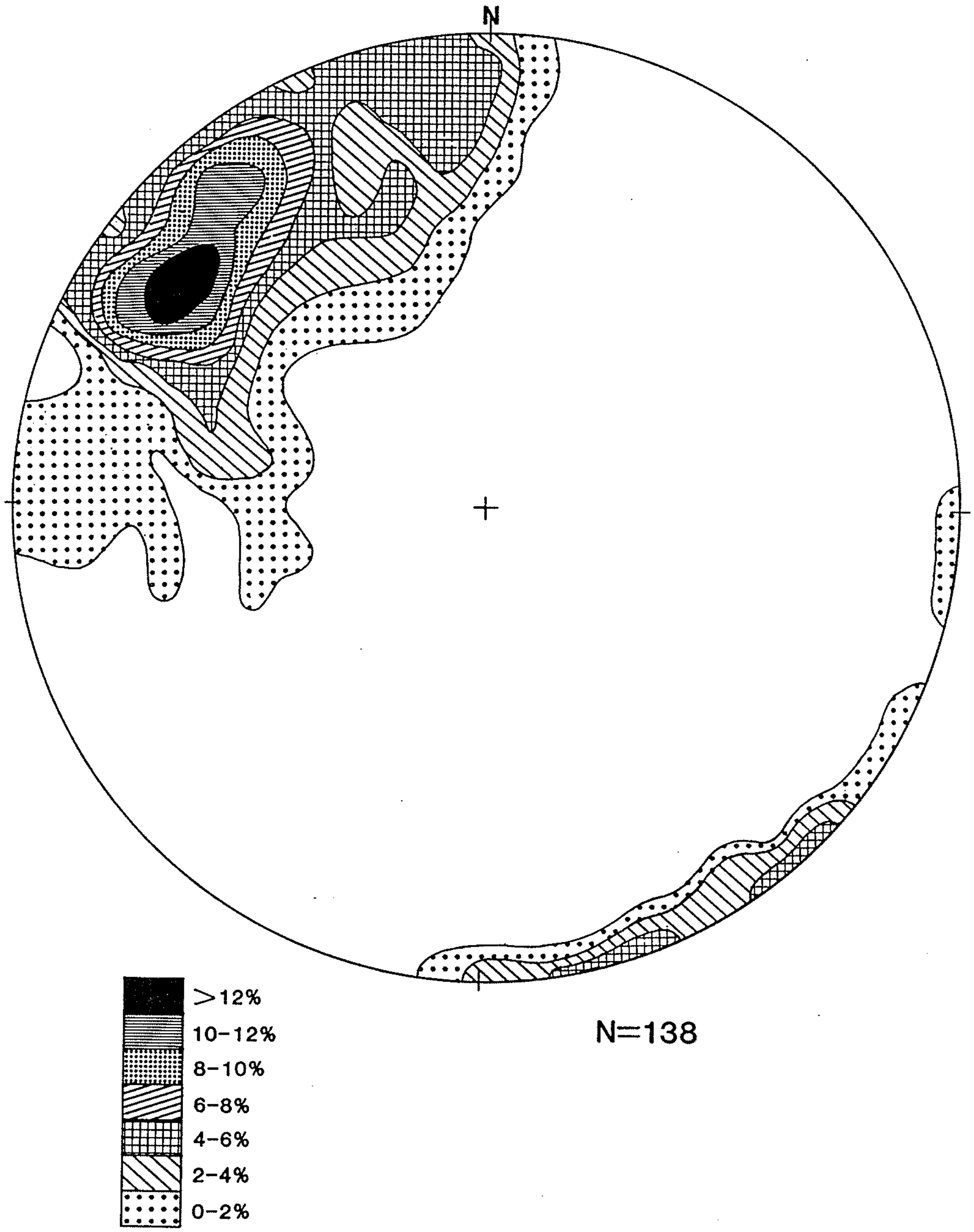

Figure 75: Equal area contour plot of the poles to the NE/SE shear zones. Twenty of the data points are measurements taken by the author in the mine. The other 118 data points were taken from the mine level plans.

The NE/SE shear zones are widely spaced throughout the SAM unit. All except one of these shear zones are very localized and their strike and down plunge lengths may range from a few metres to about 50 m and their thickness from one or two centimetres to 50 cm. The one exception is a large prominent shear zone which has a strike length of 250 m (i.e. it traverses across the whole SAM unit) and which extends over 700 m down plunge. It has a thickness of 2 m. There is insufficient data to tell whether or not this shear zone continues beyond the SAM unit. The location of this prominent shear zone is shown in Figure 61.

The dikes, the stockworks (Figure 76) and the 16-type shear zones and veins (Figure 77) all have been offset by the NE/SE shear zones. The apparent diplacement of all these features in plan view is right-lateral and the amount of apparent displacements may range up to 5 m. In cross-section 16-type shear schistosity and veins show a reorientation that can be interpreted as due to drag and which suggests reverse movement in the NE/SE shear zones (Figure 77).

The rocks within and outside the NE/SE shear zones have very similar mineralogical and textural characteristics to the rocks within and outside the 16-type shear zones. The rocks within the NE/SE shear zones also contain schistosity, slickenlines and mineral lineations. The schistosity is oriented parallel to the shear zone boundaries and it commonly exhibit slickensided surfaces. Also, within the schistosity, mineral lineations comprised of elongated aggregates of calcite, leucoxene, feldspar and quartz grains are very common. Figure 78 is an equal area plot of the slickenlines and mineral lineations on the NE/SE shear zones collected by the author from several locations in the mine. Five data points are slickenlines measurements where the other three data points are mineral lineations.

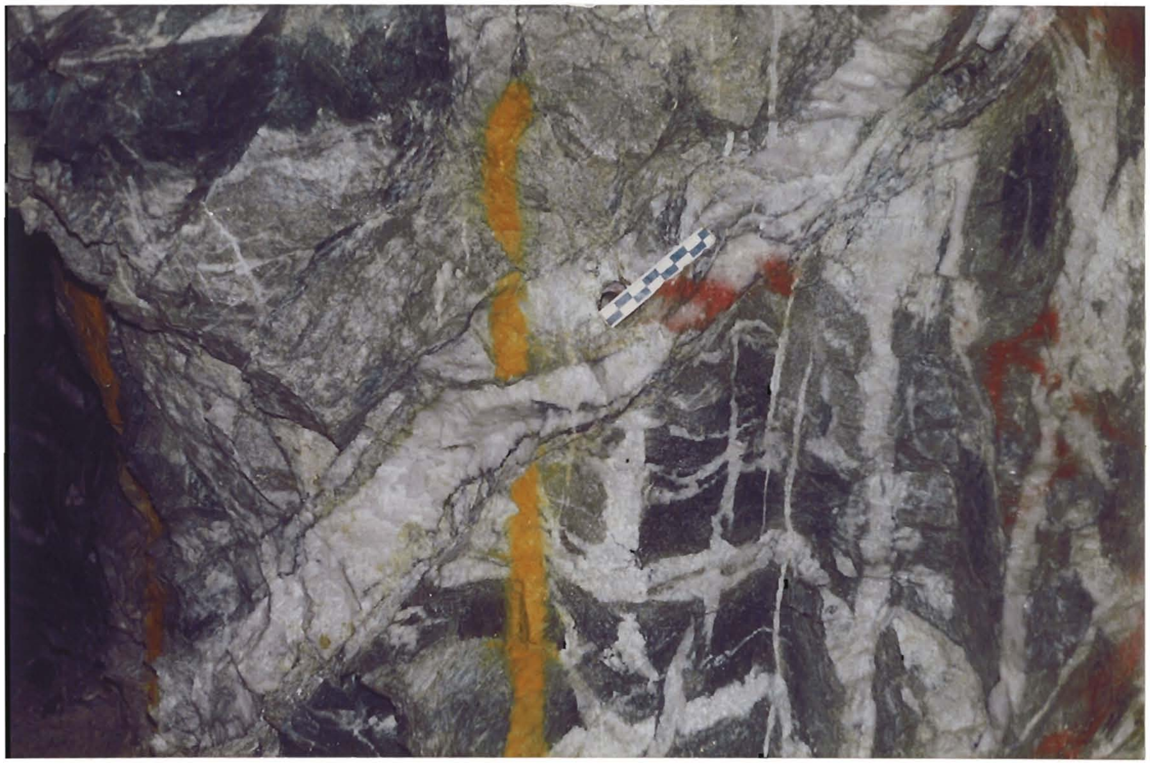

Figure 76: A NE/SE vein cross-cuts and displaces a stockwork. (NE/SE vein lower left to upper right, stockwork on lower right). The rule is 15 cm.

Figure 77: Cross section of a NE/SE vein cross-cutting and offsetting a 16-type shear zone containing thin 16-type veins.

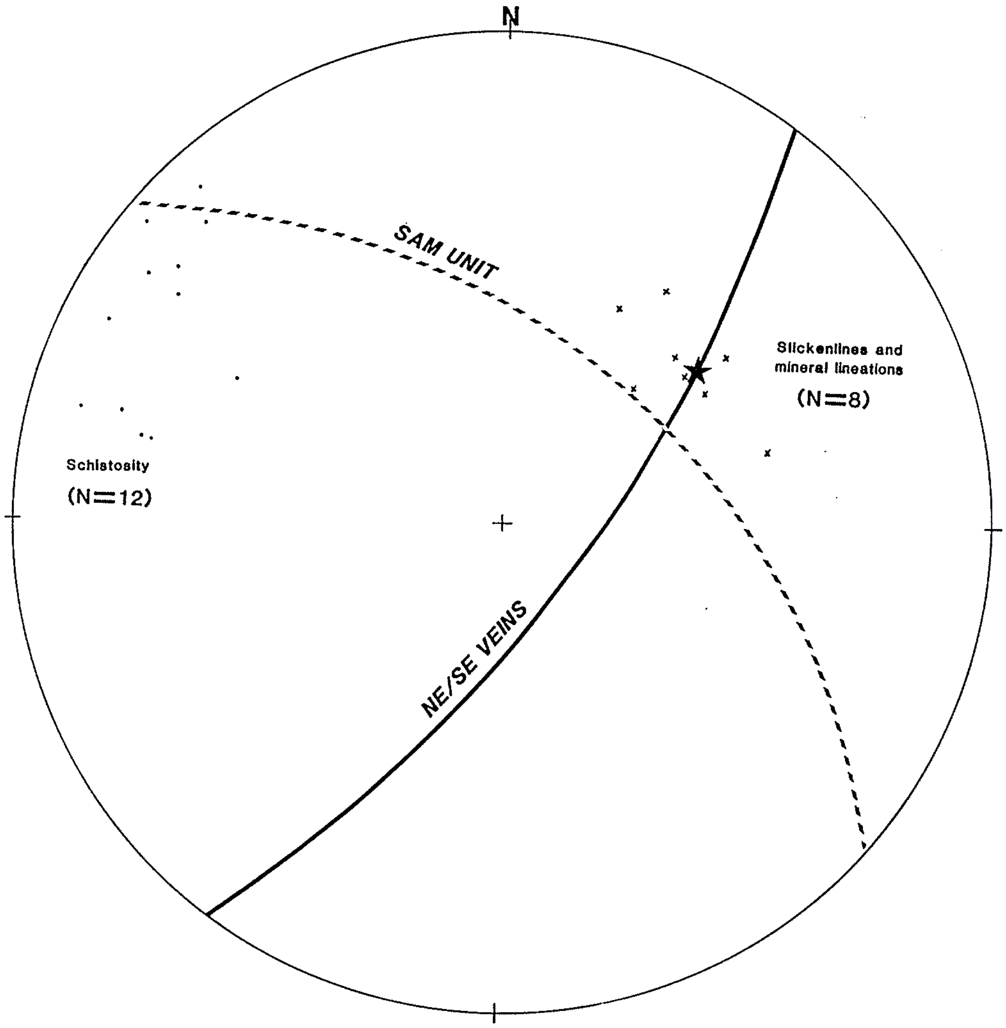

Figure 78: Stereographic plots of the directions of slickenlines and mineral lineations on the NE/SE shear zones and mean plane of the NE/SE shear zones. Five slickenlines measurements and three mineral lineation measurements were collected from several NE/SE shear zones in the mine. The star represents the best projection of these slickenlines and mineral lineations on the NE/SE shear zones.

Figure 78 also shows that the mean plane of the NE/SE shear zones passes through this cluster of points and therefore it is presumed that these slickenlines and mineral lineations lie on the NE/SE shear zones. A point on the mean NE/SE plan therefore is chosen to represent the attitude of these slickenlines and mineral lineations. If these slickenlines and mineral lineations are the products of shear movement, then the slip is pitching $39^0 NE$ on the shear zones. This orientation of slip, combined with the observed offsets of dikes and 16-type shear zones lead to the interpretation that the movement on the NE/SE shear zones is hangingwall up and to the left. Figure 79 is a synoptic projections of the mean orientations of the SAM unit, dikes, stockworks, 16-type structures, NE/SE veins and slickenlines and mineral lineations on the NE/SE shear zones. The pitch of the slip on the NE/SE shear zones is smaller than the pitch of other features on the NE/SE shear zones. Thrust movement on the NE/SE shear zones therefore have offset the above features in right-lateral fashion.

The configuration of the principal stress directions at the time of the NE/SE shear zone formation has been determined (Figure 80). The determination of this configuration is based on: (1) the orientaton of the NE/SE shear zones, (2) the slip direction indicated by slickenlines and mineral lineations on the shear zones, (3) the interpreted sense of slip (hangingwall up and to the left), and (4) the assumption that the NE/SE shear zones are shear fractures formed at approximately 30^0 to the direction of the maximum compressive principal stress (σ_1) and 60^0 to the direction of the minimum principal stress (σ_3). If the above observations and assumption are valid, then the directions of the principal stesses at the time of the NE/SE shear zone formation are $\sigma_1 = 20^0/N79^0E$, $\sigma_2 = 47^0/S13^0W$ and $\sigma_3 = 37^0/N25^0W$.

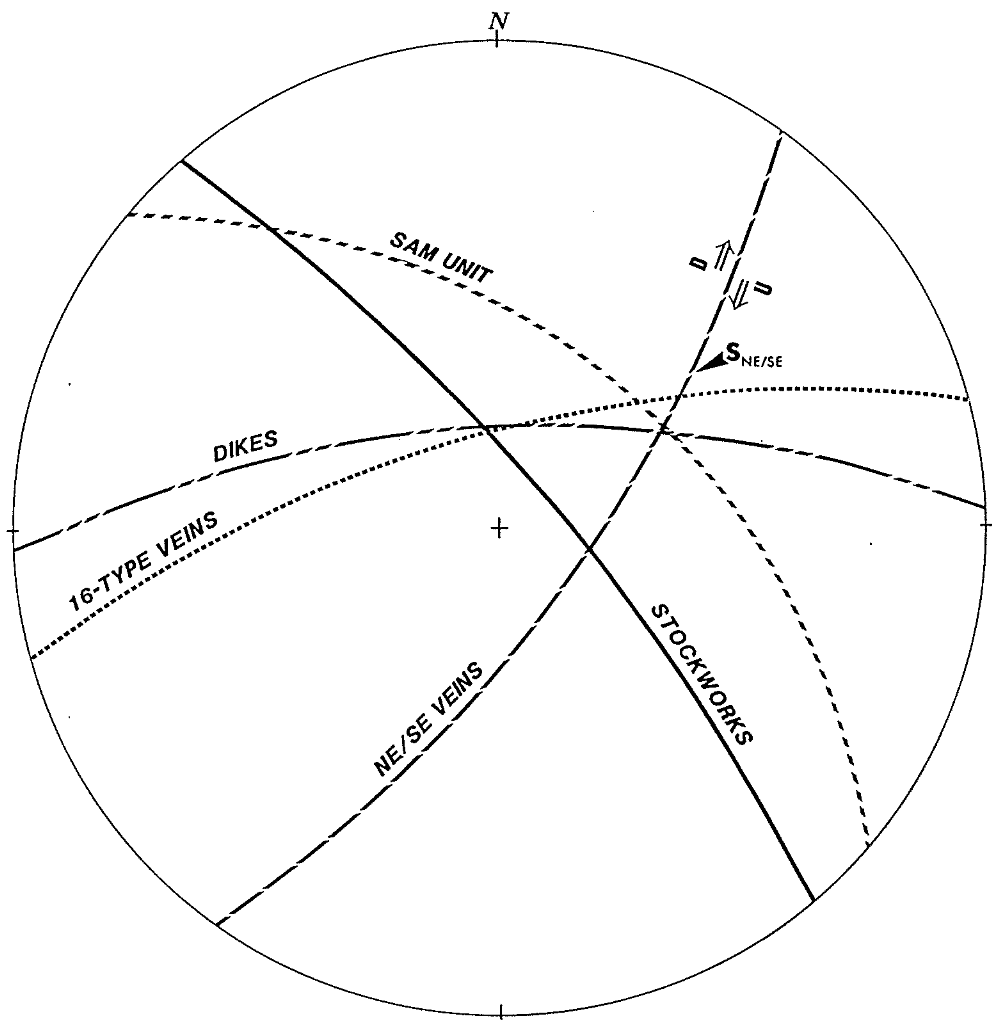

Figure 79: Synoptic projections of the mean orientations of the SAM unit, dikes, stockworks, 16-type structures, NE/SE veins and lineations on NE/SE shear zones.

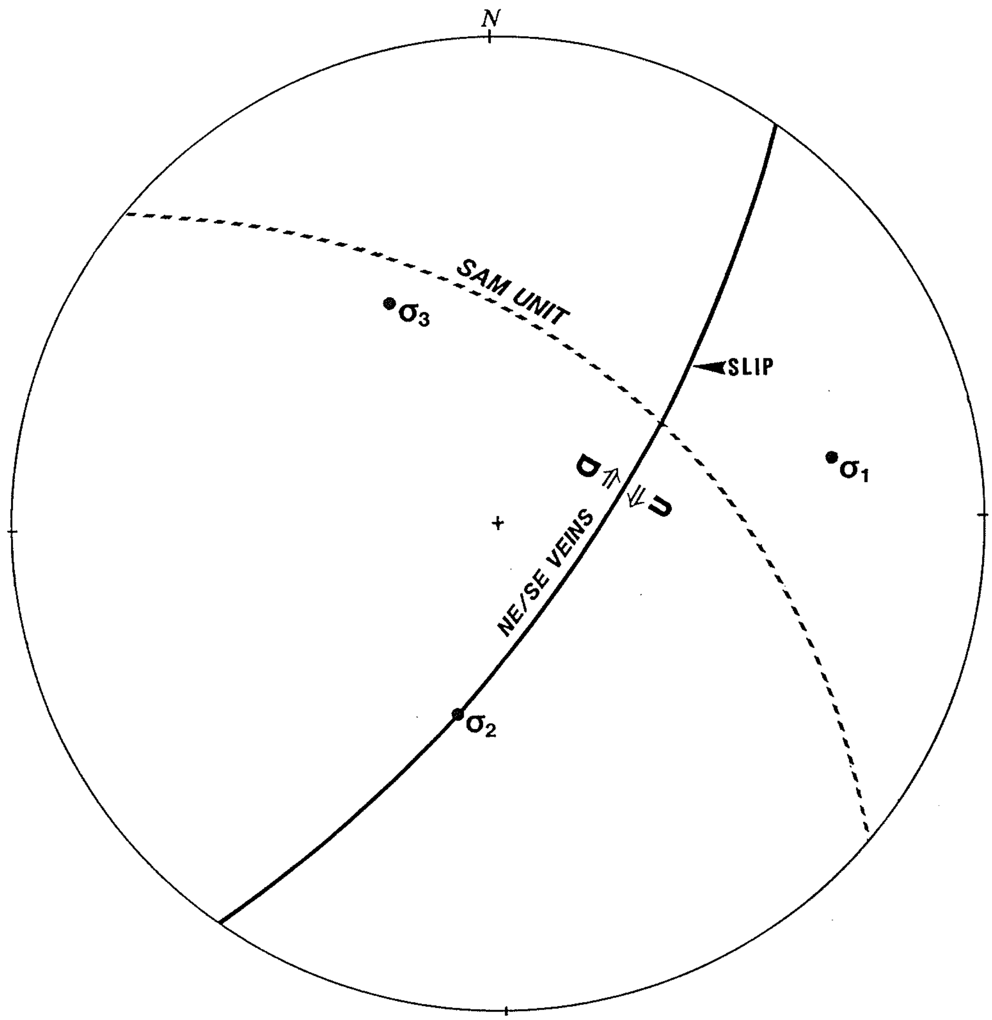

Figure 80: Interpretation of the principal stress directions in the SAM unit at the time of the NE/SE shear zones development. Assumption: $\phi = 30^0$.

8.1.2 Characteristics of the NE/SE veins

The NE/SE veins are widely spaced in the SAM unit as are the shear zones which contain them. The strike and down plunge lengths of these veins are always less extensive than the shear zones. Their strike and down plunge lengths of all except the vein in the prominent shear zone range only a few metres to 50 m and their thickness from one or two centimetres to 5 cm. Within the prominent shear zones the strike and the down plunge lengths of the vein are about 150 m and 700 m respectively, and it has a thickness of 20 m.

The NE/SE veins are made up dominantly of quartz and small amounts of carbonate, albite, pyrite and chlorite. They also contain thin slivers of schistose wall rock fragments and small amounts of stylolitic ribbon structures (Figure 74) similar to those in the 16-type veins. The sliver of wall rock fragments are always arranged parallel to the vein wall. The NE/SE veins were probably developed as a result of hydraulic tensile fracturing, by pressurized vein fluids, of strength anisotropies produced by the pre-existing NE/SE shear zones. Figure 81 is a schematic diagram in plan view showing the SAM unit after the development of the prominent NE/SE vein-filled shear zone.

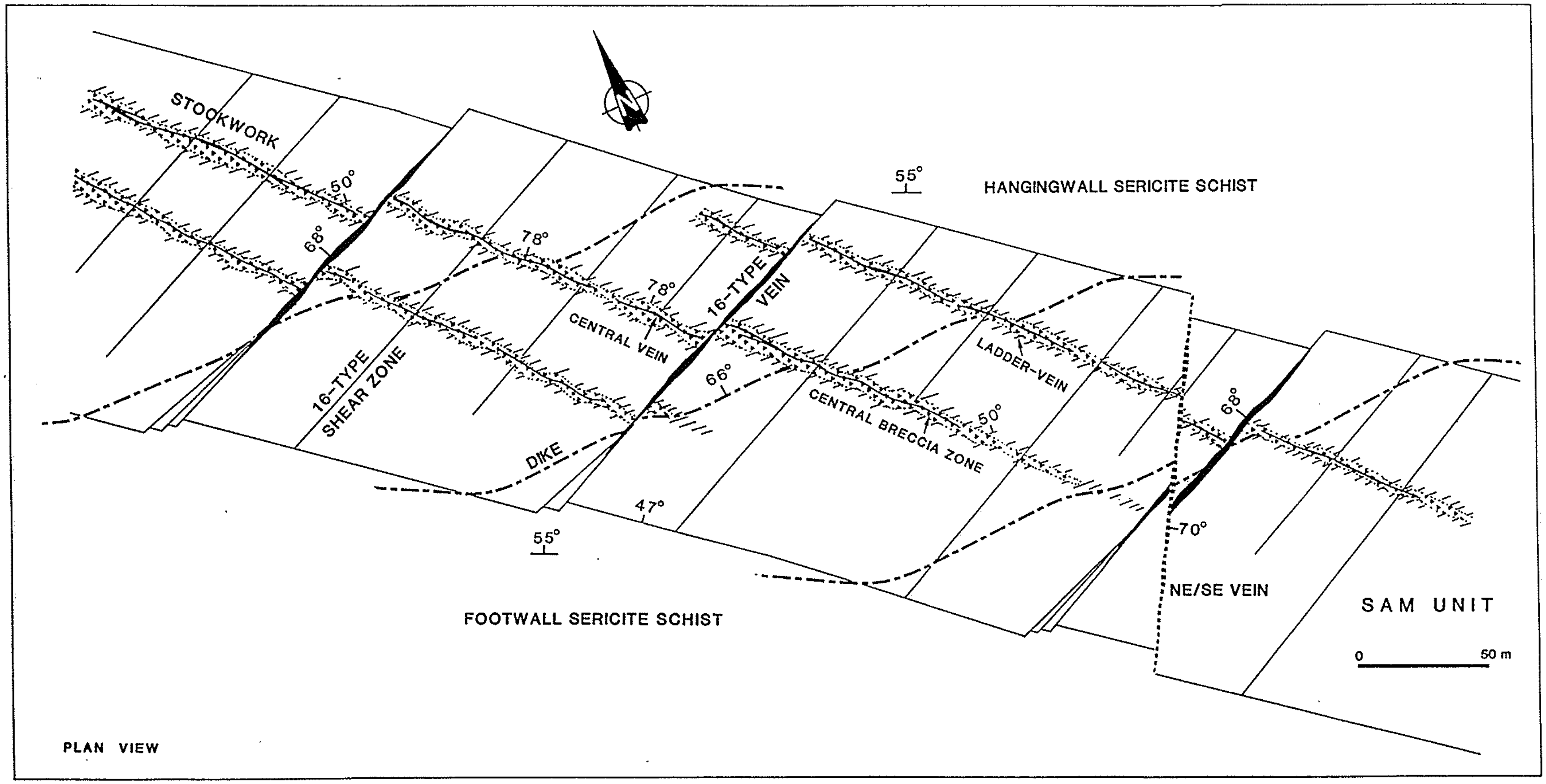

Figure 81: Schematic plan view of the SAM unit after the development of a NE/SE shear zone.

8.2 THE NW/SW VEINS

This is the final set of veins which has a different attitude than the other sets. It consists of a prominent vein on the 6th and 7th levels (Figure 61) where there are no major stockworks and a few subordinate veins at other levels in the mine. The prominent vein strikes $N55^0W$ and it dips 75^0SW. The strike and down dip lengths of this vein are about 300 m and 130 m respectively, and it has a thickness of 40 cm (Figure 82). There is no sign of it pinching out as it approaches very close to the hangingwall and footwall contacts of the SAM unit but there is insufficient evidence to tell whether it continues beyond the SAM unit or not. It has sharp contacts and the wall rock adjacent to the fracture exhibits no strain fabric. The dikes, 16-type and NE/SE sets of shear zones all have been offset by this vein-filled fracture. However, this fracture has not been observed to come in contact with the stockworks, but it is inferred that it is younger than the stockworks from the fact that it offsets the 16-type and NE/SE sets of shear zones.

Using a displaced 16-type shear zone and a NE/SE shear zone, it has been possible to determine the net slip on this fracture. The net slip pitches 45^0SE, is 7.1 m long and with hangingwall side up. Using the net slip and the assumption that the NW/SW fracture is shear fracture formed at approximately 30^0 to the direction of the maximum compressive principal stres's (σ_1) and 60^0 to the direction of the minimum principal stress (σ_3), the configuration of the principal stresses at the time of the NW/SW fracture development are: $\sigma_1 = 19^0/S11^0E$, $\sigma_2 = 54^0/N72^0W$ and $\sigma_3 = 30^0/N69^0E$ (Figure 83).

The vein is composed of mainly quartz and minor amounts of carbonate, chlorite, albite and pyrite. There are few wall rock fragments included within the vein.

Figure 82: Cross section of the most prominent NW/SW vein-filled fracture on level 6 of the San Antonio mine. The fracture cuts across 16-type schistosity. The width of the vein is about 40 cm. The exposure is a mining face looking northwest.

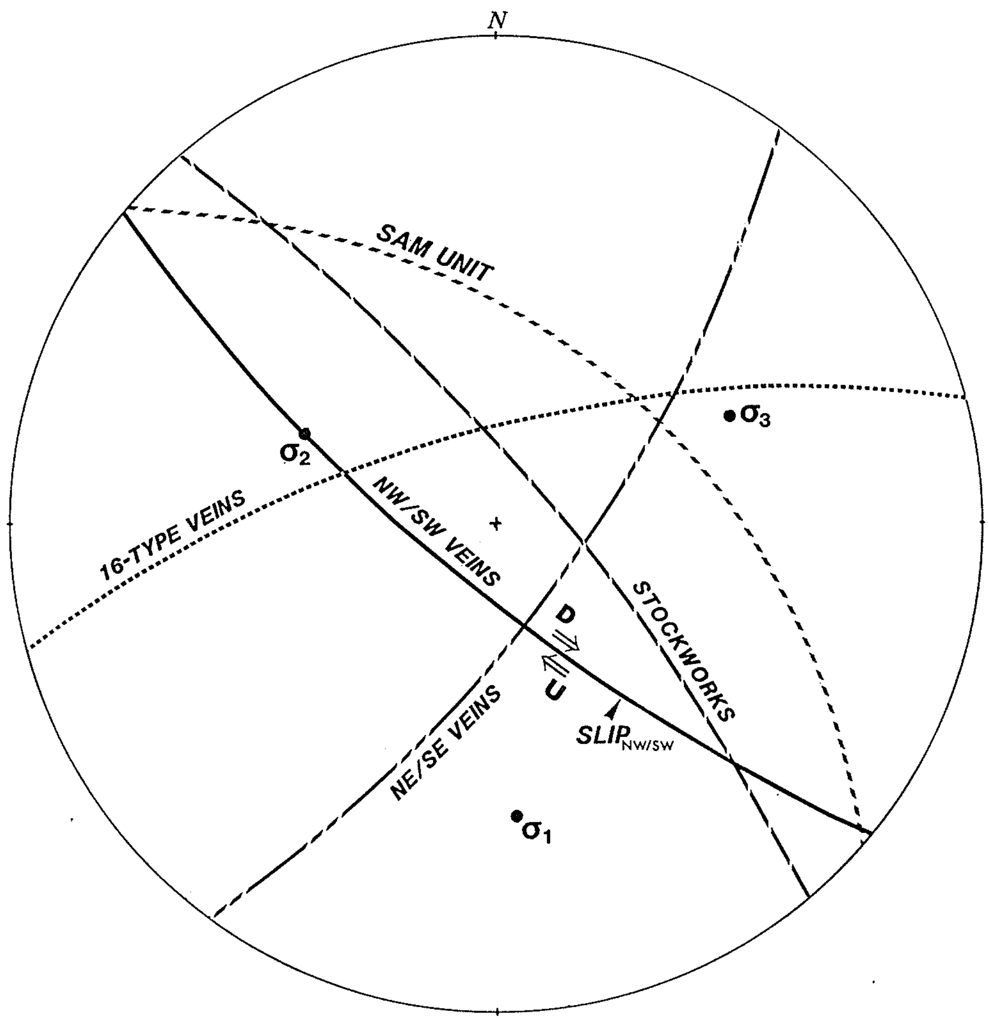

Figure 83: Interpretation of the principal stress directions in the SAM unit at the time of the main NW/SW shear fracture development. Assumptions : (1) NW/SW fracture is formed by shear and (2) $\phi = 30^0$.

The lack of strain fabrics in the wall rocks adjacent to this vein-filled fracture suggests that it is probably a brittle fault and that fracturing and vein intrusion were probably coeval to reduce the frictional resistance during displacement. Figure 84 is a schematic diagram in plan view showing the relationships between the prominent NW/SW vein-filled fracture and the dikes, 16-type and NE/SE sets of shear zones. Figure 85 is a schematic diagram in cross-section of the SAM unit showing the displacement of the hangingwall and footwall contacts of the SAM unit by the prominent NW/SW vein.

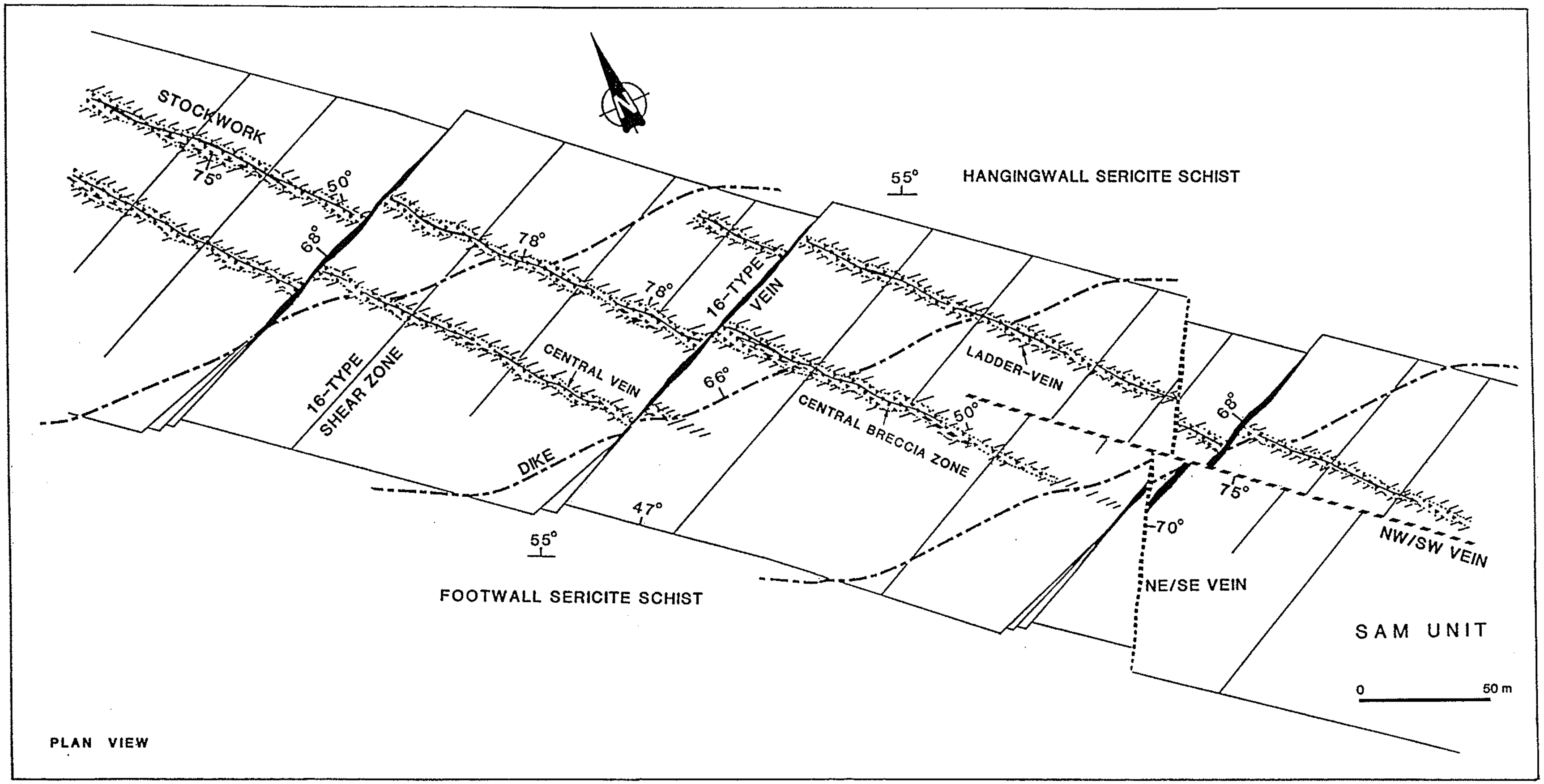

Figure 84: Schematic plan view of the SAM unit following the development of the main NW/SW fracture.

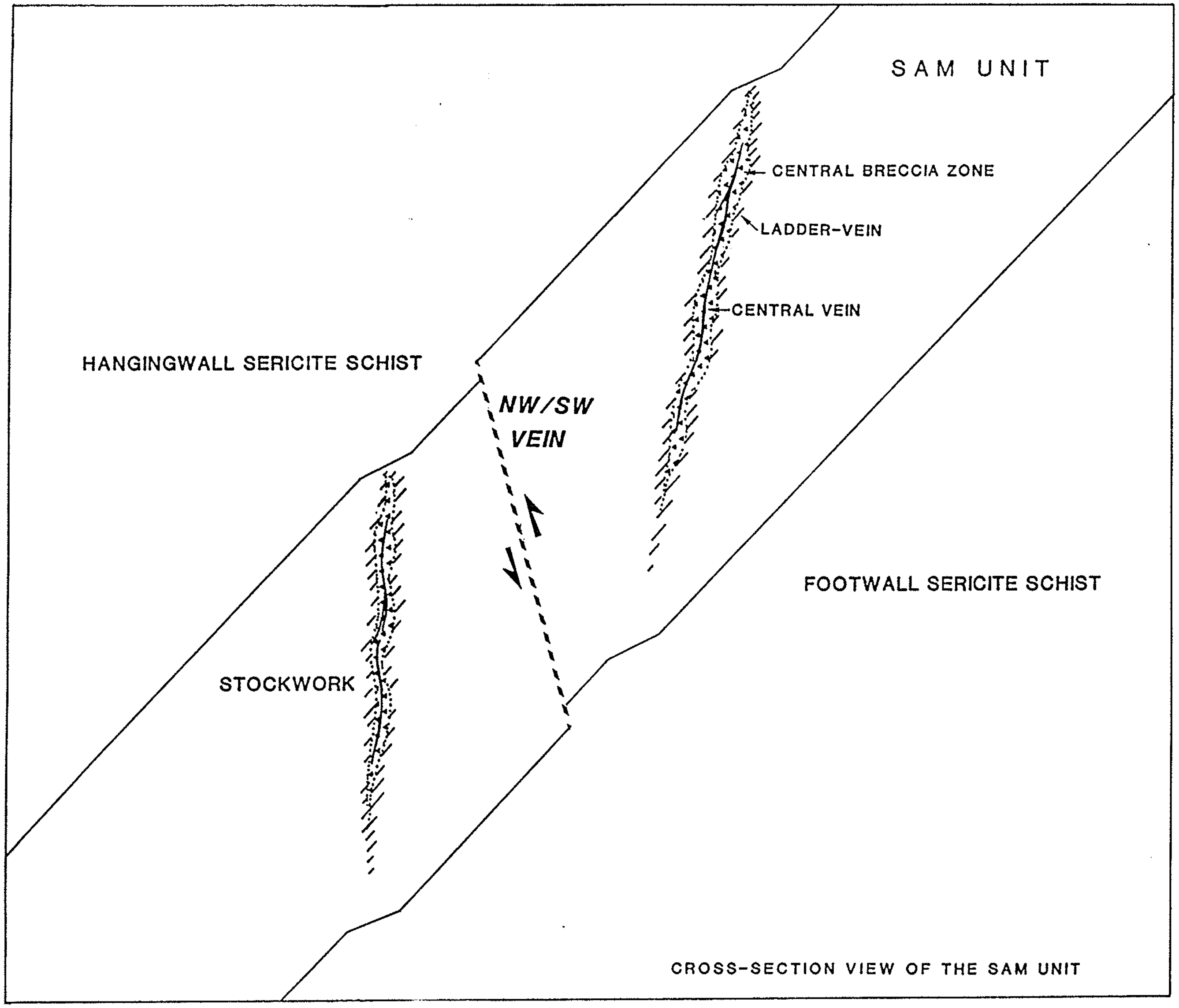

Figure 85: Schematic cross section of the SAM unit after the development of the main NW/SW fracture. Reverse movement has led to displacements of both hangingwall and footwall contacts of the SAM unit.

8.3 A SHALLOW NORTH-DIPPING FAULT

One fault with a shallow dip to the north has been recognised in the San Antonio mine. It is located on the western-most part of the 17th level of the mine. It strikes east-west and dips approximately 20^0N. The fault surface is marked by a centimetre-thick layer of brownish-dark material, and it is bordered by a metre-wide zone of brecciated wall rock on each side. The dimensions of this fault have not been determined. It cuts across a near-by stockwork on the 17th level but its relationship to the 16-type, NE/SE and NW/SW sets of structures have not been determined.

The angular wall rock fragments in the brecciated zone range from less than a millimetre to a couple of centimetres and they have been cemented together by brownish-dark material to give cataclastite characteristics. In thin sections the dark material is made up largely of very fine, prismatic tourmaline. However, the dark material in some of the vein-like fissures are isotropic, suggesting that they may be pseudotachylite.

The presence of extensive brecciation of the adjacent wall rock and small amounts of pseudotachylite suggest that brittle fracturing at high rate of strain had occurred in this fault (Davis 1984, Wise et al 1984, Ramsay and Huber 1987).

CHAPTER NINE

TIMING OF THE STRUCTURAL EVENTS WITHIN THE SAM UNIT

The cross-cutting relationships between the five major sets of fractures are very consistent throughout the SAM unit. These cross-cutting relationships are depicted diagramatically in Figure 86. The relative ages of the structures, as determined from these cross-cutting relationships are from oldest to youngest: (1) dikes, (2) stockworks, (3) 16-type veins, (4) NE/SE veins and NW/SW veins. The E-W/N fault postdates the stockworks, otherwise its age is unknown.

In the previous chapters the origin of each of the sets of fractures has been analysed separately and indepentently. Where possible fracture type, principal stress orientations and kinematic interpretations were made.

Table 1 presents these interpretations in summary form. A review of Table 1 reveals the strong likelihood that these structures are independent of one another. Not only are there clearly defined age relationships between the structures, the kinematics and stress orientation interpretations are also distinctly different for each structure.

There are three important observations that should be made concerning the relationships between the two most important sets of structures, i.e., the stockworks and the 16-type veins. (1) The stockworks and the 16-type veins apparently are not conjugate shear fractures as suggested by Stockwell (1938) and Stephenson (1971). Figure 87 illustrates how the movements on the two structures are incompatible with such an interpretation.

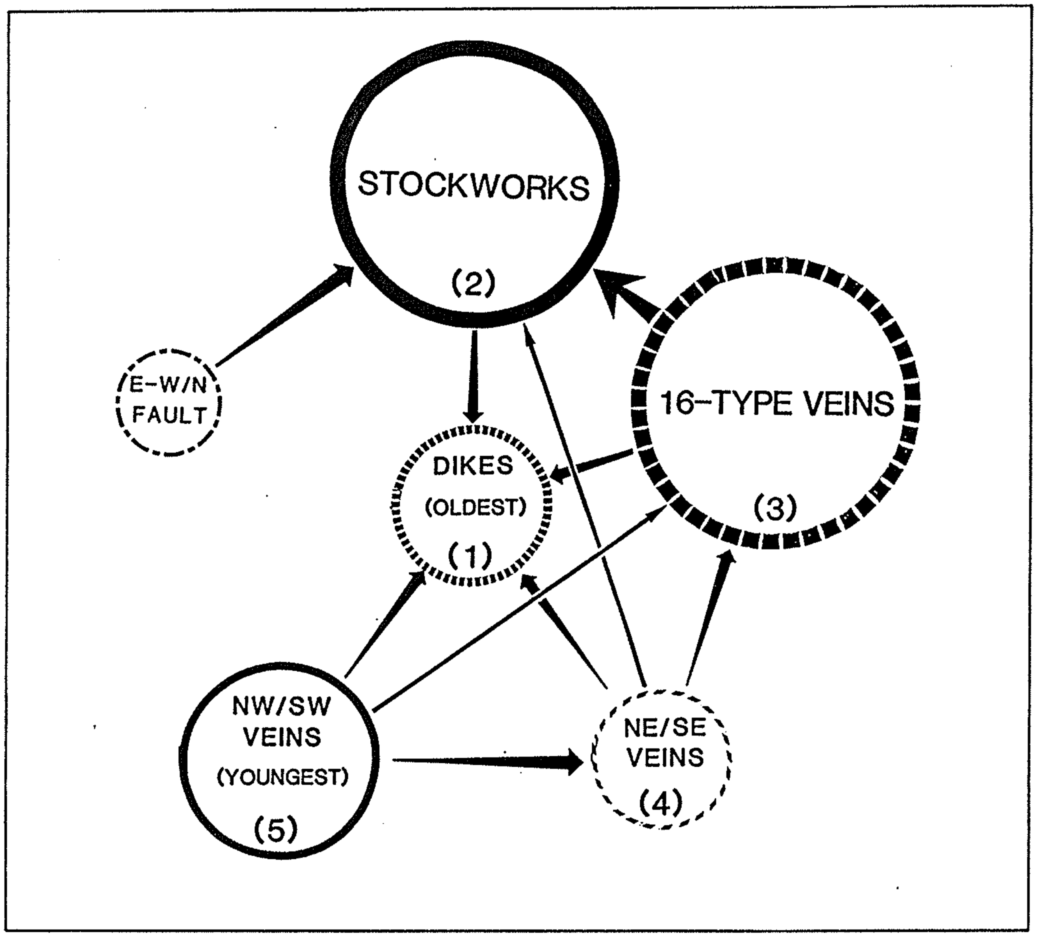

Figure 86: Relative ages of the five major fractures sets in the SAM unit based on observed cross-cutting relationships. Arrows point towards the relatively older sets.

STRUCTURES		ATTITUDE	FRACTURE TYPE	KINEMATIC ANALYSES		PRINCIPAL STRESS ORIENTATIONS			ASSUMPTION
				PITCH OF SLIP	SENSE OF SLIP	σ_1	σ_2	σ_3	
DIKES		N88°E/66°NW	Brittle hydraulic tension fractures					24°/S2°E	
STOCKWORKS	LADDER-VEINS	N83°W/50°NE	Brittle hydraulic tension fractures					40°/S7°W	
	CENTRAL BRECCIA ZONES	N40°W/78°NE	Shear ? Hydraulic ? brecciation	RANGE OF SLIP DIRECTIONS FROM 45° NW TO 69° NW	THRUST RIGHT-HANDED	40°/N5°E TO 44°/N36°E	44°/S51°E TO 19°/S44°E	32°/S75°E TO 39°/S36°W	SHEARING $\Phi=30^\circ$
	CENTRAL VEINS	N40°W/78°NE	Shear ? Tension ? brittle fractures						
16-TYPE VEINS		N75°E/68°NW	Ductile shear fractures	41° NE	THRUST LEFT-HANDED	21°/N27°E	41°/N84°W	41°/S44°E	$\Phi=30^\circ$
NE/SE VEINS		N36°E/70°SE	Ductile shear fractures	39° NE	THRUST RIGHT-HANDED	20°/N79°E	47°/S13°W	37°/N25°W	$\Phi=30^\circ$
NW/SW VEINS		N50°W/75°SW	Shear ? Tension ? brittle fractures	45° SE	THRUST RIGHT-HANDED	19°/S11°E	54°/N7°W	30°/N69°E	SHEARING $\Phi=30^\circ$

Table 1: Summary of the interpretation of the fracture type, kinematic analyses and principal stress orientations for all fracture sets.

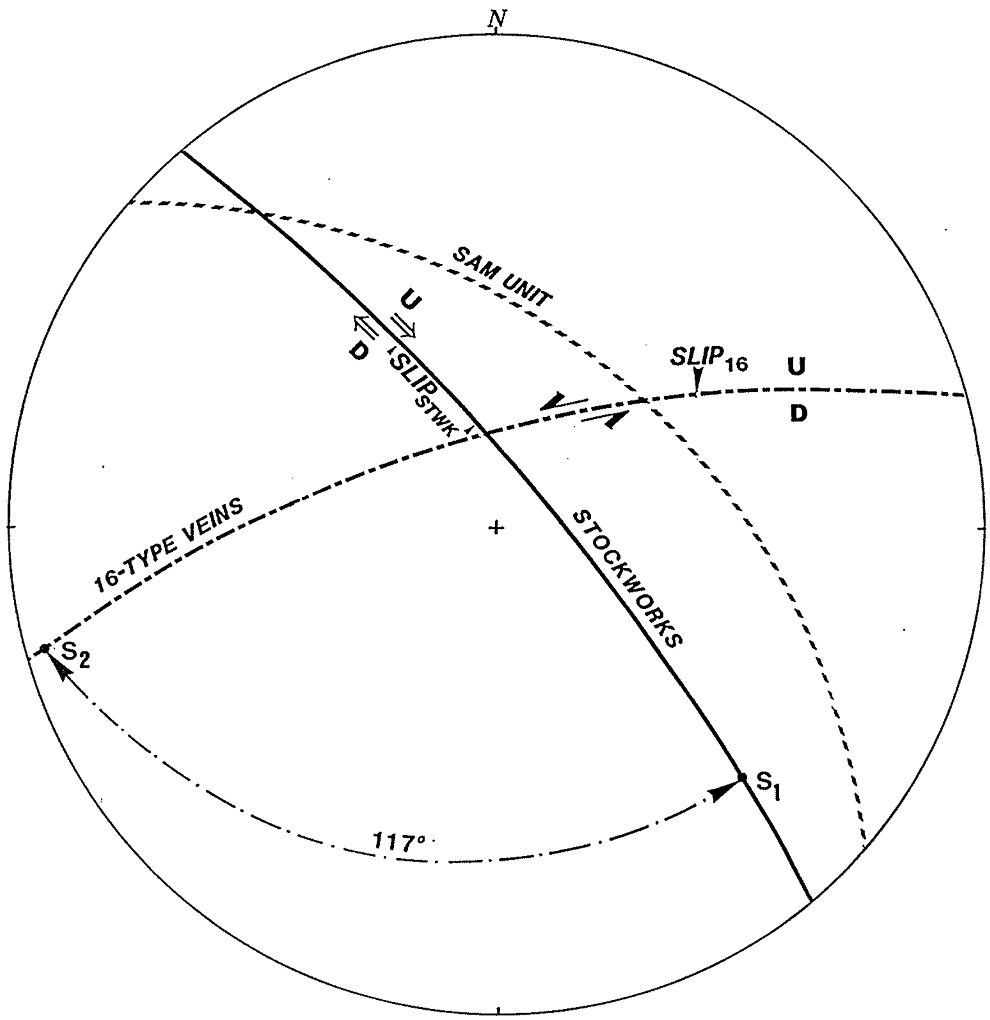

Figure 87: Synoptic stereoplot to test whether or not 16-type shear zones and stockworks represent conjugate set of shears. Observed movement on the 16-type shear zones ($SLIP_{16}$) and on the stockworks (indicated by $SLIP_{STWK}$) are incompatible with movements predicted in the conjugate model (S_1 and S_2).

Furthermore the figure also shows how the ladder-veins, as hydraulic tension fractures, could not be related to the 16-type structures. Finally, the angle between the intersection of the two features are very much higher than the angle between the intersection of an ideal conjugate shears (about 60^0 to 90^0). (2) The stockworks are not extensional zones linking en echelon 16-type shear zones as suggested by Poulsen et el (1986). The angle between the intersection of the two features are not normal to the slip direction on the 16-type shear zones (Figure 87) to comply with the model. Nor are the ladder-veins oriented normal to the slip direction on the 16-type shear zones. The stockworks in the SAM unit are not bound by 16-type shear zones but instead they are always cut across and displaced by the 16-type shear zones. In addition, stockworks have developed in the SAM unit where there are no, or few, large 16-type shear zones. (3) Although the development of the stockworks and the 16-type shear zones appears to be separate there remains the possibility that translational movement on the stockworks could have been delayed until the time of the origin of the 16-type structures and been due to the same stresses. Figure 88 shows the orientation of the maximum compressive stress interpreted for the 16-type structures. If the stockworks are considered as existing structural anisotropy, translational movement induced by the maximum compressive stress would be consistent with the observed offsets on the stockworks. The abundant vertical veinlets in the stockworks cross-cut by the 16-type shear zones are further evidence that indicate an overlap in the complete development of the stockworks and the 16-type shear zones.

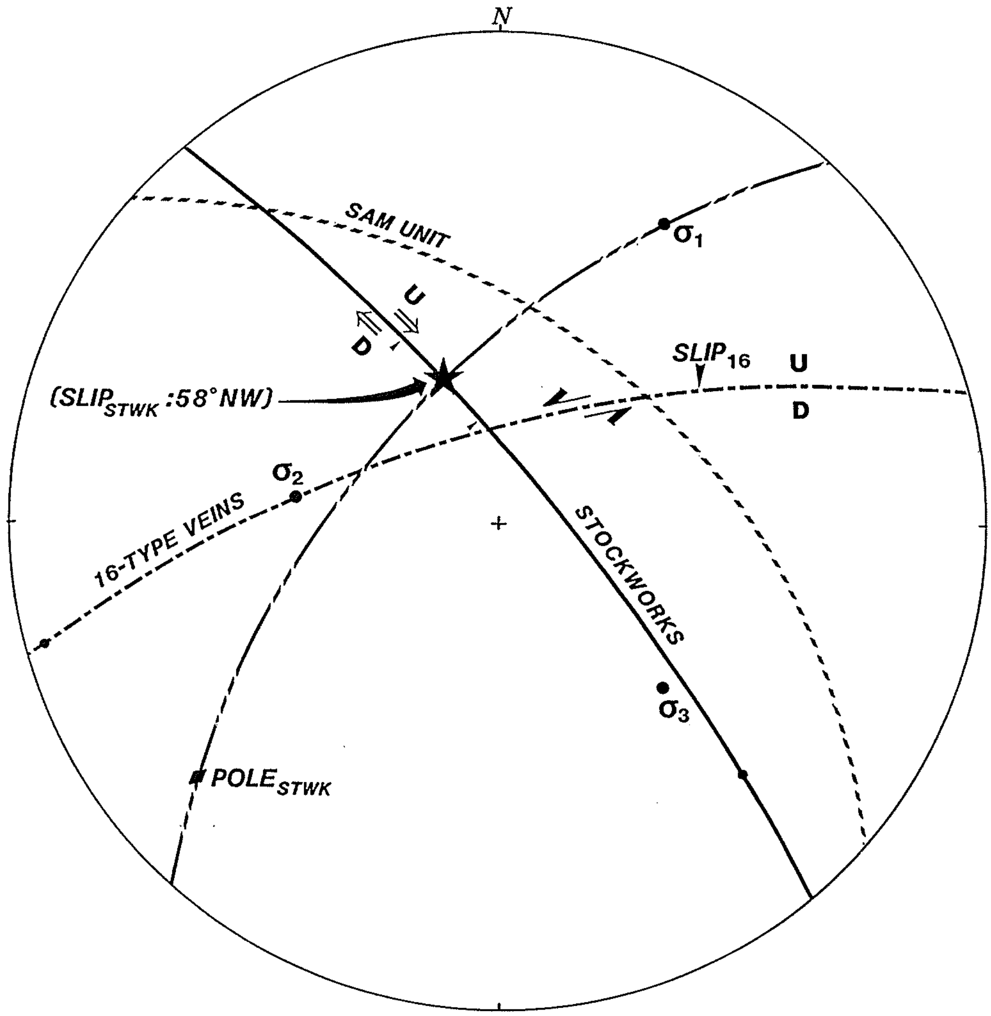

Figure 88: Synoptic diagram prepared to test the model of movement on the stockworks (as a strenght anistropy) during 16-type shear zones development. Star indicates the position of movement on the stockworks predicted by the 16-type shear maximum principal stress (σ_1); it falls within the observed range of movements on the stockworks.

Figure 89 takes these observations into account and summarizes modes of, and chronological sequence of, development of the major fractures sets within the SAM unit. On Figure 89 the changing character of deformation is indicated from brittle, in dikes and stockworks formation, to ductile in 16-type and NE/SE shear zones, and back to brittle in NW/SW fracture formation. The possibility of some pre-stockwork ductile structures is also shown. The development of the vertical veinlets in the stockworks is shown as contemporaneous with the development of the 16-type shear zones.

Although both structures and their contained veins show clear cut age relationships the vein forming fluids changed very little over this full span of time. Figure 89 also shows the mineral composition of the veins and the timing of the appearance of the minerals in the different vein sets. The mineral composition of the vein material in the stockworks, 16-type veins, NE/SE veins and NW/SW veins are very similar and they are composed of variable amounts of quartz (usually greater than 90%), carbonate, chlorite, albite and pyrite. All these minerals except chlorite were first introduced in stockworks and have appeared throughout the deposition of the subsequent vein sets. Chlorite was introduced only after the major components of the stockworks had developed and its occurrence in the stockworks is restricted to the vertical veinlets. Gold is mainly found in the stockworks and the 16-type veins but small amounts of it may also be found in the NE/SE and NW/SW vein sets.

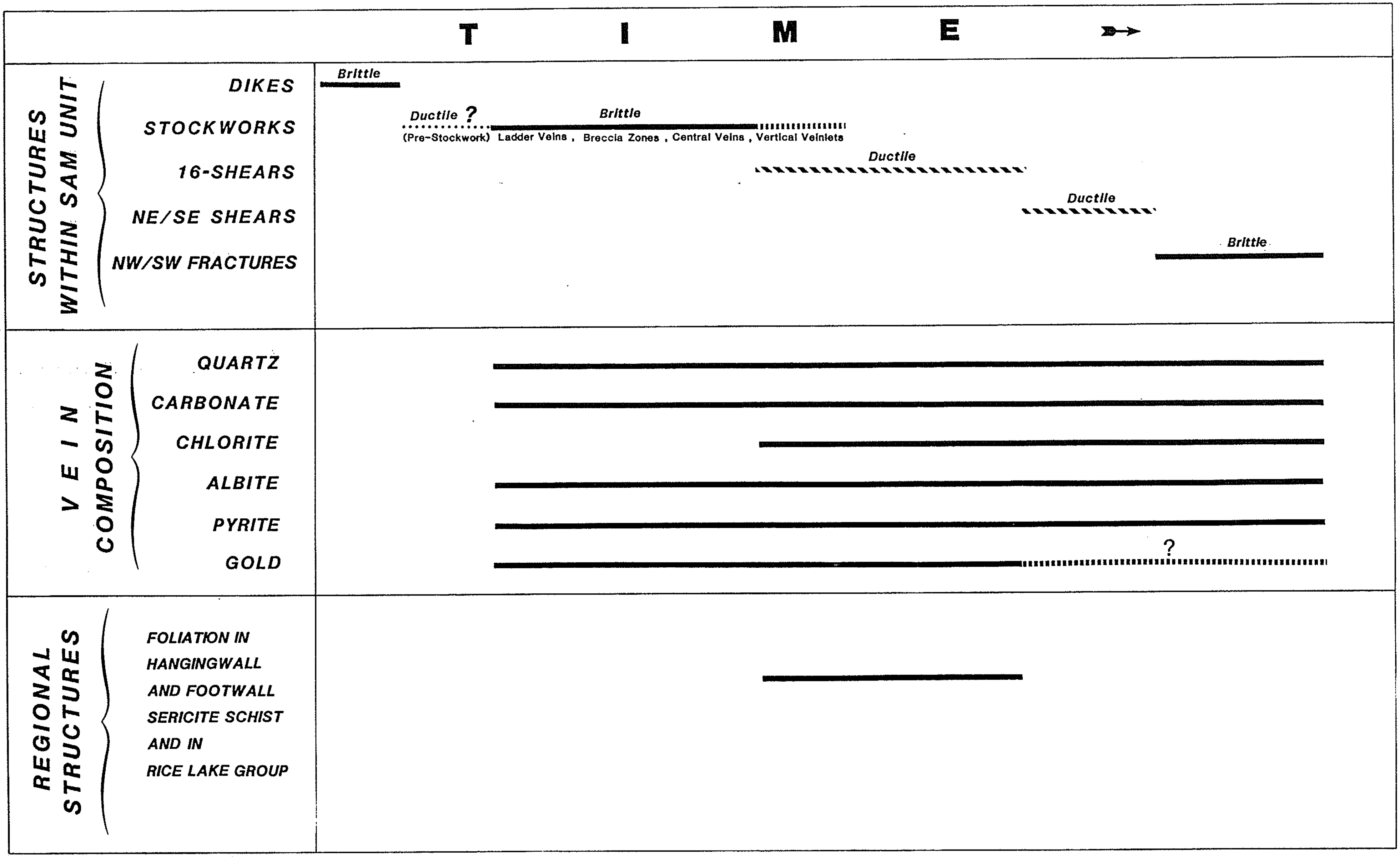

Figure 89: Relationships between the major fracture sets and the veins within the SAM unit and the regional foliation.

CHAPTER TEN

DICUSSION

The approach used in this study has been to interpret each fracture set within the SAM unit as individual entity, in its present orientation. Standard Coulomb fracturing criteria have been applied in interpreting the orientations of the principal stresses responsible for each fracture set. This approach places some limitations on some of the conclusions of the study for the following reasons. (1) The present study has considered the SAM unit to be a fixed orientation through time. Such may not be the case. A changing orientation of the SAM unit in a fixed stress field could also yield the different principal stress orientations concluded in this study. (2) Recent experimental work by Reches (1978, 1982) and Reches and Dieterich (1982) have shown that fracture orientations may respond to changing stress fields which themselves are a product of fracture development.

In addition to these points there is also the question of how the observed strain in the SAM unit is related to the surrounding more ductile rocks in the Rice Lake Group.

Deformation within the overall Rice Lake Group is characterized mainly by a prominent penetrative regional foliation and a "stretch" lineation (Poulsen et el, 1986). Deformation within the SAM unit, in contrast, is not penetrative and has been localized in five major fracture sets. Only one of these fracture sets, the 16-type shear zones, appears to be related to the regional foliation in the surrounding Rice Lake Group. The relationship is expressed in two ways. First, the 16-type shear zones of the SAM unit and the penetrative foliation in the Rice Lake Group have orientations that are similar to a refracted cleavage in a more brittle unit (SAM unit) set in a more ductile matrix (Rice Lake Group)(Figure 60). Secondly, the movement direction interpreted from the 16-type shear zones is similar to that interpreted by Poulsen et el (1986) for the development of the stretch lineation fabric in the Rice Lake Group. Figure 90 is a synoptic diagram containing the orientations of the SAM unit, the 16-type shear zones, the slip direction on the 16-type shear zones, the penetrative foliation and the stretch lineation of the Rice Lake Group. If the interpretation of Poulsen et al (1986) is correct (that the stretch lineation represents the tectonic transport direction in the Rice Lake Group) than the two movement directions almost coincide.

The foliation and stretch lineation in the Rice Lake Group have been attributed by Poulsen et al (1986) to the development of the Normandy Creek shear zone. Figure 91 shows how the 16-type shear zones and the Normandy Creek shear zone may related. Both interpretations state that the sense of movement throughout the area is north side up or thrust.

Deformational events that produced the fractures sets older and younger than the 16-type shear zones within the SAM unit have not been observed in the surrounding Rice Lake Group. There are two other regional structures, however, to which two of the fracture sets within the SAM unit may be related, the Wanipigow fault and the Manigotagan fault. Figure 92 shows the relationship between the stockworks and the Wanipigow fault. Movement on the Wanipigow fault has been interpreted to be dextral and hangingwall up by McRitchie (1971) and Poulsen et al (1986). Figure 93 shows how the NW/SW fractures may be related to the Manigotagan fault. Movement on the Manigotagan fault has been interpreted to be dextral and hangingwall up by McRitchie (1971).

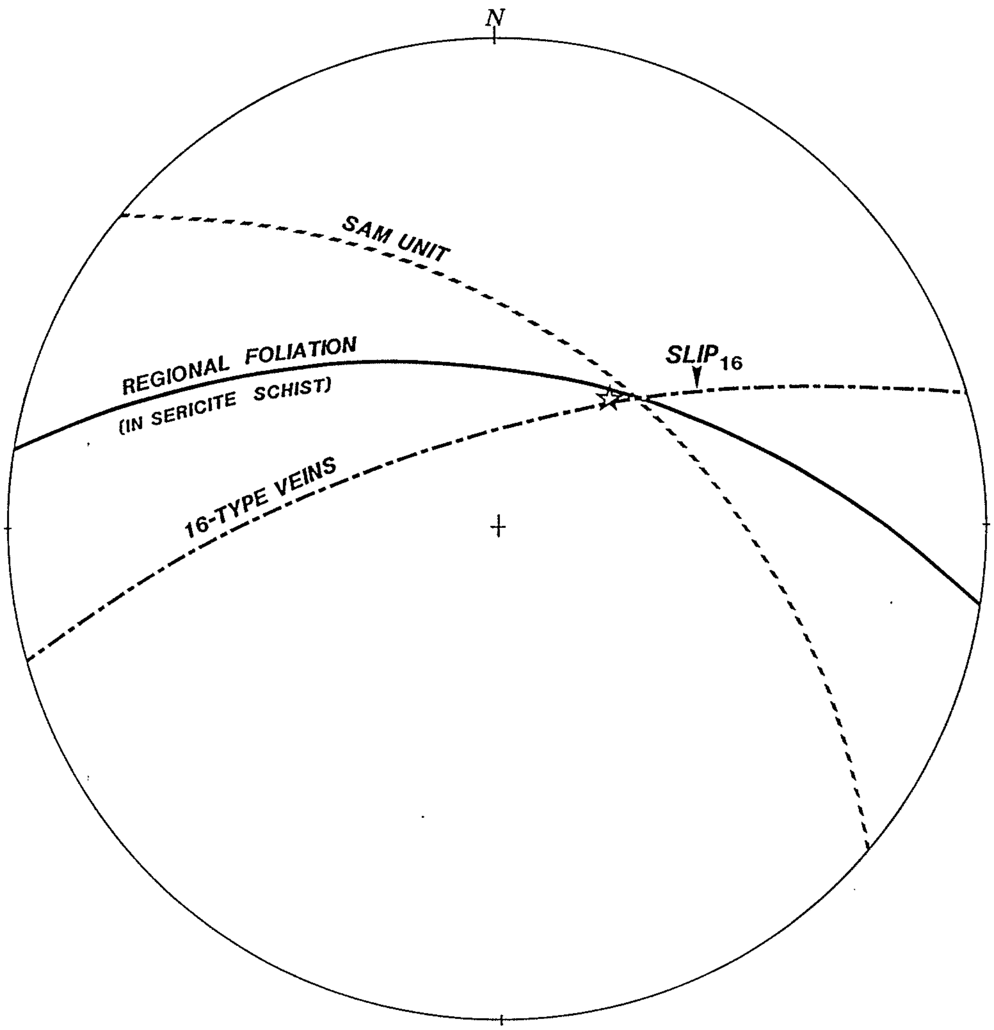

Figure 90: Synoptic diagram showing the relationships between the 16-type shear zones within the SAM unit and the regional foliation adjacent to the SAM unit. Star represents orientation of "stretch" lineation in the hangingwall and footwall sericite schist and in the Rice Lake Group. Data for regional foliation and stretch lineation are from Poulsen et al (1986).

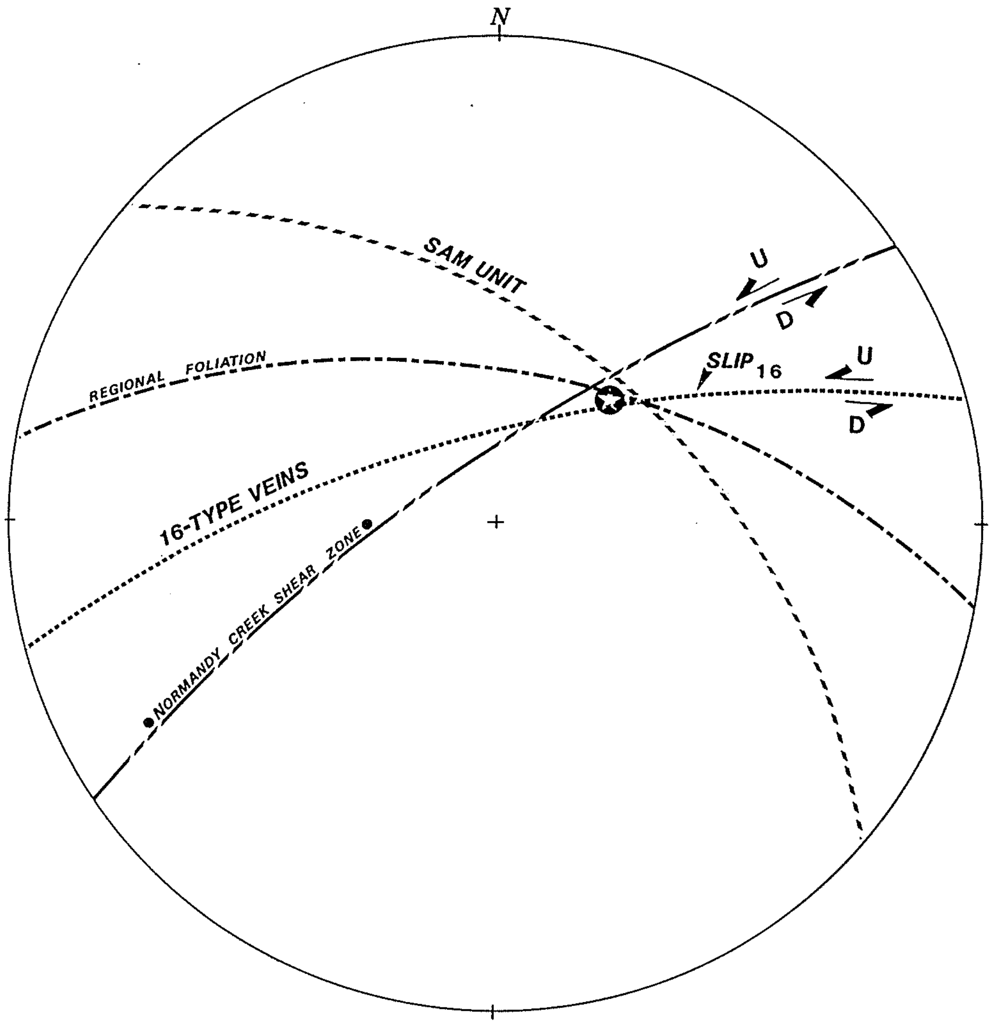

Figure 91: Synoptic diagram showing the possible genetic relationships between the 16-type shear zones and the Normandy Creek shear zone. Star represents orientation of "stretch" lineation in the hangingwall and footwall sericite schist. Data for regional foliation, stretch lineation and Normandy Creek shear zone are from Poulsen et al (1986).

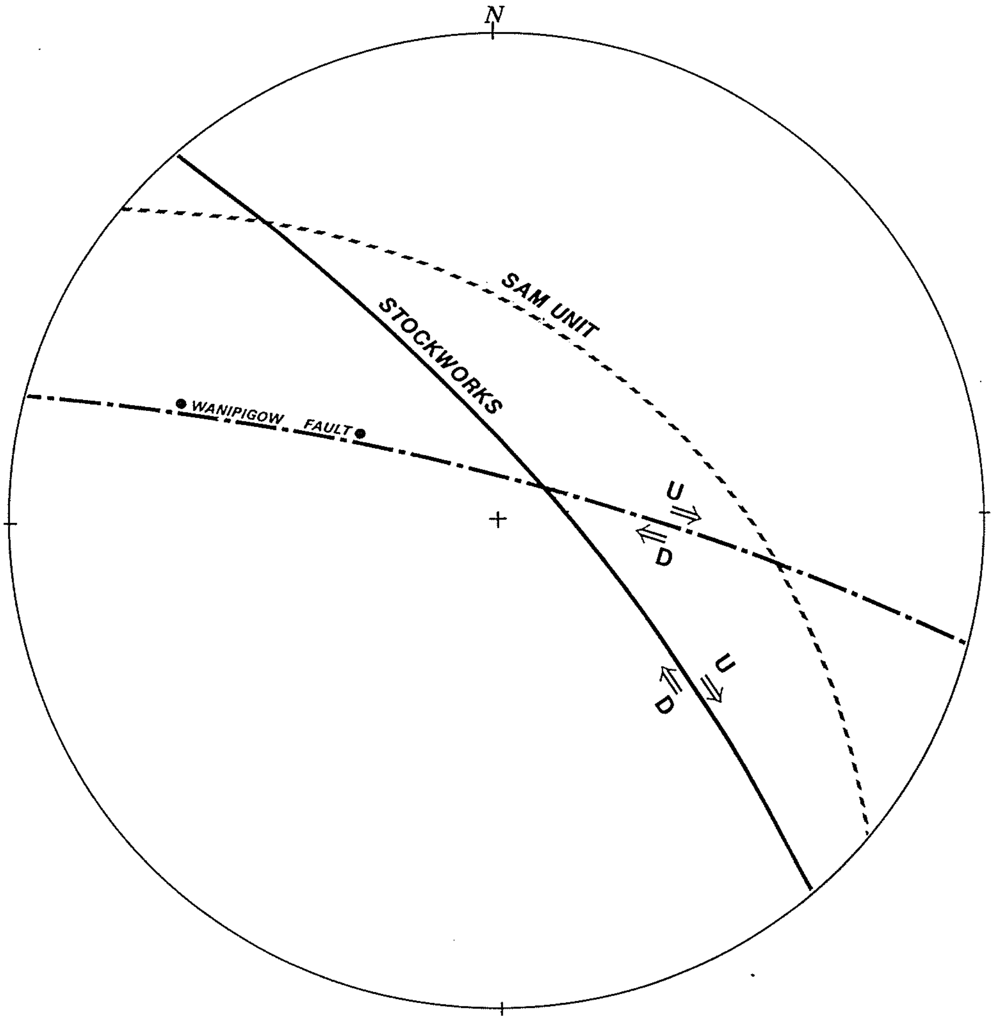

Figure 92: Synoptic diagram showing the possible genetic relationships between the stockworks within the SAM unit and the Wanipigow fault. The data for the Wanipigow fault is from McRitchie (1971) and Poulsen et al (1986).

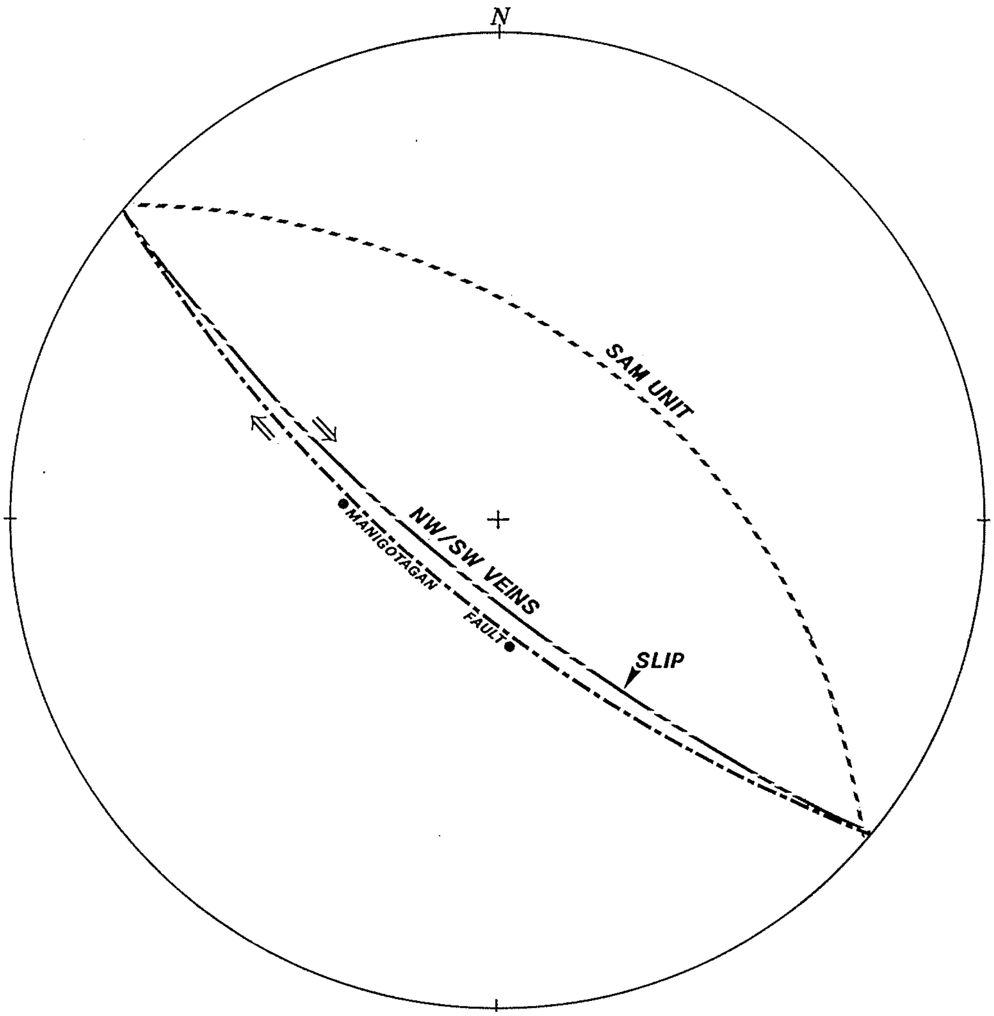

Figure 93: Synoptic diagram showing the possible genetic relationships between the NW/SW fractures and the Manigotagan fault. Data for the Manigotagan fault is from McRitchie (1971).

SELECTED REFERENCES

[1] Amukun, S. E. O. and Turnock, A. C. 1971. Composition of gold-bearing quartz vein rocks, Bissett Area, Manitoba. *Manitoba Mines Branch Publications* **71-1**, 325–336.

[2] Bailes, A. L. 1971. Geology and Geochemistry of the Pilot-Smuggler shear zones, Rice Lake Region, Southeastern Manitoba. *Manitoba Mine Branch Publication* **71-1**, 299–312.

[3] Bell, T. H. and Hammond, R. L. 1984. On the internal geometry of mylonite zones. *Jour. of Geology* **92**, 667–686.

[4] Bragg, J. G. 1943. Rock alteration at the San Antonio mine. *Canadian Mining Journal* **64**, 553–556.

[5] Davis, G. H. 1984. Structural Geology of Rocks and Regions. John Wiley and Sons NY, 492 p.

[6] De Wit, J. P. 1933. The San Antonio......The History. *San Antonio mine file.*

[7] DeHuff, G. L. Jr. 1935. Geology and gold deposits of San Antonio mine. *San Antonio mine file*, 12 p.

[8] Engelder, T. 1987. Joints and shear fractures in rocks: in B.K. Atkinson (ed.), Academic Press, N.Y., 27–69.

[9] Etheridge, M. A. 1983. Differential stress magnitudes during regional deformation and metamorphism: upper bound imposed by tensile fracturing. *Geology* **11**, 231–234.

[10] Gibson, J. C. and Stockwell, C. H. 1948. San Antonio Mine, in: *Structural Geology of Canadian Ore deposits, CIM* **1**, 315–321.

[11] Harris, J. F., Taylor, G. L. and Walper, J. L. 1960. Relation of deformational fractures in sedimentary rocks to regional and local structures. *American Assoc. Petroleum Geologists* **44**, 1853–1873.

[12] Henry, H. A. July 18, 1945. San Antonio Mine. *Canadian Finance.*

[13] Johnson, A. M. 1970. Physical processes in Geology. Freeman, Cooper and Co., San Francisco, Calif., 577 p.

[14] Lister, G. S. and Snoke, A. W. 1984. S-C mylonites. *Jour. Structural Geology* **6**, 617–638.

[15] McQuillan, H. 1973. Small-scale fracture density in Asmari formation of SW Iran and its relation to bed thickness and structural setting. *American Assoc.*

Petroleum Geologists **57**, 2367–2385.

[16] Milling, D. R., Watkinson, D. H., Poulsen, K. H., Chorlton, L. B. and Hunter, A. D. 1986. The Cameron Lake gold deposit, northwestern Ontario, Canada : Geological setting, structure, and alteration, in: A.J. Macdonald (ed.), *Proceedings of Gold '86, An International Symposium on the Geology of Gold: Toronto, 1986*, 149–169.

[17] McRitchie, W. D. 1971. The petrology and environment of the acidic plutonic rocks of the Wanipigow-Winnipeg Rivers Region, SE Manitoba in: McRitchie W.D. and Weber W.(eds.), Geology and geophysics of the Rice Lake Region, SE Manitoba. *Manitoba Mines Branch Publication* **71-1**, 7–61.

[18] Narr, W. and Lerche, I. 1984. A method for estimating subsurface fracture density in core. *Americal Assoc. Petroleum Geologists* **68**, 637–648.

[19] Phillips, W. J. 1972. Hydraulic fracturing and mineralization. *Jour. Geol. Soc. London* **128**, 337–359.

[20] Pollard, D. D. 1973. Derivation and evaluation of a mechanical model for sheet intrusions. *Tectonophysics* **19**, 233–269.

[21] Poulsen, K. H., Ames, D. E., Lau, S. and Brisbin, W. C. 1986. The structural setting of gold deposits in the Rice Lake Area, Uchi subprovince, SE Manitoba: a preliminary report.

[22] Ramsay, J. G. 1980. Shear zone geometry: a review. *Jour. Structural Geology* **2**, 83–99.

[23] Ramsay, J. G. and Huber, M. I. 1983. The Techniques of Modern Structural Geology, Volume 1: Strain Analysis. Academic Press, London. 307 p.

[24] Ramsay, J. G. and Huber, M. I. 1987. The Techniques of Modern Structural Geology Volume 2: Folds and Fractures. Academic Press, London, 309–700.

[25] Reches, Z. 1978. Analysis of faulting in 3-dimensional strain field. *Tectonophysics* **47** 109–129.

[26] Reches, Z. and Dieterich, J. H. 1982. Faulting of rocks in 3-dimensional strain fields I. Failure of rocks in polyaxial, servo-control experiments. *Tectonophysics* **95**, 111–132.

[27] Reches, Z. 1982. Faulting of rocks in 3-dimensional strain fields II. Theoretical analysis. *Tectonophysics* **95**, 133–156.

[28] Reid, J. A. 1931. Geology of San Antonio Gold Mine, Rice Lake, Manitoba. *Econ. Geol.* **26**, 644–661.

[29] Reid, J. A. 1933. San Antonio Gold Mine. CIM Annual Meeting Toronto.

[30] Richard, M. J. and Rixon, L. K. 1983. Stress configurations in conjugate quartz-vein arrays. *Jour. Structural Geology* **5**, 573–578.

[31] Sibson, R. H. 1977. Fault rocks and fault mechanisms. *J Geol. Soc. London* **283**, 684–721.

[32] Simpson, C. and Schmid, S. M. 1983. An evaluation of criteria to deduce the sense of movement in sheared rocks. *Geol. Soc. Am.(Bull)* **94**, 1281–1288.

[33] Skerl, A. C. 1955. A study of the structural setting of the San Antonio Gold Mine, Bissett, Manitoba. *San Antonio Mine file*, 40 p.

[34] Stephenson, J. F. 1971. Gold deposite of the Rice Lake - Beresford Lake Greenstone Belt, SE Manitoba. *Manitoba Mines Branch Publications* **71-1**, 337–374.

[35] Stockwell, C. H. 1938. Rice Lake - Gold Lake Area, SE Manitoba. *Geological Survey of Canada Memoir* **210**, 21–51.

[36] Suppe, J. 1985. Principles of Structural Geology. Prentice-Hall, NJ. 537 p.

[37] Theyer, P. 1983. Geology of gold environments in the Bissett/Wallace Lake Portion of the Rice Lake greenstone belt; in *Manitoba Mineral Resource Division, Report of Field Activities 1983*, 101–106.

[38] White, S. H. 1979. Grain and subgrain size variations across a mylonite zone. *Contrib. Mineral. Petrol.* **70**, 193–202.

[39] Williams, H. R., Corkery, D. and Lorek, E. G. 1985. A study of joints and stress-release buckle in Palaeozoic rocks of Niagara Peninsula, Southern Ontario. *Can. Jour. Earth Sciences* **22**, 296–300.

[40] Wilson, G. 1982. Introduction to small-scale geological structures (in collaboration with Cosgrove,J.W.). George Allen and Unwin Publ., London. 128 p.

[41] Wise, D. U. et al. 1984. Fault-related rocks: suggestions for terminology. *Geology* **12**, 391–394.

GENERAL REFERENCES

[1] Akande, S. O. 1982. Mineralogy and genesis of three vein systems, Ross Mine, Holtyre, Ontario, in Hodder R.W. and Petruk W.(eds.), *Geology of Canadian Gold Deposits. CIM Special Volume* **24**, 94–97.

[2] Anderson, O. C. and Grew, P. C. 1977. Stress corrosion theory of crack propagation with application to geophysics. *Rev. Geophys. Spac. Physics* **15**, 77–104.

[3] Aydin, A. and Johnson, A. M. 1978. Development of faults as zones of deformational bands and as slip surfaces in sandstone. *Pure and Applied Geophysics* **116**, 931–942.

[4] Bartlett, W. L., Friedman, M. and Logon J. M. 1981. Experiental folding and faulting of rocks under confining pressure.Part IX.Wrench faults in limestone layers. *Tectonophysics* **79**, 255–277.

[5] Bartram, G. R. and McGall, G. J. H. 1971. Wall-rock alteration associated with auriferous lobes in the Golden Mile, Kalgoorlie. *Special Publications Geol.Soc.Austr.* **3** 191–199.

[6] Bateman, A. M. 1950. Economic mineral deposits: structural association of vein ores. Second edition p.107-137, John Wiley and Sons Inc. NY.

[7] Bayly, B. 1986. A diagram for simultaneous fracture and flow. *Tectonophysics* **131**, 157–166.

[8] Beach, A. 1975. The geometry of en-echelon vein arrays. *Tectonophysics* **28**, 245–263.

[9] Beach, A. 1977. Vein arrays, hydraulic fractures and pressure-solution structures in a deformed flysch sequence, S.W. England. *Tectonophysics* **40**, 201–225.

[10] Beach, A. 1980. Numerical models of hydraulic fracturing and the interpretation of syntectonic veins. *Jour. Structural Geology* **2**, 425–438.

[11] Beach A. 1980. Retrogressive metamorphic processes in shear zones with special reference to the Lewisian complex. *Jour. Structural Geology* **2**, 257–263.

[12] Bell, T. H. and Etheridge, M. A. 1973. Microstructures of mylonites and their descriptive terminology. *Lithos* **6**, 337–348.

[13] Bombolakis, E. G. 1968. Photoelastic investigation of brittle crack growth

within a field of uniaxial compression. *Tectonophysics* **1**, 343–351.

[14] Bombolakis, E. G. 1968. Photoelastic study of initial stages of brittle fracture in compression. *Tectonophysics* **6**, 461–473.

[15] Bombolakis, E. G. 1976. Some constraints and aids for interpretation of fracture and fault development: *Theory , Origin, in Basement Tectonics Contribution No.* **27**, 289–305.

[16] Boyle, R. W. 1982. Gold Deposits: A review of their geological and geochemical setting, in Petruk W. and Hodder R.W.(eds.), Geology of Canadian Gold Deposits : *Can Inst. Mining Metall., Special Volume* **24**, 1–5.

[17] Brisbin, W. C. 1986 Mechanics of pegmatite intrusion. *American Mineralogist* **71**, 644–651.

[18] Brodie, K. H. and Rutter, E. H. 1985. On the relationship between deformation and metamorphism, with special reference to the behavior of basic rocks: in A.B. Thompson and D.C. Rubie (eds.), *Metamorphic Reaction Kinetics, Textures and Deformation.* Springer-Verlag, N.Y., 138–179.

[19] Bruhn, R. L. and Pavlis, T. L. 1981. Late Cenozoic deformation in the Matamuska Valley, Alaska: Three-dimensional strain in a forearc region. *Goel. Soc. Am.(Bull)* **92**, 282–293.

[20] Burg, J., Iglesias, M., Laurent, Ph., Matte, Ph. and Ribeiro, A. 1981. Variscan intracontinental deformation: The Coimbra-Cordoba shear zone, SW Iberian Peninsular. *Tectonophysics* **78**, 161–177.

[21] Castro, A. 1984. Emplacement fractures in granitic plutons (Central Extremadura batholith, Spain). *Geologische Rundschau* **73**, 869–880.

[22] Chase, F. M. 1949. Origin of the Bendigo saddle reefs with comments on the formation of ribbon quartz. *Econ. Geol.* **44**, 561–597.

[23] Chernykh, A. L. 1978. The geology and the mechanics of formation of en echelon ruptures. *Geologiya i geofizika* **19**, 31–37.

[24] Cobbold, P. R.1977. Description and origin of banded deformation structures. I. Regional strain, local perturbations, and deformation bands. *Can. J. Earth Sci.* **14**, 1721–1731.

[25] Coward, M. P. 1976. Strain within ductile shear zone. *Tectonophysics* **34**, 181–197.

[26] Currie, K. L. and Ferguson J. 1970. The mechanism of intrusion of lamprophyre dikes indicated by "offsetting" of dikes. *Tectonophysics* **9**, 525–535.

[27] Davies, J. F., Bannatyne, B. B., Barry, G. S. and McCabe, H. R. 1962. Geology and mineral resources of Manitoba: Rice Lake-Beresford Lake Area.

Manitoba Dept. of mines and natural resources, 47-52.

[28] Dougherty, E. Y. 1949. Ribbon structures in gold-quartz veins. *Econ. Geol.* **45**, 177–179.

[29] Eisbacher, G. H. 1970. Deformation mechanics of mylonitic rocks and fractured granites in Cobequid Mountains, Nova Scotia, Canada. *Geol. Soc. Am.(Bull)* **81**, 2009–2020.

[30] Engelder, T. 1987. Joints and shear fractures in rocks: in B.K. Atkinson (ed.), Fracture mechanics in rock. Academic Press, N.Y., 27–69.

[31] Etherigde, M. A. and Wilkie, J. C. 1979. Grainsize reduction, grain boundary sliding and the flow strength of mylonite. *Tectonophysics* **58**, 159–178.

[32] Etheridge, M., Wall, V. J. and Cox, S. F. 1984. High fluid pressure during regional metamorphism and deformation: implication for mass transport and deformation mechanisms. *Jour. Geophysical Res.* **89**, 4344–4358.

[33] Farmin, R. 1941. Host-rock inflation by veins and dikes at Grass Valley, California. *Econ. Geol.* **36**, 143–174.

[34] Gentile, F. 1983 Gold mineralization at San Antonio Project (Brinco Mining Ltd), Bissett, Manitoba. *CIM 85th Annual General Meeting Paper* **89**, 1–28.

[35] Goetze, C. and Evans, B 1979. Stress and temperature in the bending lithosphere as constrained by experimental rock mechanics. *Geophy. J. Res. astr. Soc.* **59**, 463–478.

[36] Graves, M. C. and Zeatilli, M. 1980. A review of the geology of gold in Nova Scotia, in Hodder R.W. and Petruk W.(eds.), *Geology of Canadian Gold Deposits: CIM Special Volume* **24**, 233–242.

[37] Grocott, J. 1981. Fracture geometry of pseudotachylyte generation zones: a study of shear fractures formed during seismic events. *Jour. Structural Geology* **3**, 169–178.

[38] Guha, J., Archambault, G. and Leroy, J. 1983. A correlation between the evolution of mineralizing fluids and the geomechanical development of a shear zone as illustrated by the Henderson 2 Mine, Quebec. *Econ. Geol.* **78**, 1605–1618.

[39] Handin, J. 1969. On the Coulomb-Mohr failure criteria. *Jour. Geophysical Res.* **74**, 5343–5348.

[40] Haynes, F. M. and Titley, S. R. 1980. The evolution of fracture-related permeability within the Ruby Star Granodiorite, Sierrita Porpyry Copper Deposit, Pima County, Arizona. *Econ. Geol.* **75**, 673–683.

[41] Hobbs, B. E., Means, W. D. and Willains, P. F. 1976. An Outline of Structural Geology. John Wiley and Sons Inc.,NY, 571 p.

[42] Hollister, V. F. 1973 Structural control and hydrothermal alteration pattern of Chaucha porphyry copper, Ecuador. *Mineral Deposita* 8, 321–331.

[43] Hugon, H. and Schwerdtner, W. M. 1985. Structural signature and tectonic history of deformed gold-bearing rocks in northwestern Ontario. *Ontario Geological Survey Miscellaneous Paper* **127**, 62–72.

[44] Hulin, C. D. 1929. Structural control of ore deposition. *Econ. Geol.* **24**, 15–29.

[45] Hurst, M. E. 1935. Vein formation ay Porcupine, Ontario. *Econ. Geol.* **30**, 103–127.

[46] Kerrich, R. and Allison, I. 1978. Vein geometry and hydrostatics during Yellowknife mineralization. *Can. J. Earth Sci.* **15**, 1653–1660.

[47] Kerrich, R. and Hodder, R. W. 1980. Archean lode gold and base metal deposits: Evidence for metal separation into independent hydrothermal systems, in Hodder R.W. and Petruk W.(eds.), *Geology of Canadian Gold Deposits: CIM Special Volume* **24**, 144–160.

[48] Kerrich, R., Allison, I., Barnett, R., Moss, S. and Starkey, J. 1980. Microstructural and chemical transformations accompanying deformation of granite in a shear zone at Mieville, Switzerland; with implications for stress corrosion cracking and superplastic flow. *Contrib. Mineral. Petrol.* **73**, 221–242.

[49] Knipe, R. J. and Wintsch, R. P. 1985. Heterogenous deformation, foliation development, and metamorphic processes in a polyphase mylonite: in A.B. Thompson and D.C. Rubie (eds.), *Metamorphic Reactions, Kinetics, Textures, and Deformation*, Springer-Verlag, NY, 180–210.

[50] Konstantinov, M. M. 1977. Genetic types of ore-bearing breccias. *International Geology Review* **20**, 289–294.

[51] Kranz, R. L. 1983. Microcracks in rocks: A review. *Tectonophysics* **100**, 449–480.

[52] Ladeira, F. L. and Price, N. J. 1981. Relationship between fracture spacing and bedding thickness. *Jour. Structural Geology* **3**, 179–183.

[53] Lajtai, E. Z. 1969. Mechanics of second order faults and tension gashes. *Geol. Soc. Am. Bull.* **80**, 2252–2272.

[54] Lajtai, E. Z. 1971. A theoretical and experimental evaluation of the Griffith theory of brittle fracture. *Tectonophysics* **11**, 129–156.

[55] Lyn, I. 1938. San Antonio Mine structural geology and geophysical programmes. *Brinco Mining Ltd file*, 22 p.

[56] Marmont, S. 1986. The geological setting of the Detour Lake gold mine, Ontario, Canada in: A.J.Macdonald(ed.), *Proceedings of Gold '86, An international symposium on the Geology of Gold: Toronto, 1986*, 81–96.

[57] Mckinstry, H. E. 1955. Structure of hydrothermal ore deposits: Bateman A.M.(ed.). *Econ. Geol. Fiftieth Anniversary Volume 1905-1955*, 170–218.

[58] Melling, D. R., Watkinson, D. H., Poulsen, K. H., Chorlton, L. B. and Hunter, A. D. 1986. The Cameron Lake gold deposit, northwestern Ontario, Canada : Geological setting, structure, and alteration, in: A.J. Macdonald (ed.), *Proceedings of Gold '86, An International Symposium on the Geology of Gold: Toronto, 1986*, 149–169.

[59] Mitcham, T. W. 1973. Origin of breccia pipe. *Econ. Geol.* **69**, 412–413.

[60] Mitra, G. 1978. Ductile deformation zones and mylonites: The mechanical processes involved in the deformation of crystalline basement rocks. *American Jour. Sci.* **278**, 1057–1084.

[61] Moore, J. McM. and Jackson,N. 1977. Structure and mineralization in the Cligga granite stock, Cornwall. *J. Geol. Soc. London* **133**, 467–480.

[62] Murrel, S. A. F. 1977. Natural faulting and the mechanism of brittle shear failure. *J. Geol. Soc. London* **133**, 175–189.

[63] Park, R. G. 1983. Foundations of Structural Geology. Blackie and Son Ltd, NY, 135 p.

[64] Paterson, M. S. 1978. Experimental rock deformation - the brittle field. Springer-Verlag 245 p.

[65] Platt, J. P. and Vissers, R. L. M. 1980. Extensional structures in anisotropic rocks. *Jour. Structural Geology* **2**, 397–410.

[66] Poirier, J. P. 1980. Shear localization and shear instability in materials in the ductile field. *Jour. Sturctural Geology* **2**, 135–142.

[67] Poulsen, K. H. 1983. Structural setting of vein-type gold mineralization in the Mine Centre-Fort Frances area: implications for Wabigoon subprovince, in Colvine A.C.(ed.), The Geology of Gold in Ontario: *Ontario Geological Survey Misc. Paper* **110**, 174–180.

[68] Ragan, D. M. 1985. Structural Geology : An Introduction to Geometrical Techniques. Third edition.John Wiley and Sons Inc., 393p.

[69] Ramsay, J. G. and Graham, R. H. 1970. Strain variation in shear belts. *Can. J. Earth Sci.* **7**, 786–813.

[70] Rehrig, W. A. and Heidrick, T. L. 1972. Regional fracturing in Laramide Stocks of Arizona and its relationship to porphyry copper mineralization. *Econ. Geol.* **67**, 198–213.

[71] Rispoli, R. 1981. Stress fields about strike-slip faults inferred from stylolites and tension gashes. *Tectonophysics* **75**, 729–736.

[72] Robert, F., Brown, A. C. and Audet, A. J. 1983. Structural control of gold mineralization at the Sigma Mine, Val d'Or, Quebec. *CIM Bulletin* **76**, 72–80.

[73] Robert, F. and Brown, A. C. 1986. Archean gold-quartz veins at the Sigma Mine, Abitibi Greenstone Belt, Quebec. Part I: Geologic relations and formation of the vein system. *Econ. Geol.* **81**, 578–592.

[74] Robert, F. and Brown, A. C. 1986. Archean gold-bearing quartz veins at the Sigma Mine, Abitibi Greenstone belt, Quebec. Part II : Vein paragenesis and hydrothermal alteration. *Econ. Geol.* **81**, 593–616.

[75] Roering, C. 1968. The geometrical significance of natural en echelon crack arrays. *Tectonophysics* **5**, 107–123.

[76] Rutter, E. H. and Brodie, K. H. 1985. The permeation of water into hydrating shear zones: in A.B. Thompson and D.C. Rubie (eds.), *Metamorphic Reactions, Kinetics, Textures, and Deformation.* Springer-Verlag, NY 242–250.

[77] Secor, D. T. Jr. 1965. Role of fluid pressure in jointing. *Am. J. Sci.* **263**, 633–646.

[78] Segall, P. and Simpson, C. 1986. Nucleation of ductile shear zones on dilatant fractures. *Geology* **14**, 56–59.

[79] Sibson, R. H., Moore, J. McM. and Rankin, A. H. 1975. Seismic pumping - a hydrothermal fluid transport mechanism. *J. Geol. Soc. London* **131**, 653–659.

[80] Sibson, R. H. 1980. Transient discontinuities in ductile shear zones. *Jour. Structural Geology* **2**, 165–171.

[81] Sibson, R. H. 1981. Controls on low stress hydro-fracture dilatancy in thrust, wrench and normal fault terrains. *Nature* **289**, 665–667.

[82] Sibson, R. H. 1985. Stopping of earthquake ruptures at dilational fault jogs. *Nature* **316**, 248–251.

[83] Spence, D. A. and Turcotte, D. 1985. Magma-driven propagation of cracks. *J. Geophys. Res.* **90**, 575–580.

[84] Suppe, J. 1983. Geometry and kinetics of fault-bend folding. *American Jour. Sci.* **283**, 684–721.

[85] Tchalenko, J. S. 1970. Similarities between shear zones of different magnitudes. *Geol. Soc. Am.(Bull)* **81**, 1625–1640.

[86] Travis, G. A., Woodall, R. and Bartram, G. B. 1971. The geology of the Kalgoorlie Goldfield. *Special Publications Geol. Soc. Austr.* **3**, 175–190.

[87] Vernon, R. H. 1974. Controls of mylonite compositional layering during non-cataclastic ductile deformation. *Geol. Magazine* **111**, 121–123.

[88] Vernon, R. H. 1983. Grain-size reduction and foliation development in a deformed granitoid batholith. *Tectonophysics* **92**, 123–145.

[89] Wernicke, B. and Burchfiel, B. C. 1982. Modes of extensional tectonics. *Jour. Structural Geology* **4**, 105–115.

[90] White, S. H. and Knipe, R. J. 1978. Transformation and reaction-enhanced ductility in rocks. *Jour. Geol. Soc. Lond.* **135**, 513–516.

[91] White, S. H., Burrow, S. E., Carreras, J., Shaw, N. D. and Humphreys, F. J. 1980. On mylonite in ductile shear zones. *Jour. Structural Geology* **2**, 175–187.

[92] Wood, P. C., Burrows, D. R., Thomas, A. V. and Spooner, E. T. C. 1986. The Hollinger-McIntyre gold quartz vein system, Timmins, Ontario, Canada; Geologic characteristics, fluid properties and light stable isotope geochemistry: in A.J. Macdonald (ed.), *Proceeding Volume, An International Symposium on the geology of gold deposits*, 56–80.

[93] Wright, J. F. 1932. Geology and mineral deposits of parts of SE Manitoba. *Geological Survey of Canada Memoir* **169**, 79–86.

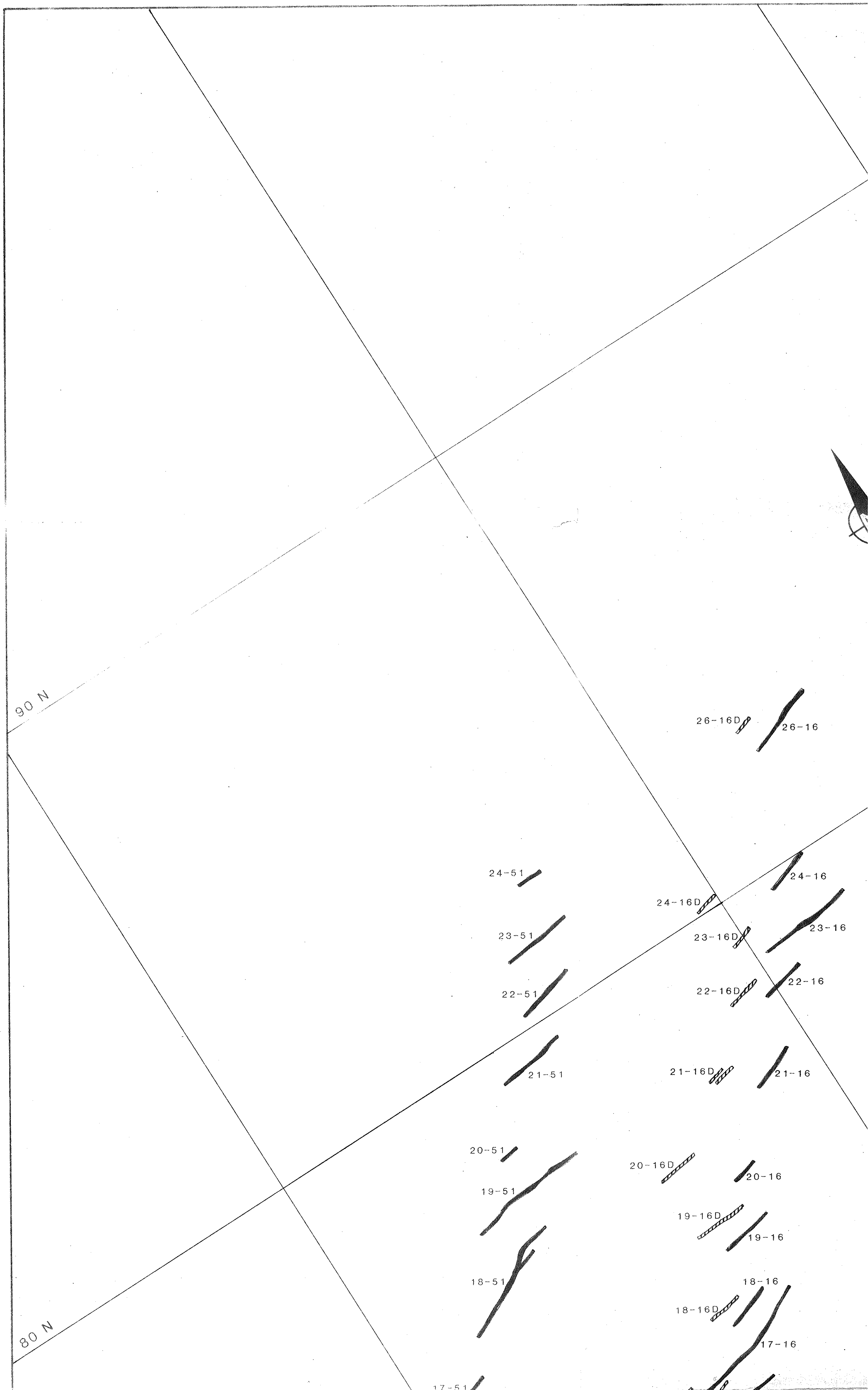
90 N
80 N
26-16D
26-16
24-51
24-16D
24-16
23-51
23-16D
23-16
22-51
22-16D
22-16
21-51
21-16D
21-16
20-51
20-16D
20-16
19-51
19-16D
19-16
18-51
18-16
18-16D
17-16
17-51

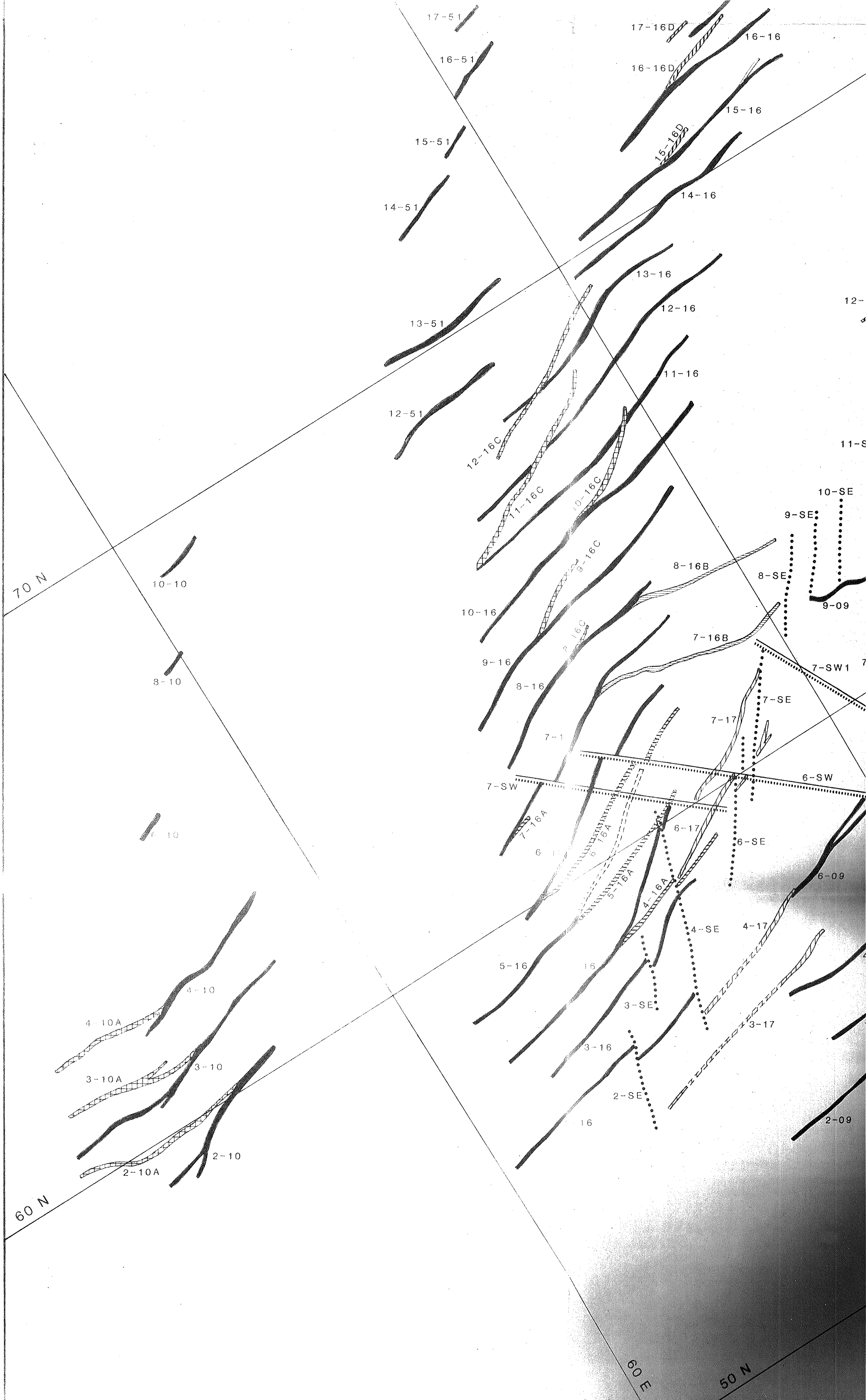

17-51
16-51
15-51
14-51
13-51
12-51
10-10
8-10
4-10
4-10A
3-10A
3-10
2-10A
2-10
70 N
60 N
60 E
50 N
17-16D
16-16
16-16D
15-16
15-16D
14-16
13-16
12-16
11-16
12-16C
11-16C
10-16C
9-16C
10-16
9-16
8-16
8-16B
7-16B
7-17
7-SW
7-16A
6-17
5-16A
4-16A
5-16
3-16
3-SE
2-SE
4-SE
4-17
3-17
6-SW
6-SE
7-SE
7-SW1
8-SE
9-SE
10-SE
9-09
6-09
2-09

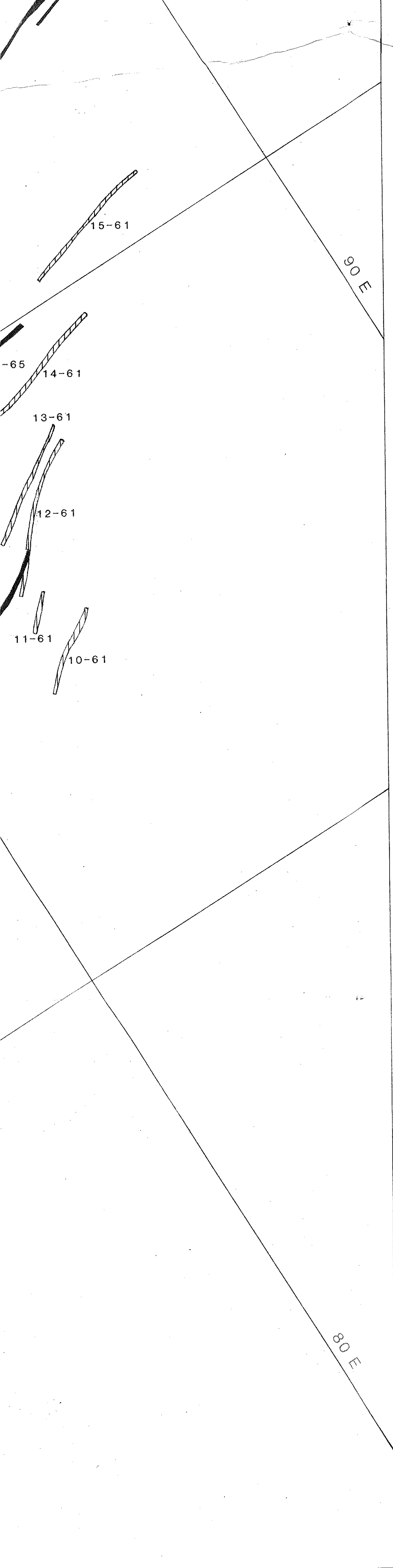

NE/SE VEINS AND NW/SW VEINS

16-TYPE VEINS
(2-16 : LEVEL -VEIN NUMBER)

NE/SE VEINS
(2-SE : LEVEL-VEIN IDENTIFICATION)

NW/SW VEINS
(6-SW : LEVEL-VEIN IDENTIFICATION)

0 30 60 90 120 m

Figure 61

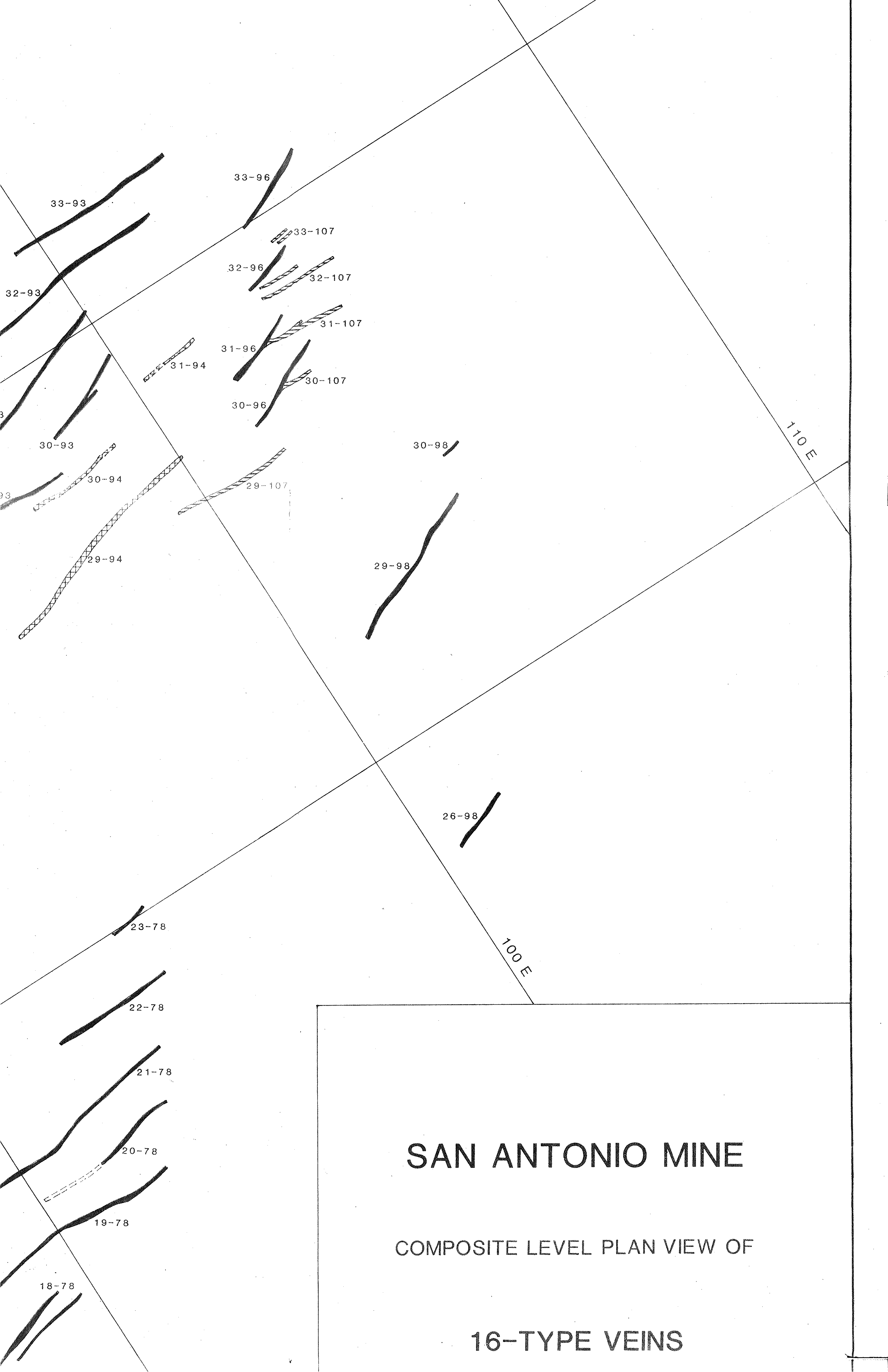

SAN ANTONIO MINE

COMPOSITE LEVEL PLAN VIEW OF

16–TYPE VEINS

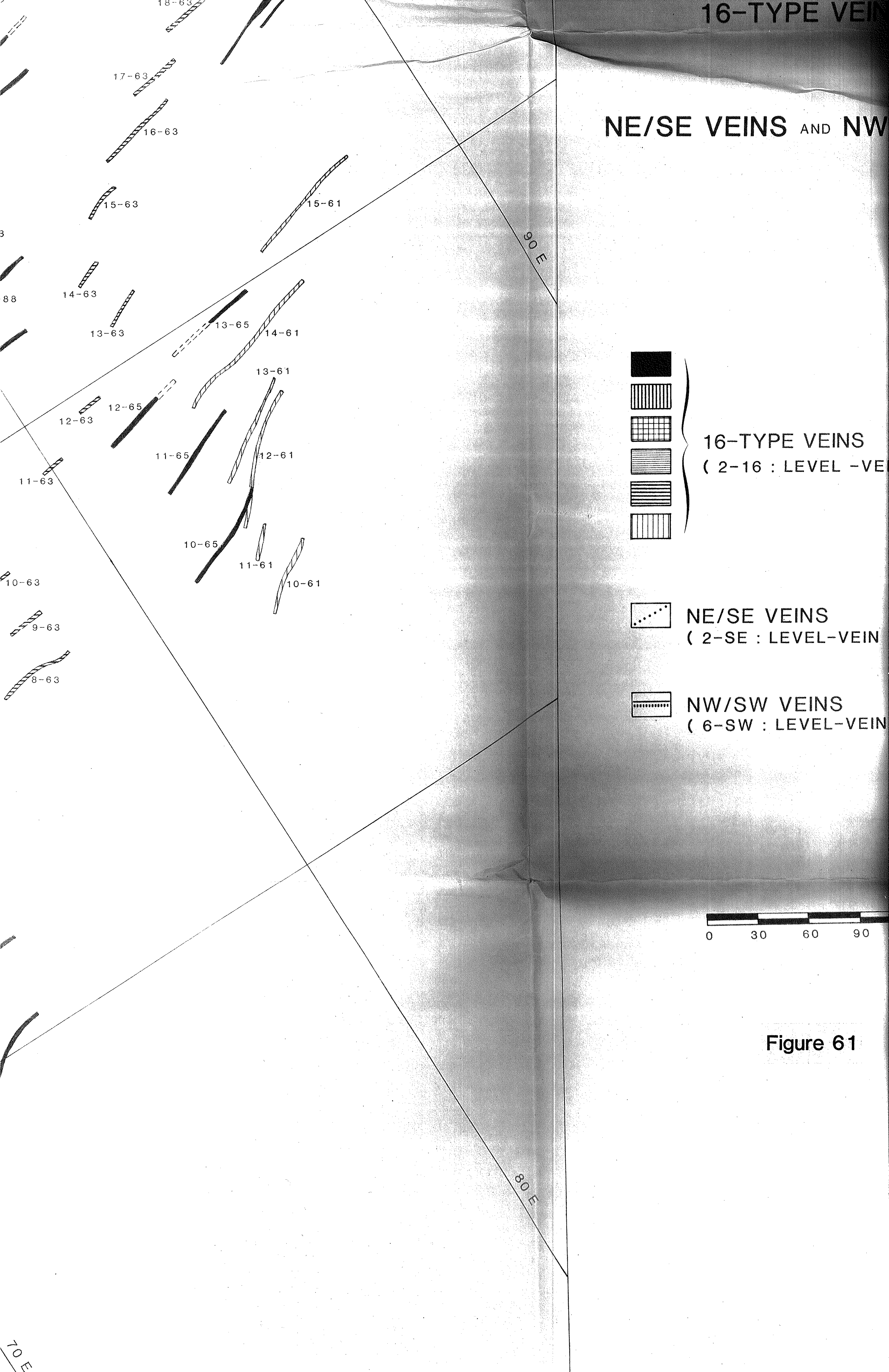
16-TYPE VEI
NE/SE VEINS AND NW
18-63
17-63
16-63
15-63
15-61
14-63
13-63
13-65
14-61
13-61
12-65
12-63
11-65
12-61
11-63
10-65
11-61
10-61
10-63
9-63
8-63
90 E
80 E
70 E
16-TYPE VEINS
(2-16 : LEVEL -VE
NE/SE VEINS
(2-SE : LEVEL-VEIN
NW/SW VEINS
(6-SW : LEVEL-VEIN
0
30
60
90

Figure 61

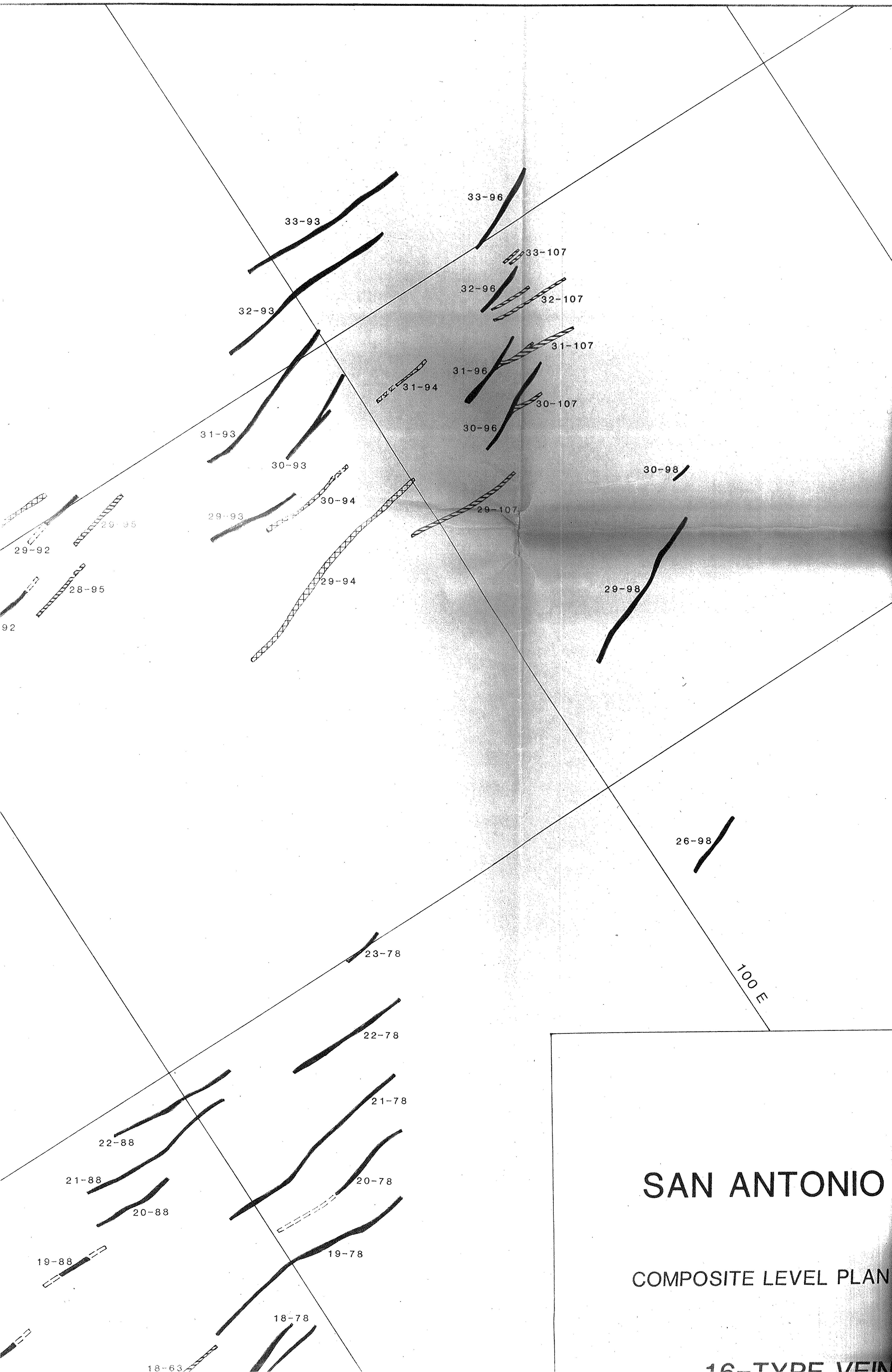

33-93
32-93
31-93
30-93
29-93
33-96
33-107
32-96
32-107
31-107
31-96
31-94
30-107
30-96
30-94
30-98
29-107
29-92
28-95
92
29-94
29-98
26-98
100 E
23-78
22-78
21-78
22-88
21-88
20-78
20-88
19-88
19-78
18-78
18-63
SAN ANTONIO
COMPOSITE LEVEL PLAN

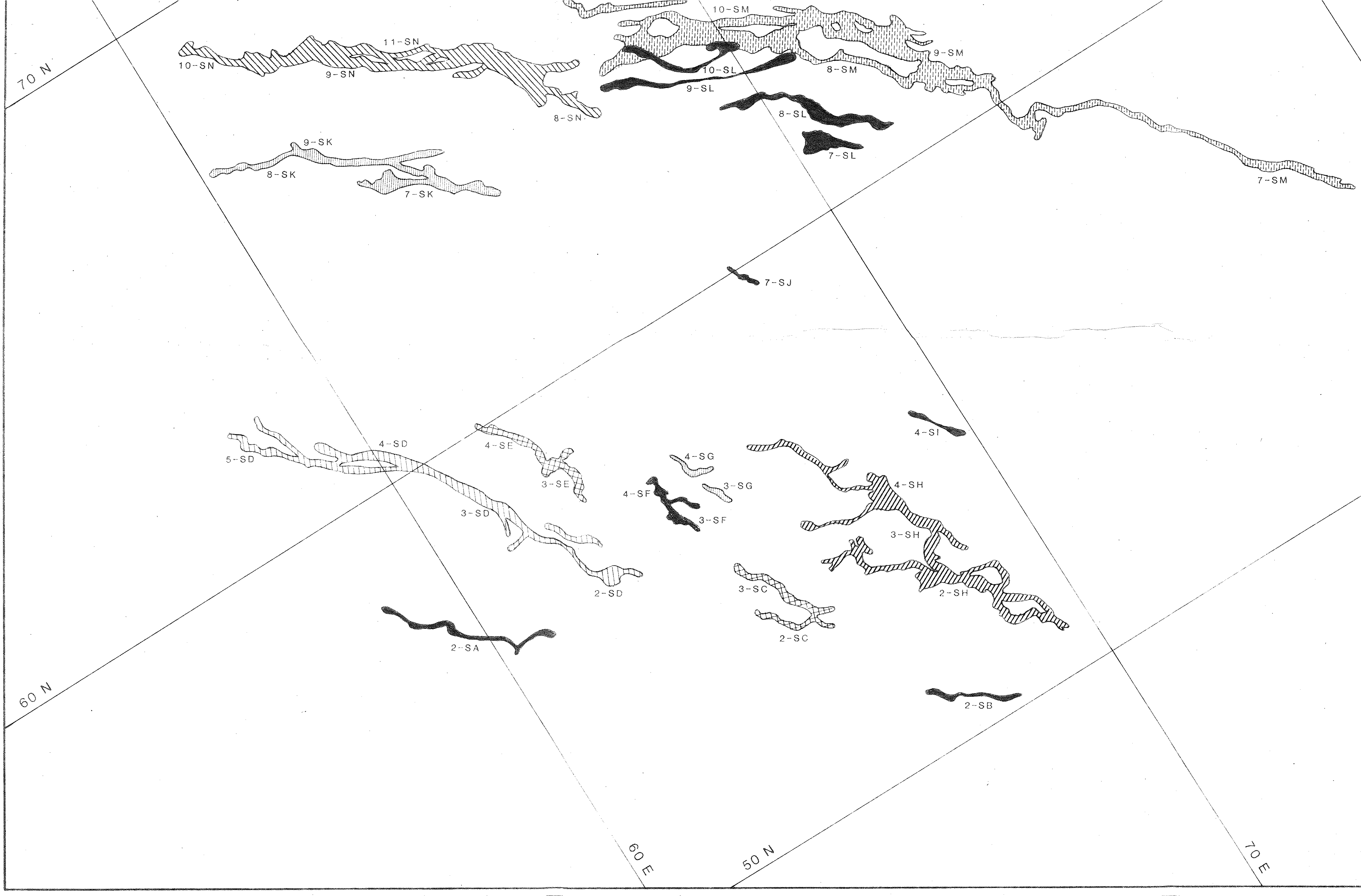

10-SM
11-SN
10-SN
9-SN
9-SM
10-SL
8-SM
9-SL
8-SN
8-SL
9-SK
7-SL
8-SK
7-SM
7-SK
70 N
7-SJ
4-SI
4-SD
4-SE
5-SD
4-SG
3-SG
3-SE
4-SH
4-SF
3-SF
3-SD
3-SH
2-SD
3-SC
2-SH
2-SC
2-SA
60 N
2-SB
60 E
50 N
70 E

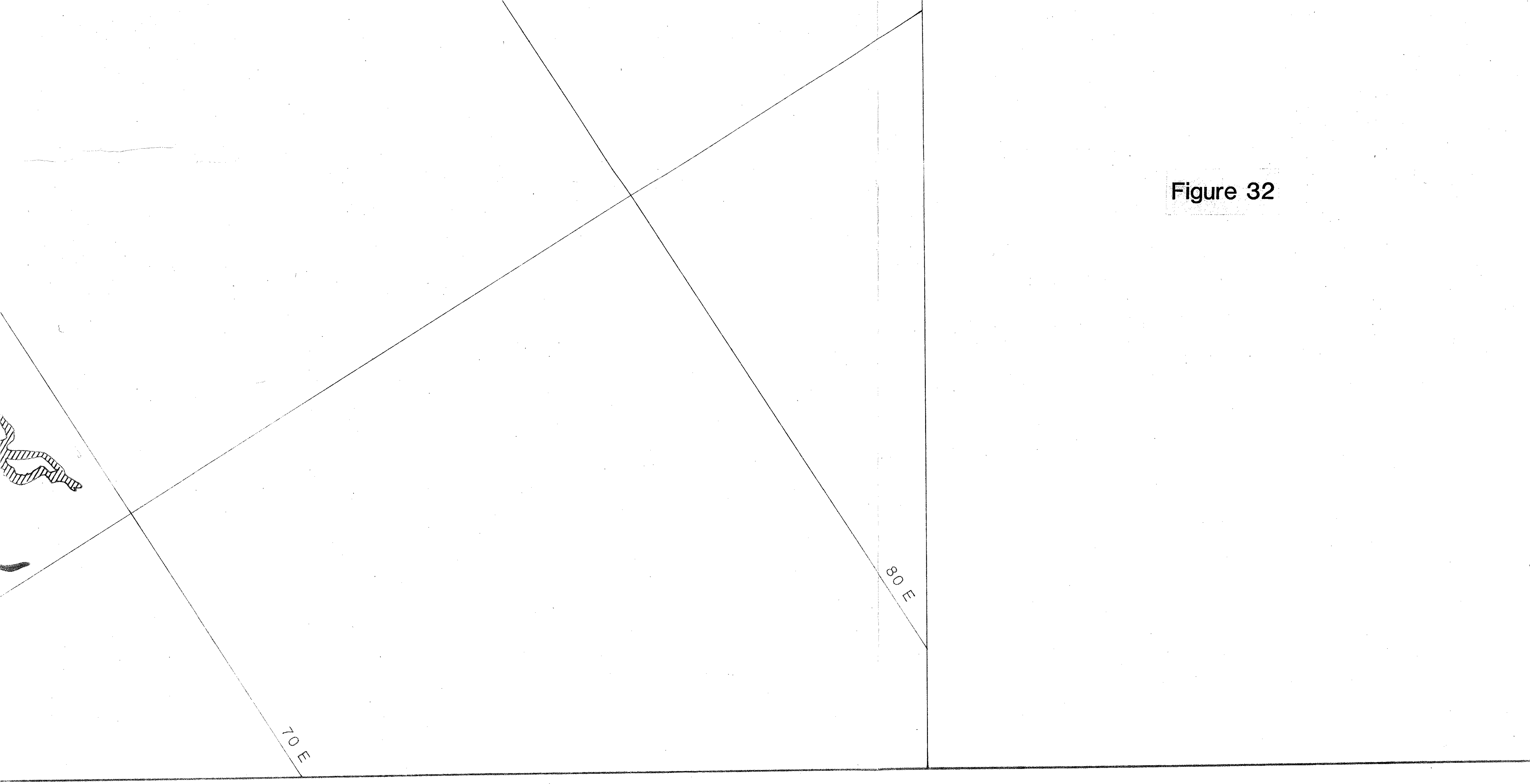

Figure 32

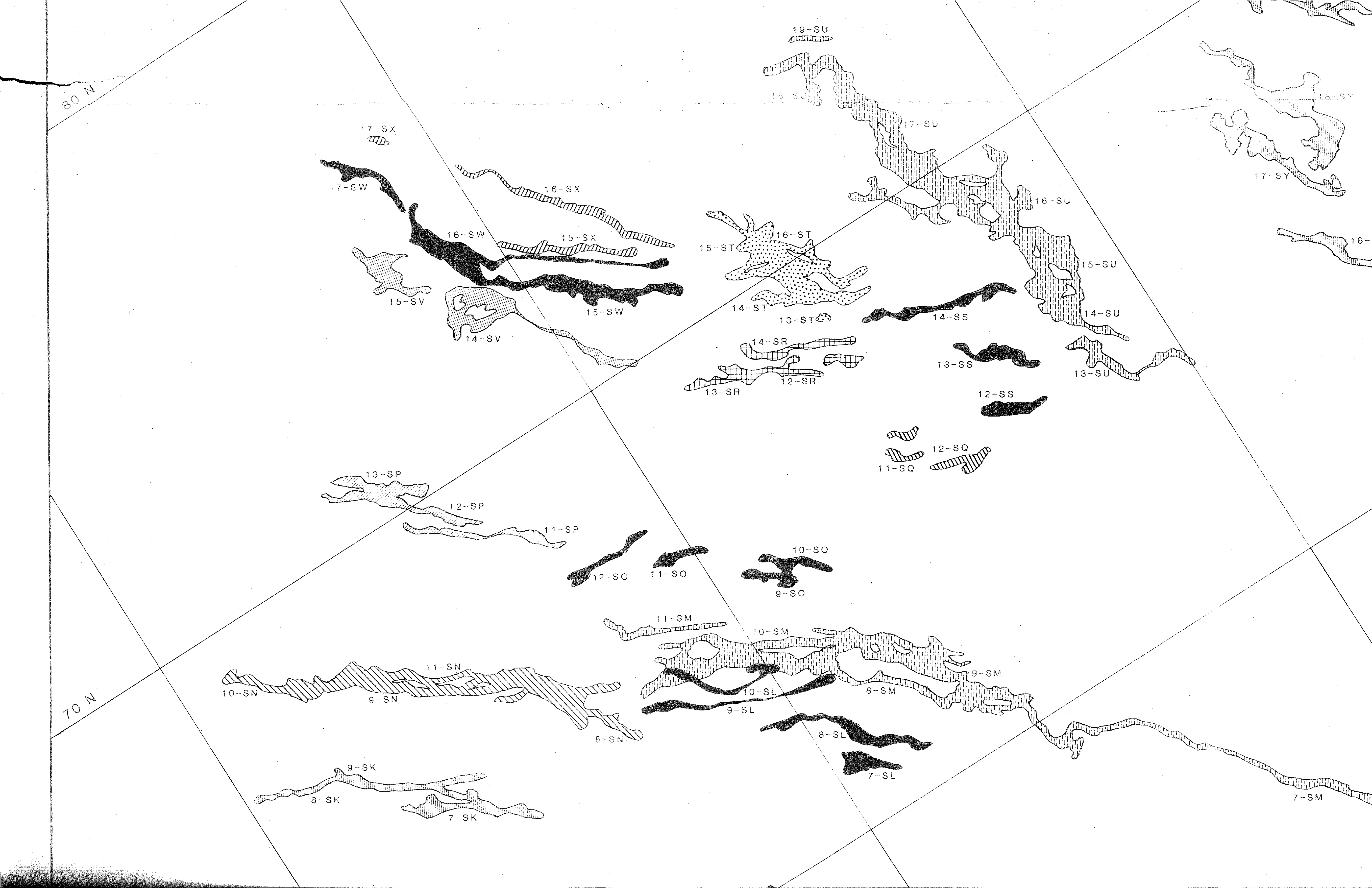
80 N
70 N
19-SU
18-SU
17-SU
16-SU
15-SU
14-SU
13-SU
18-SY
17-SY
17-SX
16-SX
15-SX
17-SW
16-SW
15-SW
15-SV
14-SV
16-ST
15-ST
14-ST
13-ST
14-SS
13-SS
12-SS
14-SR
13-SR
12-SR
12-SQ
11-SQ
13-SP
12-SP
11-SP
10-SO
12-SO
11-SO
9-SO
11-SM
10-SM
9-SM
8-SM
7-SM
11-SN
10-SN
9-SN
8-SN
10-SL
9-SL
8-SL
7-SL
9-SK
8-SK
7-SK

SAN ANTONIO MINE

COMPOSITE LEVEL PLAN VIEW OF

STOCKWORKS

2-SA : LEVEL-STOCKWORK IDENTIFICATION

0 30 60 90 120 m


23-SZ
24-SZ
22-SZ
21-SY
N

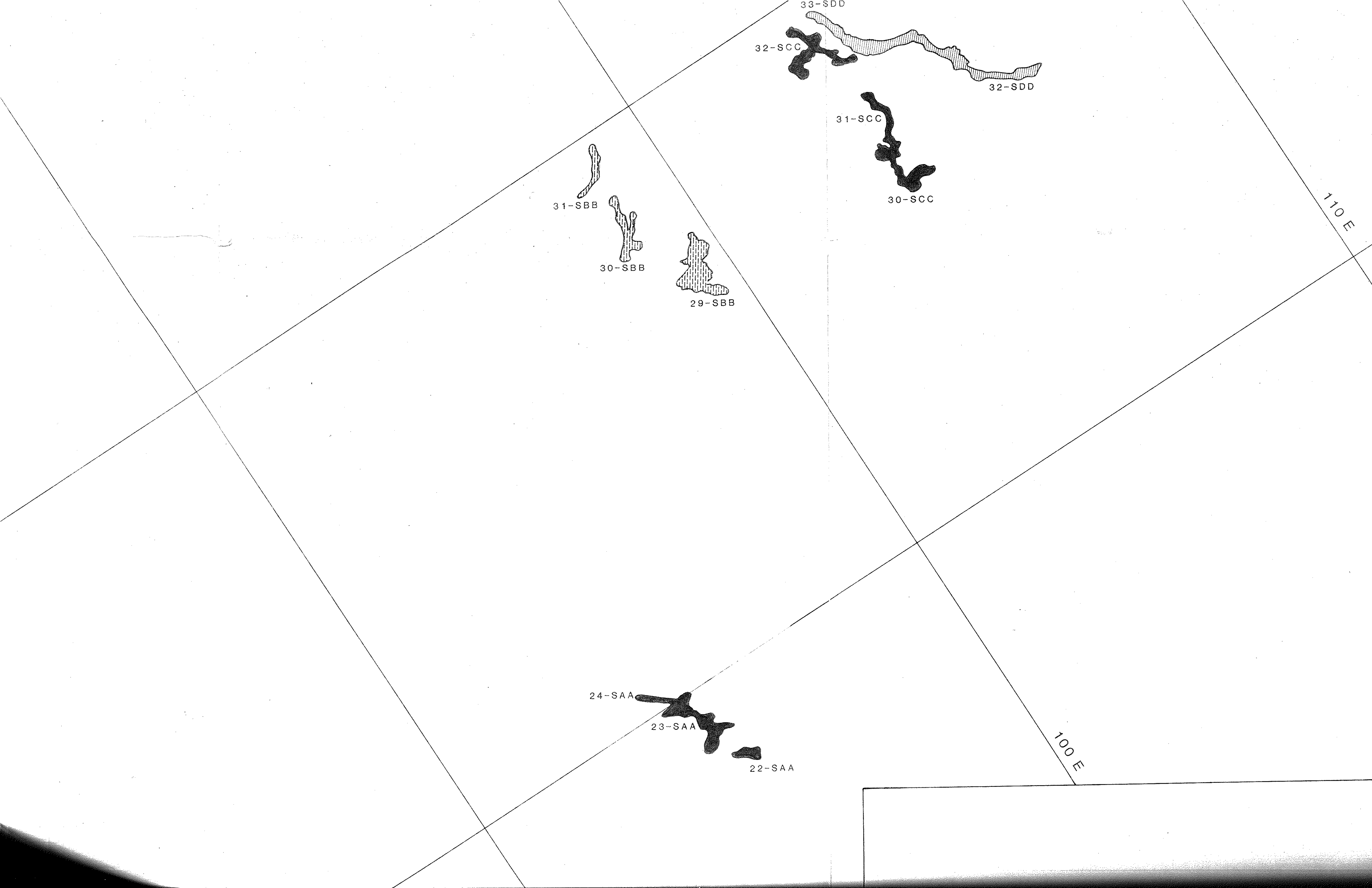
33-SDD
32-SCC
32-SDD
31-SCC
30-SCC
31-SBB
30-SBB
29-SBB
110 E
24-SAA
23-SAA
22-SAA
100 E

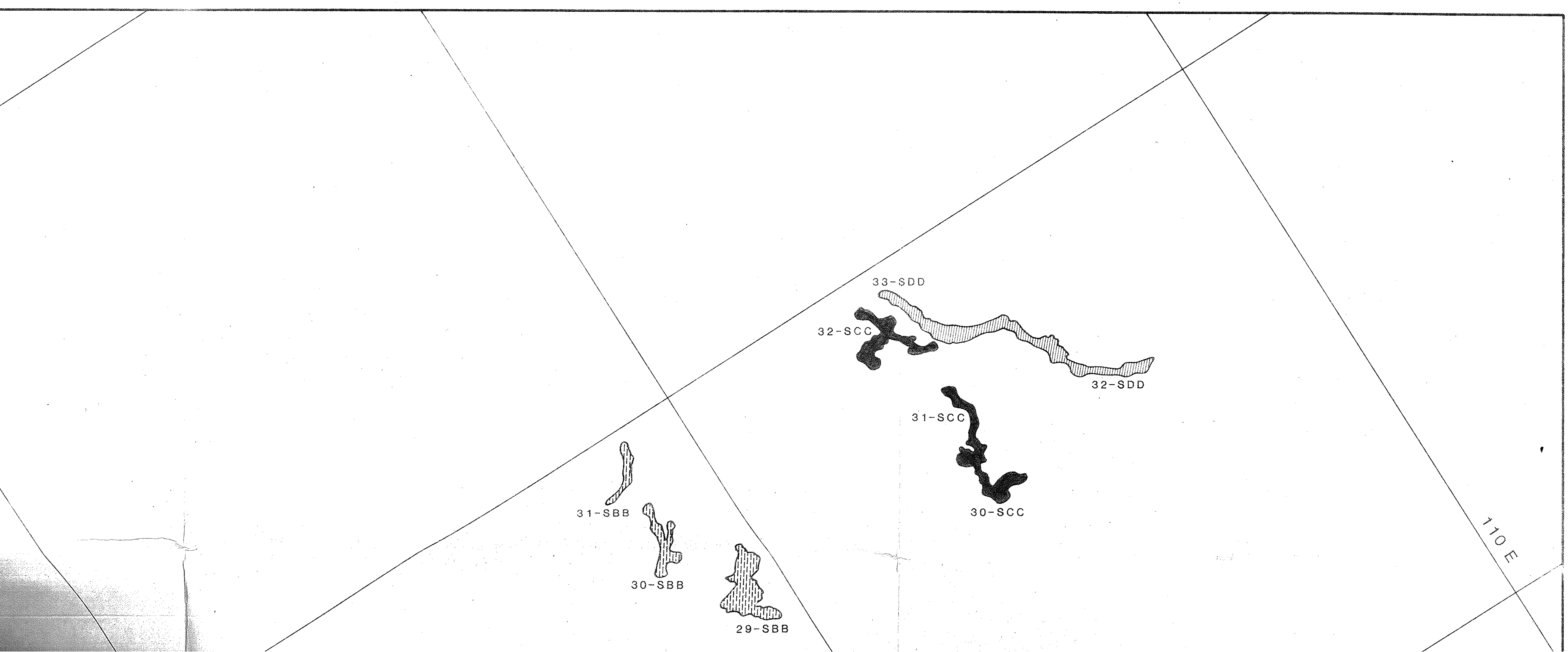
33-SDD
32-SCC
32-SDD
31-SCC
30-SCC
31-SBB
30-SBB
29-SBB
110 E


N